DISSERTATION

submitted to the
Combined Faculties for the Natural Sciences and for Mathematics
of the Ruperto-Carola University of Heidelberg, Germany
for the degree of
Doctor of Natural Science

Presented by
Daniel António Burgos Espadinha, M.Sc.
Born in Valencia, Venezuela

Oral examination: 18.12.2015

Exploring combined treatment strategies to target quiescent chronic myeloid leukemia (CML) stem cells

Referees: Prof. Dr. Andreas Trumpp

Prof. Dr. Alwin Krämer

ABSTRACT

Chronic myeloid leukemia (CML) was one of the first malignancies suggested to be driven by leukemic stem cells (LSCs) and currently serves as a disease model for stem cell based malignancies. The constitutively active BCR-ABL tyrosine kinase, created by a reciprocal translocation between chromosomes 22 and 9, drives progression of this leukemia and is thus an ideal target for drug design. Research has led to the development of the tyrosine kinase inhibitor (TKI) Imatinib, which selectively and potently inhibits the BCR-ABL kinase, leading to a rapid hematologic and cytogenetic response in most CML patients. However, following years of treatment with Imatinib, remaining residual LSCs can lead to a relapse of the disease on cessation of treatment, highlighting the need for a curative approach to eliminate both the bulk of leukemia as well as the LSCs.

Quiescence has been proposed as a potential mechanism through which LSCs remain resistant to TKI treatment, and therefore pushing these cells into cycle may make them susceptible to TKI, leading to their eradication.

Recently, our group has demonstrated that the cytokine Interferon-alpha (IFNα) can very efficiently drive quiescent hematopoietic stem cells (HSCs) into an active cell cycle. Here, we have investigated whether IFNα is also capable of activating quiescent BCR-ABL expressing LSCs. Furthermore, we have explored whether IFNα-induced activation makes LSCs more susceptible to Imatinib treatment and investigated the potential beneficial effect of a combined treatment with IFNα and Imatinib. To address these questions we used CML mouse models in which BCR-ABL expression is mainly targeted to the HSC population.

Here we could demonstrate that upon IFNα exposure, quiescent LSCs enter an active cell cycle and proliferate similarly as HSCs. Furthermore, we have tested several treatment schemes for a combined treatment in our mouse models. Interestingly, the continuous administration of Imatinib together with pulsed exposures to IFNα led to a more significant reduction of the leukemic burden when compared to either of the treatments alone.

Furthermore, we also investigated the influence of the leukemic cells on the behavior of wt cells in our CML mouse models. Here, we could show that leukemic cells induced an alteration of the wt cell population distributions in a way that mimic the leukemic compartment. This effect may be mediated by a leukemia-induced modification of the cytokine repertoire that we have also characterized in the leukemic BM. In addition, by examining the reconstitution ability of the wt cells that coexisted with the leukemic cells, we could show that exposure to a leukemic environment impairs the function of wt progenitors and HSCs.

Taken together, our data indicate that a combined strategy of continuous TKI administration together with pulsed activation of LSCs through IFNα exposure is more advantageous than TKI alone and may thus avoid relapse of the disease by eradicating LSCs. Moreover, our data suggest that the presence of leukemic cells is detrimental for the wt cells, impairing the function of wt progenitors and HSCs.

ZUSAMMENFASSUNG

Die chronische myeloische Leukämie (CML) war eine der ersten Erkrankungen, bei denen leukämischen Stammzellen (LSCs) als Krankheitsauslöser vermutet wurden und dient daher heutzutage als Modell für Stammzell-basierte Krankheiten. Die konstitutiv aktive BCR-ABL Tyrosinkinase, die durch eine reziproke Translokation zwischen Chromosom 22 und 9 erzeugt wird, ist der Auslöser der CML und bietet daher einen idealen therapeutischen Angriffspunkt für rationales Wirkstoffdesign. Fortschritte in der Wirkstoffforschung haben zu der Entwicklung des Tyrosinkinase-Inhibitoren (TKI) Imatinib beigetragen, welches potent und selektiv die Kinase Funktion von BCR-ABL inhibiert und somit zu einer schnellen hematologischen und zytogenetischen Antwort in der Mehrheit der CML Patienten führt. Allerdings verbleiben auch nach jahrelanger Imatinib Behandlung restliche LSCs, welche die Ursache für einen leukämischen Rückfall nach Beendigung der Behandlung sein können. Dies betont die Notwendigkeit für einen heilenden Therapieansatz, welcher sowohl die Mehrheit der leukämischen Zellen als auch die LSCs eliminiert.

Quieszenz wurde als möglicher Mechanismus vorgeschlagen, durch welchen LSCs resistent gegenüber TKI Behandlung bleiben. Daher könnte eine erzwungene Zellzyklusaktivierung diese ruhenden LSCs für eine TKI Behandlung sensibilisieren was zu ihrer Vernichtung führt.

Vor kurzem konnte unsere Gruppe zeigen, dass das Zytokin Interferon-Alpha (IFNα) ruhende hämatopoetische Stammzellen (HSCs) sehr effizient in den aktiven Zellzyklus treibt. In dieser Arbeit wurde untersucht ob IFNα auch ruhende BCR-ABL exprimierende LSCs aktivieren kann und ob diese IFNα-vermittelte Aktivierung LSCs empfänglich für eine Imatinib Behandlung macht. Zusätzlich wurde die potenziell nützliche Wirkung einer Kombinationsbehandlung von IFNα und Imatinib getestet. Für diese Fragestellungen wurden CML Mausmodelle verwendet, in welchen BCR-ABL Expression hauptsächlich auf die HSC Population beschränkt ist. Wir konnten zeigen, dass ruhende LSCs, ähnlich wie HSCs, nach IFNα-Behandlung in den Zellzyklus eintraten und proliferierten. Außerdem wurden mit Hilfe unserer Mausmodelle mehrere Behandlungsstrategien für eine Kombinationsbehandlung getestet. Hierbei zeigte eine kontinuierliche Imatinib Behandlung in Kombination mit einer wiederkehrenden IFNα Behandlung eine signifikante Reduktion der leukämischen Last im Vergleich zu den jeweiligen Einzelbehandlungen.

Des Weiteren haben wir den Einfluss von leukämischen Zellen auf das Verhalten von wildtyp (wt) Zellen in unseren CML Mausmodellen untersucht. In diesem Zusammenhang konnten wir zeigen, dass leukämische Zellen eine Veränderung in der Zusammensetzung der wt Zellpopulationen hervorrufen, sodass diese die Verteilung der leukämischen Zellen imitiert. Dieser Effekt könnte durch eine durch die Leukämie ausgelösten Änderung des Zytokin-Milieus herbeigeführt werden, welches wir im leukämischen Knochenmark charakterisiert haben. Außerdem konnten wir mit Hilfe von Rekonstitutionsexperimenten mit wt Zellen, welche mit leukämischen Zellen koexistierten, zeigen, dass eine leukämische Umgebung die Funktion von wt Vorläufern und HSCs beeinträchtigen kann.

Zusammenfassend zeigen unsere Daten, dass eine Kombinationsbehandlung bestehend aus kontinuierlicher TKI Behandlung und einer wiederkehrenden Aktivierung von LSCs durch IFNα Behandlung vorteilhafter als eine einfache TKI Behandlung ist und daher den Rückfall der Krankheit durch das Beseitigen der LSCs verhindern könnte. Außerdem deuten unsere Daten darauf hin, dass die Anwesenheit von leukämischen Zellen einen schädlichen Einfluss auf wt Zellen hat, indem diese die Funktion von wt Vorläufern und HSCs beeinträchtigen.

TABLE OF CONTENTS

1. INTRODUCTION

1.1 Hematopoietic stem cells

1.1.1 Discovery of hematopoietic stem cells

The hematopoietic stem cell (HSC) research field was initiated in the 1950s with the demonstration that lethally irradiated mice could be rescued from death by transplantation of bone marrow (BM) from healthy mice, which was able to reinitiate blood cell production (Ford et al., 1956; Nowell et al., 1956). The concept of a specific population of cells being able to generate diverse hematopoietic cell types was first demonstrated in the 1960s, with the observation that colonies formed in the spleen of transplanted mice arose from a single cell and contained different mature cell lineages (Becker et al., 1963; Till and Mc, 1961; Wu et al., 1967). The existence of HSCs was then finally proved in 1977 with the demonstration that a particular BM cell was able to give rise to all blood cell types of both the myeloid and lymphoid lineages (Abramson et al., 1977).

The HSCs were the first adult stem cells to be prospectively isolated (Spangrude et al., 1988) and to become commonly used for clinical applications such as the BM transplantation for the treatment of leukemia and autoimmune disorders (Weissman, 2000). Nowadays, HSCs are one of the most extensively studied and characterized stem cells and serve as model for other adult stem cells.

1.1.2 Function of hematopoietic stem cells

Hematopoietic stem cells (HSCs) are at the apex of the hierarchically organized hematopoietic system and are responsible for the life-long maintenance of blood production (Kondo et al., 2003). In the classical model of hematopoietic lineage commitment, HSCs give rise to multipotent progenitors (MPPs), which have the ability to rapidly amplify their numbers and differentiate into lineage-committed progenitors (Morrison et al., 1997a; Morrison and Weissman, 1994). In turn, these committed progenitors, which include the common lymphoid progenitors (CLP), common myeloid progenitors (CMP), granulocyte macrophage progenitors (GMP) and megakaryocyte-erythrocyte progenitors (MEP), proliferate extensively and differentiate into mature blood cells (Fig. 1.1) (Akashi et al., 2000; Kondo et al., 1997).

The simplistic view of the classical model has been challenged by several studies such as the discovery of the lymphoid-primed progenitor cells (LMPPs), which are capable of giving rise to B and T cells as well as granulocytes and macrophages, but not erythrocytes or platelets (Adolfsson et al., 2005). Moreover, recent studies have demonstrated the existence of heterogeneity within the HSC pool in terms of lineage-biased differentiation potentials (Benz et al., 2012; Dykstra et al., 2007; Ema et al., 2014; Gekas and Graf, 2013; Haas et al., 2015; Morita et al., 2010; Sanjuan-Pla et al., 2013). Furthermore, it has recently been suggested that HSCs are able to directly give rise to several lineage-committed progenitors within one cell division (Yamamoto et al., 2013). Thus, whereas it was initially believed that HSCs would give rise to MPPs, which in turn would branch into either myeloid or lymphoid common progenitors, increasing evidence demonstrates the existence of additional alternative pathways down the hematopoietic tree.

HSCs are not only able to generate any cell of the hematopoietic system but also have the ability to self-renew by dividing asymmetrically and thus ensuring that one daughter cell remains an HSC (Kondo et al., 2003). They reside in the trabecular bone area of the bone marrow (BM) of adults and are a rare population of cells, comprising approximately 0.001-0.01% of total BM cells in mice (Oguro et al., 2013) and 0.01-0.2% of total BM mononuclear cells in humans (Pang et al., 2011).

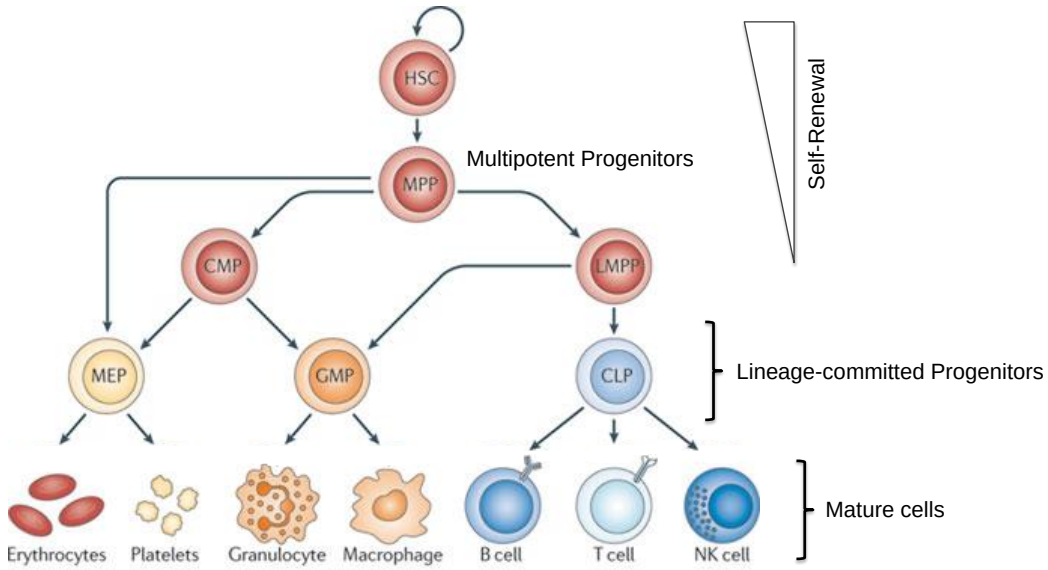

Figure 1.1: The Hematopoietic Hierarchy
The hematopoietic stem cells (HSCs) reside at the top of the hierarchically organized hematopoietic system and have long-term self-renewal capacity as well as the potential to give rise to any blood lineage. During the differentiation process, progenitor cells gradually loose the self-renewal and multi-lineage reconstitution capacity. Whereas multipotent progenitors (MPPs) and lymphoid-primed progenitor cells (LMPPs) have the potential to give rise to cells from both the myeloid and lymphoid branch, the megakaryocyte-erythrocyte progenitors (MEP), granulocyte-macrophage progenitors (GMP) and common lymphoid progenitors (CLPs) are already restricted to a specific lineage. More recently, it has been shown that HSCs have also the potential to bypass the stepwise differentiation process and within one cell division give rise to committed progenitors. (Figure adapted from (Cedar and Bergman, 2011))

1.1.3 Hematopoietic stem cell markers

The isolation of very pure fractions of HSCs has been made possible through the combination of functional assays with fluorescence activated cell sorting (FACS). The golden standard to assess HSC function consists in the ability of the cell to reconstitute the hematopoietic system of lethally irradiated mouse recipients. Since the irradiation eradicates the majority of hematopoietic cells, including the HSCs, the mouse would not be able to survive. The transplanted HSCs occupy the vacated niche space and are not only able to generate all mature blood cell types but also to self-renew and therefore maintain blood production through the entire life span of the recipient. Furthermore, they carry the ability to sustain the hematopoietic system over serial transplantations. In contrast, progenitors are only able to reconstitute the hematopoietic system for a limited span of time and are not able to be serially transplanted due to the lack of long-term self-renewal ability (reviewed in (Weissman and Shizuru, 2008)).

Through the combination of FACS and transplantation assays, HSCs began to be identified by cell surface markers. An enriched population for murine HSCs was found within the lineage$^-$ (negative for a combination of mature blood cell markers), Sca-1$^+$ and c-Kit$^+$ (LSK) cells (Uchida et al., 1994). The purity of the HSC population was further refined with the addition of more cell surface markers. The addition of CD34, as an exclusion marker, was shown to increase the purity of HSCs in the LSK compartment to more than 1 in 5 (Osawa et al., 1996). More recently, the inclusion of the CD150 and CD48 markers from the signaling lymphocytic activation molecule (SLAM) family led to a further refined purity. The combination of all the markers mentioned above enable the isolation of a highly purified population (LSKCD150+CD48-CD34-) where approximately 1 in 2 cells are long-term repopulating HSCs as opposed to 1 in 10^5 in the total BM (Kiel et al., 2005; Wilson et al., 2009). Alternative positive HSC markers, such as EPCR and ESAM, have also been described, however they seem to be redundant with the previously described marker combination and do not further increase purity (Balazs et al., 2006; Yokota et al., 2009).

1.1.4 Quiescent hematopoietic stem cells

During homeostasis, more than 70% of HSCs in the adult BM are kept quiescent in the G_0 state of the cell cycle (Wilson et al., 2008). Through quiescence, the genome integrity of HSCs is preserved by avoiding damage linked to cell replication (Bakker and Passegue, 2013; Pietras et al., 2011; Walter et al., 2015). The

remaining HSC fraction is responsible for continuously replenishing numerous mature blood cell types, which have an inherent limited life span. However, in order to meet the organism‘s needs upon hematopoietic stress conditions such as infection, inflammation, toxic insult and bleeding, quiescent HSCs are able to react to a large array of signals and enter the cell cycle and proliferate (Cheshier et al., 2007; Essers et al., 2009; Takizawa et al., 2011; Trumpp et al., 2010; Wilson et al., 2007; Yanez et al., 2009; Zhang et al., 2008).

HSCs have the ability to sense and rapidly meet the organism demands for blood cell production through receptors for cytokines, chemokines and danger-associated molecular patterns (Takizawa et al., 2012).

1.1.5 Hematopoietic stem cell niche

Adult HSCs reside in specialized niche microenvironments within the BM. Many of the stem cell properties are modulated by the interplay between HSCs and the BM microenvironment. The HSC niche is composed of an extensive array of specialized cells that provide chemical and physical cues essential for HSC maintenance and function. Some of the cellular components exert their effect through cell-to-cell contact whereas others employ secreted agents such as cytokines and chemokines. Many different cell types contribute to the HSC niche including mesenchymal stem cells (MSCs), endothelial cells (ECs), megakaryocytes, sympathetic nerve cells, osteoblasts (OBs) and macrophages (Fig. 1.2) (reviewed by (Mendelson and Frenette, 2014; Morrison and Scadden, 2014)).

HSCs are able to reside in a variety of places within the trabecular region of long bones, including the area close to the sinusoidal endothelium or near the endosteum (Kiel and Morrison, 2008; Wilson and Trumpp, 2006). It has been proposed that the HSCs more close to the endosteum are kept quiescent, whereas the remaining ones fulfill homeostatic functions (Grassinger et al., 2010; Kunisaki et al., 2013). However, the exact definition and functional relevance of the different niche subtypes is still under debate and further experiments and advances in the current techniques are needed. The visualization of HSCs in their microenvironment is hindered by technical issues, such as the inability to use as many fluorochromes simultaneously as flow cytometry and the inherent disruption of the BM architecture upon sectioning of the bone.

HSC quiescence is regulated by secreted factors from the niche cells, including transforming growth factor beta-1 (TGF-β1), stem cell factor (SCF), thrombopoietin (TPO), angiopoietin 1 (ANGPT1) and platelet factor 4 (PF4 or CXCL4) (Pietras et al., 2011). The regulators of HSC homing and positioning in the niche include the

chemokine stromal-derived factor 1 (SDF1α or CXCL12) and its C-X-C chemokine receptor type 4 (CXCR4), extracellular matrix (ECM) proteins such as fibronectin or hyaluronic acid, diverse selectins and adhesion molecules like vascular cell adhesion protein 1 (VCAM-1). The HSC proliferation and differentiation is influenced by cytokines like interleukin 7 (IL-7) and erythropoietin (EPO) or by cell-bound molecules like notch ligands (Mendelson and Frenette, 2014; Morrison and Scadden, 2014; Schepers et al., 2015).

In order to fulfill the organism's requirement during infection or BM stress, the niche cell composition and cytokine repertoire is believed to be altered in order to induce a demand-adapted hematopoiesis (Takizawa et al., 2012).

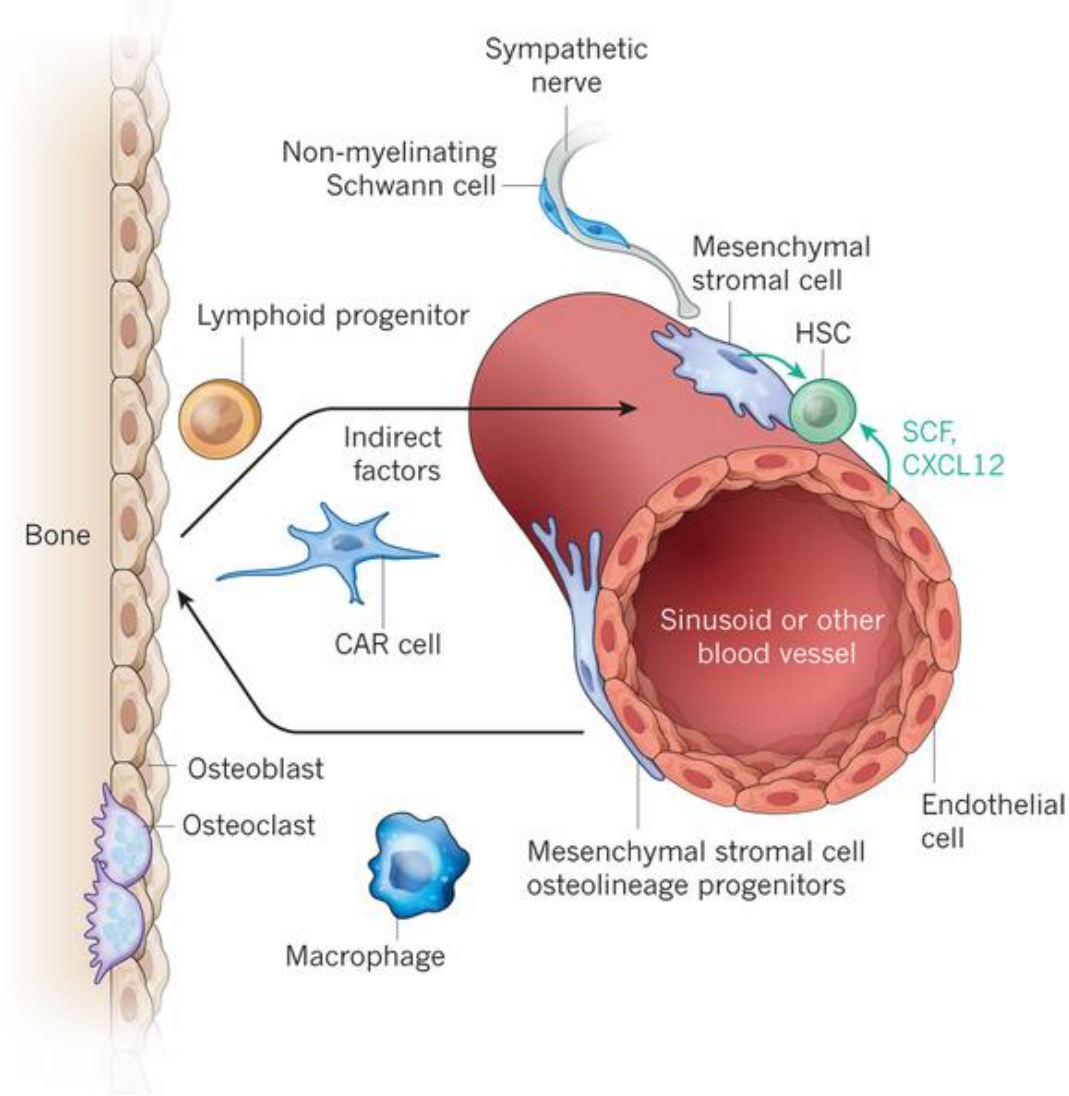

Figure 1.2: The hematopoietic stem cell niche
The hematopoietic stem cells (HSC) reside in specialized niches in the bone marrow. The HSC niche is composed by a variety of cells including mesenchymal stem cells, endothelial cells, megakaryocytes, sympathetic nerve cells, osteoblasts and macrophages. HSC maintenance is regulated by an array of factors, such as SCF and CXCL12 produced by MSCs and endothelial cells. (Figure from: (Morrison and Scadden, 2014))

1.1.6 Activation of hematopoietic stem cells with interferon-alpha

Interferon-alpha (IFNα) has been shown to be involved in a wide range of biological functions by regulating the transcription of more than 300 IFN-stimulated genes (ISGs), encoding host defense, antiviral, immunomodulatory, cell cycle, apoptotic, and transcription factor proteins (de Veer et al., 2001). More precisely, this cytokine has been primarily known for its role in resistance to viral infections, anti-proliferative effects, and enhancement of innate and adaptive immune responses (Belardelli et al., 2002; Stark et al., 1998). In the course of infection, IFNα was shown to be produced by virally infected cells as well as stimulated innate immune cells such as macrophages and dendritic cells (DCs) (Fitzgerald-Bocarsly et al., 2008; Trinchieri, 2010).

More recently, a new role for IFNα has been unveiled. It has been demonstrated that IFNα is able to push HSCs out of quiescence into active cell cycle (Essers et al., 2009). In a matter of hours after *in vivo* administration of IFNα in mice, quiescent HSCs are efficiently induced to enter an active cell cycle and proliferate. The binding of IFNα to the interferon-α/β receptor (IFNAR) leads to the phosphorylation of the signal transducer and activator of transcription 1 (STAT1) and up-regulation of a panel of IFNα-inducible genes (ISGs) (Essers et al., 2009). After a few days following IFNα acute exposure, the HSCs return back to quiescence. A recent report has suggested that upon chronic IFNα exposure, the HSCs proliferate only for a limited time, after which the response to IFNα is blocked as a safeguard mechanism (Pietras et al., 2014).

In previous studies, IFNα was demonstrated to have an anti-proliferative effect against many cell types *in vitro* (Borden et al., 2007), suggesting that IFNα signals are perceived differently depending on the cell context.

Interestingly, IFNγ has also been recently shown to induce mouse quiescent HSCs into an active cell cycle in the context of a bacterial infection through an IFNα independent signaling pathway (Baldridge et al., 2010).

1.2 Origins of leukemia

Normal, self-renewing tissues are built in a hierarchical way, containing a population of stem cells responsible for the life-long maintenance of the tissue. Furthermore, research in recent years has suggested that different types of cancer show a small population of cells with stem cell properties, the so-called cancer stem cells (CSCs) (Cho and Clarke, 2008; Dick, 2008; Reya et al., 2001; Trumpp and Wiestler, 2008). Evidence for the existence of a cancer stem cell population initially came from the field of leukemia research, where it was shown that a subgroup of leukemic cells had clonogenic activity *in vitro* and the ability to transplant the disease into mice (Bonnet and Dick, 1997; Lapidot et al., 1994; Wang and Dick, 2005). Therefore these cells were called leukemic stem cells (LSCs). Interestingly, their cell surface marker phenotype was the same as HSCs.

HSCs continuously face intrinsic and extrinsic stresses that cause DNA damage, which if not accurately resolved lead to mutations (Bakker and Passegue, 2013). Over time these mutations accumulate and can lead to malignant transformation (Welch et al., 2012). The transformed HSCs maintain the ability to self-renew but the capacity to originate the different lineages of blood cells is deregulated (Passegue et al., 2003). Additionally, LSCs can also arise from transformed progenitors that reacquire the stem cell capability for self-renewal (Eppert et al., 2011; Goardon et al., 2011; Jamieson et al., 2004; Krivtsov et al., 2006; Wang et al., 2010).

The LSCs are the disease-initiating cells and upon serial transplantation are able to propagate the leukemia, recreating the primary tumor and its heterogeneity in the recipient mouse. In order to support their maintenance and activity, the leukemic cells have the ability to remodel the BM microenvironment (Tabe and Konopleva, 2014).

The LSCs have been shown to resist against most current therapies. Since irradiation and many cytotoxic drugs can only induce cell death in proliferating cells, they are not able to target the largely quiescent LSCs. Furthermore, LSCs have been shown to be resistant not only to irradiation and chemotherapy but also to targeted therapies like immunotherapy and tyrosine kinase inhibitors (Guzman and Allan, 2014). As a consequence, LSCs are believed to be responsible for the majority of treatment failure and relapse cases. Therefore, from a clinical perspective, the targeting of LSCs is of utter importance.

1.3 Chronic myeloid leukemia

Chronic myeloid leukemia (CML) is a myelo-proliferative disease, characterized by uncontrolled growth of myeloid cells (Sawyers, 1999). Every year, 1-2 individuals per 100,000 people are diagnosed with CML, accounting for 15% of all newly diagnosed cases of leukemia in adults (Jemal et al., 2010).

Although relatively rare, it is one of the best-characterized malignancies and one of the first shown to be driven by leukemic stem cells (LSCs). Today, it serves as a model disease for stem cell based malignancies.

CML arises as a consequence of a reciprocal translocation between chromosomes 22 and 9 resulting in “Philadelphia chromosome” (Ph), which yields the BCR-ABL fusion protein (Fig. 1.3) (Goldman and Melo, 2001; Groffen et al., 1984; Rowley, 1973).

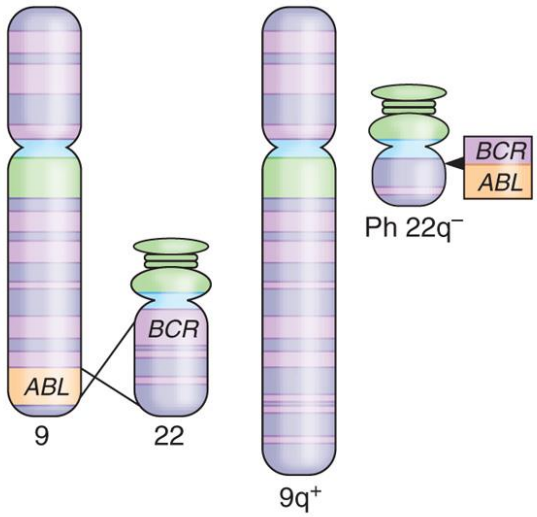

Figure 1.3: Philadelphia chromosome
As a result of a reciprocal chromosomal translocation between chromosomes 9 and 22, the “Philadelphia chromosome” is originated, given rise to the BCR-ABL fusion protein. (Figure from: (Lydon, 2009))

1.3.1 Disease phases

CML usually presents in a chronic phase (CP) but, if not treated, progresses to an accelerated phase (AP) and ultimately ends in a terminal phase called blast crisis (BC) that is clinically similar to an acute leukemia (Sawyers, 1999). The first large data collection of the disease development was derived from the atomic bomb survivors (Lange et al., 1954; Preston et al., 1994). It was observed that following a prolonged latent period, the majority of patients (85%) presented in the CP, however after a 5-year window they progressed through an AP to a BC. Although, within 5

years most patients usually progress to BC, this is variable between individuals, with some patients remaining in CP for up to 20 years and others progressing to BC in just a few months (Cortes, 2004). When comparing the genetic abnormalities between the different CML phases, a far higher significant increase in point mutations and chromosomal aberrations is detected in the BC (Brazma et al., 2007; Grossmann et al., 2011).

1.3.2 Symptoms, signs and diagnosis

The majority of patients are diagnosed during the CP of the disease upon routine physical examinations or blood tests. Around 30-50% of the newly diagnosed patients in the USA are asymptomatic. For the remaining CP patients, the most common presented symptoms include fatigue, weight loss, malaise, easy satiety and left upper quadrant fullness or pain. Upon medical examination, increased white blood cell (WBC) counts and splenomegaly are usually detected. Typically, the diagnosis of CML is finalized when the presence of the Ph chromosome is confirmed by conventional cytogenetics or *fluorescent in situ hybridization* (FISH) as well as the presence of the BCR-ABL fusion transcript by the highly sensitive reverse transcriptase-polymerase chain reaction (RT-PCR) (Jabbour and Kantarjian, 2014).

1.3.3 The role of BCR-ABL as driver of chronic myeloid leukemia

The constitutively active BCR-ABL tyrosine kinase leads to deregulation of a large array of signal transduction pathways, resulting in leukemic cell growth, proliferation and survival (Fig. 1.4) (Mandanas et al., 1993) (Deininger et al., 2000; Kharas and Fruman, 2005; Ren, 2005). Similar to other cancers, some of the key cell survival pathways being altered include PI3K/AKT/mTOR, RAS/RAF/MEK/ERK, and JAK/STAT. In CML, the BCR-ABL deregulated pathways not only inhibit apoptosis and stimulate proliferation but also lead to an increased production of reactive oxygen species (ROS) within mitochondria (Bolton-Gillespie et al., 2013; Nieborowska-Skorska et al., 2012). In turn, increased levels of ROS lead to oxidative DNA damage, characterized by increased DNA point mutations and double stranded breaks, which due to unfaithful and ineffective DNA repair mechanisms, lead to aberrant chromosomal alterations.

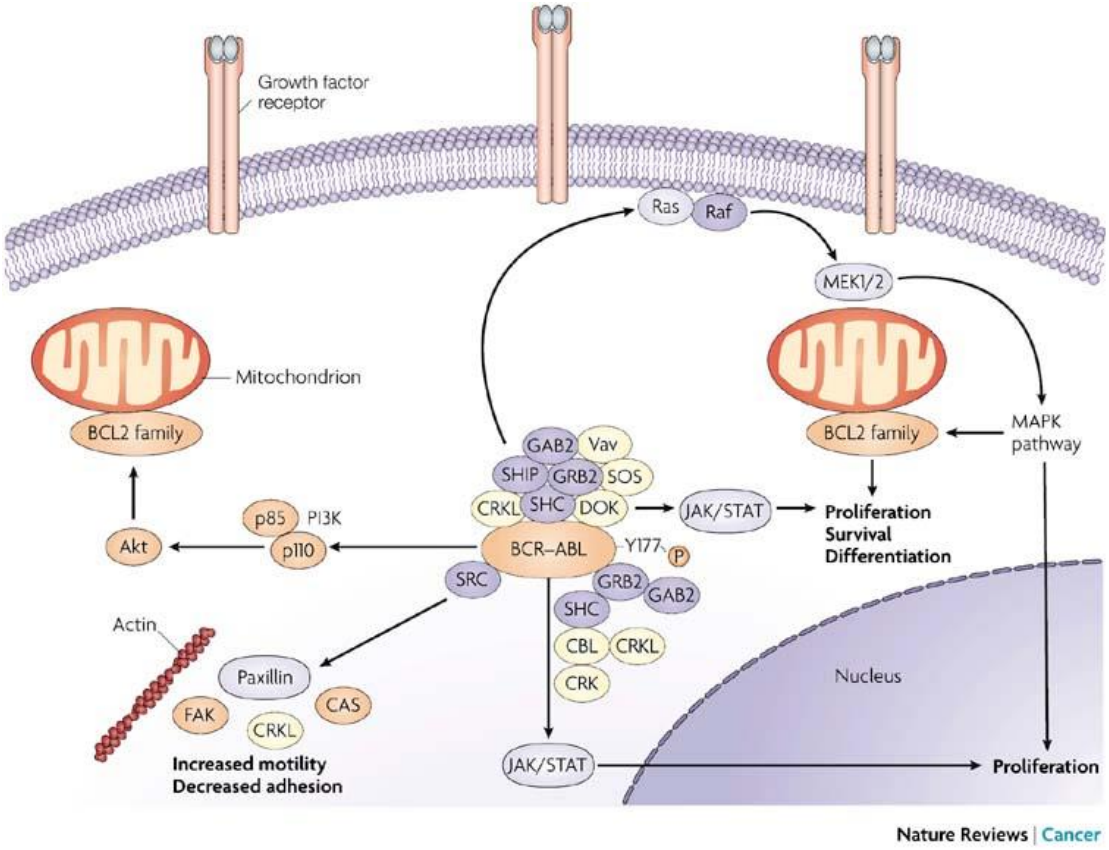

Figure 1.4: BCR-ABL signaling
Several signal transduction pathways are deregulated by the constitutively active BCR-ABL tyrosine kinase, including PI3K/AKT/mTOR, RAS/RAF/MEK/ERK and JAK/STAT, ultimately resulting in leukemic cell survival, growth and proliferation. (Figure from: (Weisberg et al., 2007))

1.3.4 Initial treatment strategies

Until the end of the 20th century, the CML therapy was restricted to nonspecific agents, evolving from the primitive usage of arsenic containing compounds in the 19th century, to the administration of busulfan, hydroxyurea and, later on, interferon-alpha (IFNα) (Silver et al., 1999).

Interferon was used for the first time to treat CML patients in 1983 (Talpaz et al., 1983). In the first trial, 5 out of 7 patients achieved complete hematological response (CHR) after being treated with high doses of IFNα, and the splenomegaly detected in 3 patients was reverted. From then on, IFNα became the drug of choice to treat CML patients. The remission rate and survival were improved, as compared to the previously used agents, and the 5-year survival rates were increased from 42% to 57% (1997). However, IFNα was associated to a wide range of significant side effects that interfered with the quality of life and therefore the long-term usage was not possible in many patients. In some cases, allogeneic stem cell transplantation (AlloSCT) was able to reverse disease development. However, not only was this intervention restricted to a limited number of patients with exceptional performance

status and available suitable stem cell donor but also was associated with a high risk of morbidity and mortality.

1.3.5 Imatinib targeted therapy

Since the constitutively active BCR-ABL kinase is the driving force behind this leukemia, it is thus an ideal target for drug development. This led to the development of the tyrosine kinase inhibitor (TKI) Imatinib (Gleevec), which selectively and potently inhibits the BCR-ABL kinase by blocking the ATP binding site, resulting in complete abrogation of BCR-ABL kinase activity (Druker and Lydon, 2000). Imatinib very efficiently targets BCR-ABL positive CML cells, leading to a rapid hematologic and cytogenetic response. With the development of Imatinib, the treatment and management of CML patients was revolutionized, resulting in a significantly improved prognosis, response rate, overall survival, and patient outcome, compared to previous therapeutic regimens (Druker et al., 2006; Hochhaus et al., 2009; O'Brien et al., 2003). The 8-year overall survival was improved from approximately 20% to 80-90% (Jabbour and Kantarjian, 2014; Jemal et al., 2010).

Nonetheless, after years of treatment with Imatinib, residual leukemic cells remain present in most patients, leading to a relapse of the disease upon discontinuation of treatment (Goldman, 2009; Michor et al., 2005). Consequently, most CML patients currently need to be treated with TKI indefinitely, with risks of toxicity, lack of compliance, drug resistance, relapse, and associated expense.

1.3.6 Second- and third-generation tyrosine kinase inhibitors

The identification of mutations in the BCR-ABL kinase domain that confer resistance to imatinib and were associated with disease relapse led to the development of the second-generation TKIs, dasatinib, nilotinib, and bosutinib (Golas et al., 2003; Lombardo et al., 2004; Weisberg et al., 2005). Dasatinib is 350 times more potent than imatinib *in vitro* (O'Hare et al., 2005; Tokarski et al., 2006) and is also know to inhibit the Src family of kinases (Shah et al., 2004). Nilotinib is a structural analog of imatinib with a 50 times higher affinity to the BCR-ABL ATP binding site *in vitro* (Weisberg et al., 2005). The second-generation TKIs were shown to be active against the majority of imatinib-resistant single-mutants, with the exception of the T315I mutation (Weisberg et al., 2007). This led to the development of the third-generation TKI, ponatinib (O'Hare et al., 2009), which represents the only TKI with activity against the T315I mutation (Cortes et al., 2012; Cortes et al., 2013). However, the acquisition of multiple mutations can still render BCR-ABL resistant to ponatinib (Zabriskie et al., 2014).

At the present time, imatinib, dasatinib or nilotinib are recommended for the initial treatment of CML-CP (O'Brien et al., 2013). Although the second-generation TKIs seem to induce faster cytogenetic and molecular responses, the 5-year overall survival has not been significantly different from imatinib and their impact in long-term overall survival remains unclear (Fava et al., 2015). Furthermore, long-term toxicity events associated with the second-generation TKIs, have been raising concerns for their use, especially in specific groups of patients (Fava et al., 2015).

1.3.7 Response and resistance to tyrosine kinase inhibitors

After patients initiate treatment, the first aim is to achieve complete hematological response (CHR) by bringing the blood cell counts back to normal values. In case the treatment is stopped at this point, the blood counts rapidly come back to abnormal values. Therefore, the second objective consists in obtaining complete cytogenetic response (CCyR) by achieving Ph chromosome negativity. More importantly, the main objective is to achieve a major molecular response (MMR) by bringing the levels of BCR-ABL transcripts down to less than 0.1%, as assessed by the highly sensitive RT-PCR technique (Baccarani et al., 2013).

The European Leukemia Net (ELN) defines an optimal response to a first line TKI when BCR-ABL transcript levels detected at 3 months are ≤10%, at 6 months <1%, and from 12 months onwards ≤0.1%. In the other hand, a failed response is characterized by BCR-ABL levels of >10% at 6 months and >1% at 12 months or loss of CCyR, CHR, MMR or detection of additional clonal chromosomal abnormalities in Ph^+ cells (Baccarani et al., 2013). The majority of patients that begin TKI treatment while in CP respond to the therapy and achieve CHR after a few weeks. Typically, 6 months after the beginning of treatment, CCyR is achieved and by 1 year MMR (BCR-ABL1 <0.1%) is reached. Although the majority of patients reach the clinic when at the CP of the disease, 10-15% already present AP or BC. Even from the patients that initially present CP, 7% have additional chromosomal aberrations other than t(9,22). In both these groups of patients, the frequency of resistance development and progression to BC is higher.

When patients are administrated with Imatinib as a first line therapy, approximately 50% remain with the same therapy at 5 years and eventually 30-40% of them achieve undetectable minimal residual disease (UMRD) (Hehlmann et al., 2011; Kantarjian and Cortes, 2011; Kantarjian et al., 2009). However, even for these patients with optimal response the ELN management guidelines recommend indefinite continuation of the TKI therapy. When TKI discontinuation trials were conducted with patients under UMDR, approximately 50% developed molecular

relapse and therefore therapy restart was undergone (Legros et al., 2012; Mahon et al., 2010; Ross et al., 2013; Rousselot et al., 2014; Rousselot et al., 2007). When discontinuation trials were performed with the second-generation TKIs dasatinib and nilotinib, the relapse rate was not markedly reduced as compared to imatinib.

From the group of patients that fail to respond to the TKI therapy, according to the ELN established thresholds, approximately 50% develop TKI resistance due to mutations that occur in the BCR-ABL kinase domain (Khorashad et al., 2013). These mutations alter the conformation of BCR-ABL and decrease the drug binding affinity. Over 50 different mutations have been reported, each with a distinct sensitivity to the several available TKIs.

Some patients fail to respond not only to the first line TKI but also to multiple TKI treatments without the occurrence of mutations in the BCR-ABL kinase domain. The drivers of this form of BCR-ABL independent resistance are still not entirely known. Some studies suggest that the activation of additional oncogenes like the SRC family kinases LYN (Dai et al., 2004; Donato et al., 2003; Mahon et al., 2008; Pene-Dumitrescu and Smithgall, 2010; Wu et al., 2008) and FYN (Grosso et al., 2009) or an increased presence of FGF2 in the BM (Traer et al., 2014) may contribute to the BCR-ABL independent resistance. Interestingly, ponatinib, which has the additional potential of inhibiting the FGF receptor and LYN kinase (O'Hare et al., 2009), was shown to be able to overcome FGF2-mediated resistance in the absence of BCR-ABL kinase mutations (Traer et al., 2014). Furthermore, ponatinib was shown to overcome resistance in several TKI-resistance cell lines (Cassuto et al., 2012). However, in a trial with resistant patients, it was only able to lead 27% of the patients to achieve MMR and the expected survival remained low (Cortes et al., 2013).

1.3.8 Chronic myeloid leukemia stem cells and resistance

In CML CP it has been demonstrated that mutations at the stem cell level are responsible for disease progression (Nieborowska-Skorska et al., 2012). The induction of high levels of ROS and oxidative damage by BCR-ABL in the leukemic stem cells leads to the formation of mutations in the BCR-ABL kinase domain as well as mutations associated with progression to BC. Even in the presence of TKI, the leukemic stem cells continue to accumulate genetic abnormalities.

In the case of CML BC it has been suggested that mutations in the GMP population, especially at the level of the WNT/β-catenin pathway, might render them with self-renewal capacity and turn them into BC leukemic stem cells (Jamieson et al., 2004; Minami et al., 2008; Stuart et al., 2009). However, additional characterization of this potential leukemia initiating cells in BC is required.

By making use of sensitive PCR techniques and functional stem cell assays, it has been shown that even when patients achieve UMRD, persistent BCR-ABL+ stem cells still remain present (Chomel et al., 2011; Chomel and Turhan, 2011; Chu et al., 2011).

In an inducible BCR-ABL transgenic mouse model of CML it was demonstrated that after shutting off BCR-ABL expression, the leukemic stem cells were able to survive and reinitiate leukemia upon BCR-ABL reactivation (Hamilton et al., 2012). Similarly, human CD34+ CML cells remained alive even when BCR-ABL was knocked down. Furthermore, human CD34+ CML cells exposed to dasatinib were able to withstand apoptosis, maintain their function and proliferate once the TKI was washed out, independently of the presence of mutations in the kinase domain (Corbin et al., 2011; Hamilton et al., 2012).

The most primitive, quiescent leukemic stem cells from CML CP, which resist TKI treatment, can then lead to a relapse of the disease upon discontinuation of treatment. The majority of relapses occur within the first 6 months after treatment stoppage (Mahon et al., 2010).

1.3.9 Chronic myeloid leukemia microenvironment

At the time of diagnosis, circulating CML $CD34^+$ cells can be detected in the peripheral blood of patients and present a downregulation of CXCR4 and defects in adhesion signaling (Jin et al., 2008; Weisberg et al., 2012). However, after TKI treatment initiation they are cleared from the blood and the resistant LSCs are believed to reside in the BM microenvironment.

The CML cells have been shown to alter the BM microenvironment. For example, in an inducible BCR-ABL transgenic CML mouse model, the leukemic cells were shown to produce G-CSF, which led to decreased expression of CXCL12/SDF1 by the BM (Zhang et al., 2012). Additionally, the leukemic clone has been shown to modify the expression levels of other cytokines in the BM such as IL-1α, IL-1β, MIP1α, MIP1β, LIF and TNFα. Similarly, CXCL12, G-CSF, MIP1β and MIP2 were shown to be differentially regulated in CML human samples.

The alterations in the BM niche induced by the leukemic cells offer a competitive growth advantage for the leukemic versus healthy cells. This mechanism has been exemplified through the production of TNFα by the leukemic cells promoting clonal dominance for the LSCs (Fleischman et al., 2011; Gallipoli et al., 2013a) as well as the induction of PIGF production and secretion by the BM stroma promoted by the leukemic cells contributing to disease development (Schmidt et al., 2011).

The signals from the BM microenvironment can also contribute to the protection of LSCs against TKI. The adhesion of the leukemic cells to the BM stroma through the N-cadherin receptor has been shown to confer protection to the LSCs through enhanced cytoplasmic N-cadherin-β-catenin complex formation and increased β-catenin nuclear translocation (Zhang et al., 2013).

So far, no therapies targeting the altered CML BM microenvironment have been introduced in the clinics.

1.3.10 Treatment tolerance and adherence

A group of patients fails to respond to the TKI therapy, not because of resistance acquisition, but due to the development of drug toxicity or poor compliance. A study focusing on patients in long-term imatinib treatment showed that 25-30% of the patients face side effects such as muscle cramps, fatigue, edema and musculoskeletal pain (Efficace et al., 2011). Only 20% of the patients reported the absence of any side effects. Actually, the incidence of side effects revealed by this study might be underestimated since it only included patients that were already able to tolerate imatinib for 3 years. The occurrence of side effects has a direct impact on the patient compliance to the TKI therapy. According to the ADAGIO study, 71% of the patients took less imatinib than the prescribed dose and only 14% were completely complaint (Noens et al., 2009). In another study focusing on CML patients that had reached CCyR on long-term imatinib therapy, 26% of patients were reported to take less than or equal to 90% of the prescribed dose (Marin et al., 2010). The intake of ≤90% versus >90% of the prescribed dose of imatinib had a significant impact on the MMR (28 versus 94%, $P < 0.001$) and CMR/UMRD (0 versus 44%, $P = 0.002$).

Apart from the short-term side effects, over time some patients can develop more severe complications that can become life-threatening, such as gastrointestinal bleeding, vascular events (e.g. hypertension, myocardial infarction, peripheral vascular occlusion and stroke), fluid retention (e.g. pleural and pericardial effusions), liver toxicity, pancreatitis, cardiac effects (e.g. prolongation of QTc, cardiac failure, arrhythmias), pulmonary hypertension, myelosuppression and infection. The majority of these side effects are observed with all TKIs but the frequency and severity of a particular effect varies between different TKIs. Recently, a phase 3 trial evaluating ponatinib versus imatinib as front line therapy for CP CML patients (NCT01650805) had to be stopped and subsequently ponatinib was temporarily withdrawn in USA due to the high incidence of vascular side effects (Cortes et al., 2013; Cortes et al., 2014; Quintas-Cardama, 2014).

All TKIs share the occurrence of side effects and compliance issues, therefore an approach that enables the complete eradication of the CML cells and consequently the possibility of treatment discontinuation is needed.

1.3.11 Chronic myeloid leukemia prevalence and associated expense

The development of TKIs revolutionized the management and treatment of CML patients. The overall survival of CML patients has been markedly increased as compared to previous therapeutic approaches. As a consequence the prevalence of CML has increased over time. It has been estimated that the prevalence in USA will increase from 70,000 cases in 2010 to 112,000 in 2020, reaching a plateau of 181,000 in 2050 (Huang et al., 2012). Already in the present time, since TKI therapy is expensive and needs to be taken indefinitely, some countries are not able to afford their prescription, emphasizing the need for a curative approach (2013).

1.3.12 Imatinib versus second- and third- generation tyrosine kinase inhibitors

When patients are diagnosed with CML in CP, the ELN recommends the administration of imatinib, nilotinib or dasatinib as a first line therapy. The decision between imatinib or second-generation TKI administration has to consider the balance between potential benefits and risks. In some particular cases, such as the existence of BCR-ABL kinase mutations, the choice for a more potent TKI is clear. The usage of third-generation TKIs is only advised when patients present with the T315I mutation. However, when patients present in CP without additional genetic abnormalities, taking into account the concerns regarding the side effects of the long-term usage of the newer agents, the decision might fall on imatinib, the TKI more extensively studied and with the safest track record.

2. AIM

The emergence of TKI targeted therapy revolutionized the treatment of CML patients, leading to a significant increase of the remission rates and overall survival, as compared to previous therapeutic approaches. However, even in patients under remission following years of TKI therapy, residual quiescent LSCs remain present that can lead to a relapse of the disease upon treatment discontinuation. Therefore, patients are required to undergo TKI treatment indefinitely, emphasizing the need for a curative approach able to target the quiescent LSCs.

Quiescence has been proposed as a potential mechanisms responsible for conferring treatment resistance to LSCs. Therefore, finding a way to activate LSCs into an active cell cycle might render them susceptible to TKI treatment, ultimately leading to the elimination of all CML cells

Previous studies have demonstrated that the cytokine IFNα can very efficiently drive quiescent HSCs into an active cell cycle. However, the effect of IFNα on LSCs has remained unknown. Thus, one aim of this thesis was to investigate whether IFNα is capable of activating quiescent LSCs in a similar way as in HSCs. Additionally, we wanted to test whether the IFNα induced activation would make the LSCs susceptible to the TKI treatment and investigate the potential benefit of the combined treatment. To address these questions we made use of CML mouse models in which BCR-ABL expression is mainly targeted to the HSC population. To model the situation of a CML patient, in which both healthy and CML cell populations coexist, mixed BM chimeras were generated by co-transplanting LSCs with wild-type HSCs. Moreover, in this experimental setup we also aimed to characterize the interplay between leukemic and healthy cells in the mixed BM chimeras. More specifically, we wanted to investigate the influence of the leukemic cells on the healthy cells across distinct populations of the hematopoietic tree, ranging from mature cells, to committed progenitors and finally HSCs.

3. RESULTS

3.1 Targeting quiescent leukemic stem cells through a combined treatment strategy

TKIs selectively and potently inhibit the BCR-ABL kinase, leading to a rapid hematologic and cytogenetic response in CML patients. However, following years of patient treatment, remaining residual LSCs can lead to a relapse of the disease on cessation of treatment. The reason for treatment resistance of LSCs is highly debated, with one of the mechanisms suggested being the quiescence of the LSCs. Our group has previously demonstrated that the cytokine IFNα can very efficiently drive quiescent HSCs into an active cell cycle (Essers et al., 2009). Thus, we have investigated whether IFNα was capable of activating quiescent BCR-ABL expressing LSCs in a similar way as in HSCs. Furthermore we tested whether the IFNα induced activation makes the LSCs susceptible to the TKI treatment and investigated the potential benefit of the combined treatment. We addressed these questions in mouse models that mimic the situation of the CML patient.

3.1.1 Inducible model of BCR-ABL expression → SCLtTA/BCR-ABL

In our initial studies we made use of the double-transgenic (dtg) SCLtTA/BCR-ABL mouse model, which inducibly and reversibly expresses BCR-ABL under the control of the 3' enhancer of the murine stem cell leukemia (SCL) gene (Koschmieder et al., 2005), thus targeting BCR-ABL expression to the HSC population (Fig. 3.1). More specifically, in one transgene, the 3' enhancer of the SCL gene targets the tetracycline transactivator (tTA) expression to the HSC population, whereas in the other transgene, BCR-Abl is under the control of the Tetracycline Response Element (TRE). Therefore, in the presence of doxycycline (DOX), the tTA is rendered incapable of binding to the TRE and thereby BCR-Abl expression is abrogated. Upon removal of DOX from the drinking water, the tTA is capable of binding to the TRE, inducing the expression of BCR-Abl in the HSCs.

The dtg mice, carrying both the SCLtTA and TRE-BCR-ABL transgenes, were always analyzed in comparison to control single-transgenic (stg) mice (carrying only one of the transgenes and therefore unable to express BCR-ABL). Both mouse lines were kept on DOX from the moment they were born until they reached adulthood (8-10 weeks old).

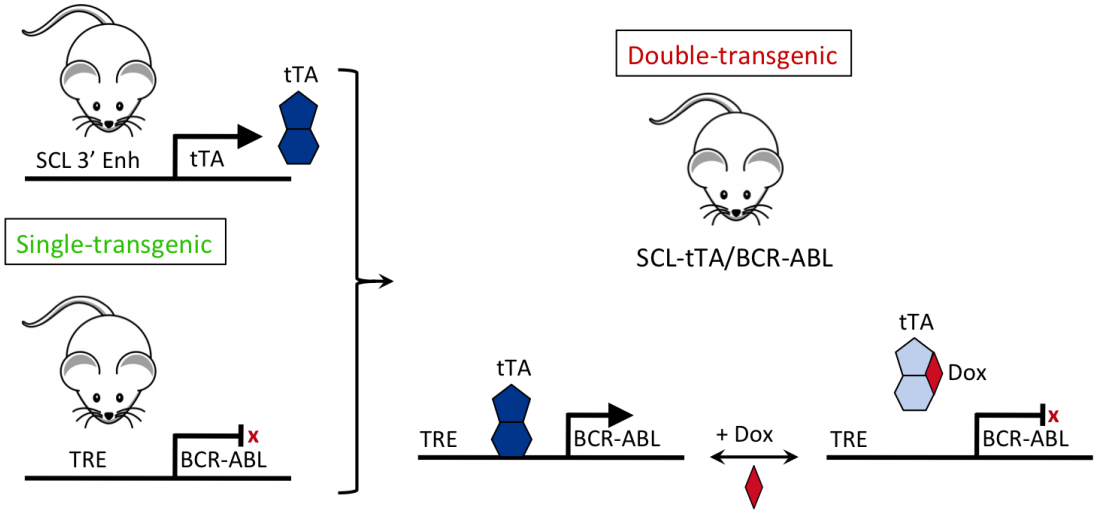

Figure 3.1: Inducible SCLtTA/BCR-ABL Tet-OFF mouse model.
The SCLtTA transgenic line expressing the tetracycline transactivator (tTA) under the control of the 3' enhancer of the murine stem cell leukemia (SCL) gene was crossed with the TRE-BCR-ABL transgenic line in which BCR-ABL expression is regulated by the Tetracycline Response Element (TRE). The resulting double-transgenic (dtg) mouse inducible and reversibly expresses BCR-ABL, in a doxycycline (DOX) dependent manner, under the control of the 3' enhancer of the murine stem cell leukemia (SCL) gene, thus targeting BCR-ABL expression mainly to the HSC population. The transgenic lines were kept on a FVB/N genetic background.

3.1.1.1 SCLtTA/BCR-ABL mice develop a chronic phase CML-like disease

In order to confirm the development of leukemia by the inducible SCLtTA/BCR-ABL Tet-OFF mouse model, the blood was monitored every second week after DOX removal until signs of leukemia were detected. The blood samples were analyzed by Hemavet to quantify the blood cell counts and additionally were stained and analyzed by flow cytometry to ascertain changes in the distribution of cell populations. Over the course of time, a statistically significant increase in the white blood cell (WBC) count could be detected in the dtg as compared to the stg mice (Fig. 3.2 A). More specifically, the monocytes (MO) (Fig. 3.2 B) and neutrophils (NE) (Fig. 3.2 C) counts were elevated whereas there was no difference in the eosinophils (EO) (Fig. 3.2 D) or lymphocytes (LY) (Fig. 3.2 E) counts.

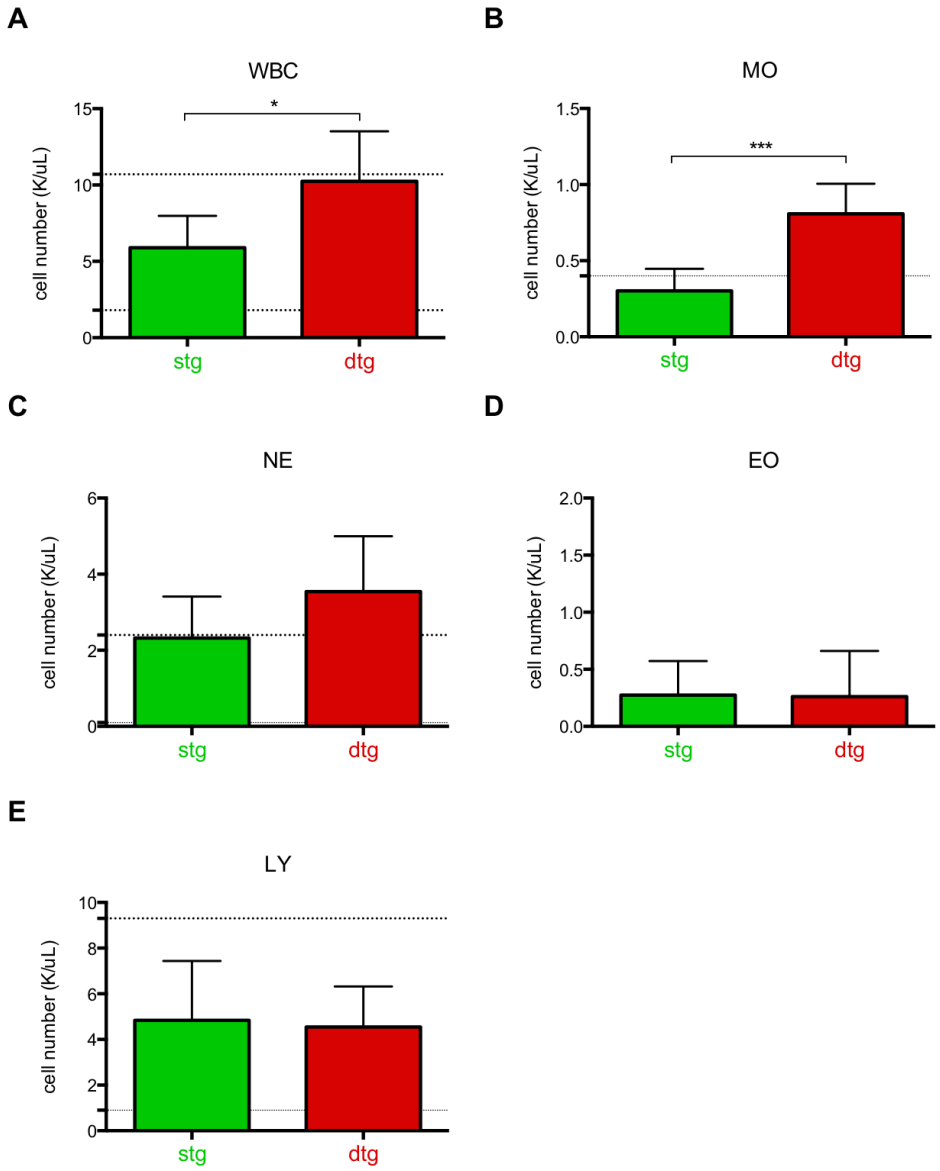

Figure 3.2: Blood cell count analysis of the SCLtTA/BCR-ABL mice.
The blood of SCLtTA/BCR-ABL double-transgenic (dtg) and control single-transgenic (stg) mice was analyzed 30 weeks after doxycycline removal from the drinking water. The blood cell counts were analyzed by HEMAVET and the white blood cell (A), monocytes (B), neutrophils (C), eosinophils (D) and lymphocytes (E) were monitored. The dashed lines delineate the normal range of the blood cell counts. Data are presented as mean ± SD with n ≥ 3. The significance was determined using an unpaired, two-tailed student's t-test (* $p < 0.05$, ** $p < 0.01$, *** $p < 0.001$).

Further analysis revealed a decrease in the body weight and an increase in the spleen size of the dtg as compared to the stg mice (Fig. 3.3 A-C). Moreover, when examining the spleen cells by flow cytometry, a statistically significant increase in the mature ($CD11b^{+}Gr1^{high}$) and immature ($CD11b^{+}Gr1^{low}$) granulocytes was detected in the dtg mice as opposed to the stg mice (Fig. 3.3 D+E). Finally, an expansion of the granulocyte population in the BM of the dtg mice was identified through flow cytometry, whereas the stg mice retained normal values (Fig. 3.3 F).

Taken together, we could confirm that the SCLtTA/BCR-ABL mice develop signs of a chronic myeloproliferative disorder resembling human chronic-phase CML.

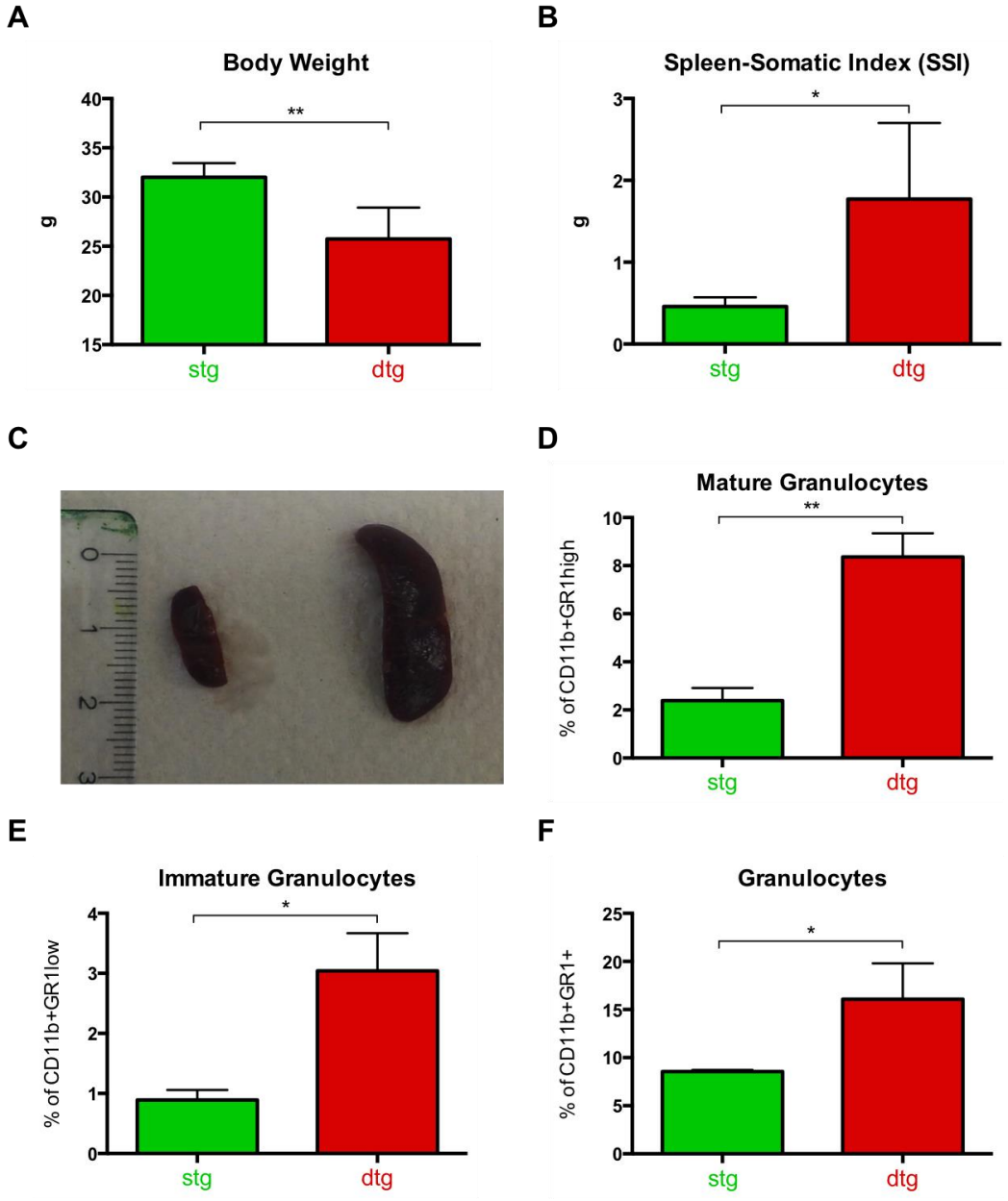

Figure 3.3: Bone marrow and spleen analysis of the SCLtTA/BCR-ABL mice.
The SCLtTA/BCR-ABL dtg and control stg mice were analyzed 30 weeks after doxycycline removal from the drinking water. (A) The body weight of dtg and stg mice was monitored. (B) The spleen was isolated and the formula (g spleen mass/g mouse mass)×100 was used to calculate the spleen-somatic index (SSI). (C) Representative picture of the macroscopic appearance of the spleen of stg and dtg mice. (D) The spleen mature granulocytes ($CD11b^{+}Gr1^{high}$) were examined by flow cytometry. (E) The immature granulocytes ($CD11b^{+}Gr1^{low}$) from the spleen were monitored through flow cytometry. (F) The bone marrow (BM) cells were stained and the granulocyte population ($CD11b^{+}Gr1^{+}$) was investigated by flow cytometry. Data are presented as mean ± SD with n ≥ 3. The significance was determined using an unpaired, two-tailed student's t-test (* $p < 0.05$, ** $p < 0.01$).

3.1.1.2 Effects of IFNα on the SCLtTA/BCR-ABL cells

Our group has previously shown that IFNα can very efficiently drive HSCs out of quiescence into an active cell cycle via the interferon-α/β receptor (IFNAR) and

STAT1 signaling (Essers et al., 2009). However, whether IFNα has similar effects on quiescent LSCs is not known. Therefore, we first addressed whether INFα is able to activate LSCs, and whether the effect of IFNα on LSCs is comparable to the effect of INFα on HSCs.

In order to challenge the mice with IFNα, we made use of polyinosinic-polycytidylic acid (pIC), a synthetic analogue of double-stranded RNA (dsRNA) that leads to the production of INFα. Both leukemic dtg and healthy stg mice were injected with PBS or pIC and 20h later the BM cells were isolated. The stem cells were then subjected to a combined intracellular staining with the active cell cycle marker Ki67 together with the DNA dye Hoechst33342, in order to monitor the cell cycle status through flow cytometry. Through this assay, the cells can be distinguished as being quiescent in G_0 ($Ki67^{-}Hoechst^{low}$) or cycling in G_1 ($Ki67^{+}Hoechst^{low}$) or S, G_2 and M phases ($Ki67^{+}Hoechst^{high}$). As expected, in the stg healthy mice challenged with IFNα, the HSCs were induced to exit G_0 phase and enter an active cell cycle (Fig. 3.4 A). Interestingly, when the leukemic dtg mice were challenged with IFNα, the LSCs were also induced to exit the G_0 phase and enter an active cell cycle to a comparable extend as the HSCs in the stg mice (Fig. 3.4 A). To assess whether the increase of HSCs in the active cell cycle was accompanied by increased proliferation, we performed a 5-Bromo-2-deoxyuridine (BrdU) incorporation assay. Since BrdU is a thymidine base analog, it becomes incorporated by actively dividing cells upon DNA replication. Mice were treated with BrdU for 14h before analysis of the stem cells by flow cytometry. As expected, the HSCs from stg mice were induced to proliferate when challenged with IFNα (Fig. 3.4 B). Interestingly, upon challenge with IFNα, the LSCs in the dtg mice were induced to proliferate to the same extend as the HSCs in the stg mice (Fig. 3.4 B).

Recently, Bhattacharya et al. suggested that BCR-ABL leads to the degradation of the interferon-α/β receptor (IFNAR) and consequently impairs the response to INFα (Bhattacharya et al., 2011). However the majority of the study was carried out using cell lines. Even though no impairment in the response to INFα was detected in the SCLtTA/BCR-ABL mice, we analyzed the level of IFNAR expressed on LSCs. In line with our previous data, both healthy HSCs as well as LSCs had similar levels of IFNAR both at steady state and after stimulation with INFα (Fig. 3.4 C).

In conclusion, we demonstrated that IFNα induces BCR-ABL-expressing stem cells to exit G_0 phase, enter an active cell cycle and increase proliferation to similar levels as healthy HSCs.

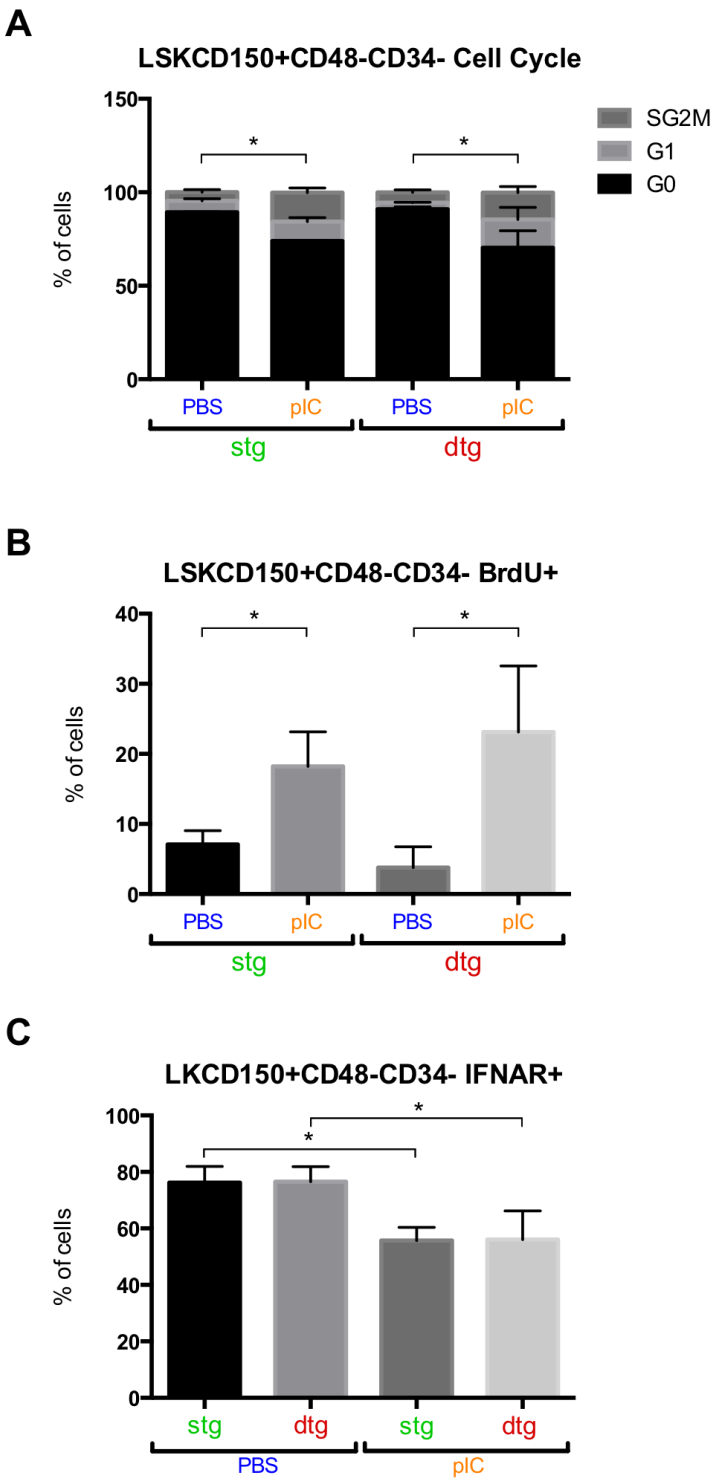

Figure 3.4: Effect of IFNα on the stem cells of SCLtTA/BCR-ABL mice.
The SCLtTA/BCR-ABL double-transgenic (dtg) and control single-transgenic (stg) mice were analyzed 30 weeks after doxycycline removal from the drinking water. Mice were intraperitoneally injected with a single dose of pIC (5mg/kg) or PBS and 20 hours later the stem cells from the bone marrow were isolated, stained, fixed, permeabilized and analyzed by flow cytometry. (A) The cell cycle status of stem cells ($LSKCD150^{+}CD48^{-}CD34^{-}$) was determined by Ki67/Hoechst intracellular staining (G_0: $Ki67^{-}$ $Hoechst^{low}$; G_1: $Ki67^{+}Hoechst^{low}$; SG_2M: $Ki67^{+}Hoechst^{high}$). (B) Mice were treated with BrdU, 14 hours before analysis, followed by quantification of the incorporation levels in the stem cells ($LSKCD150^{+}CD48^{-}CD34^{-}$). (C) The levels of the interferon-α/β receptor (IFNAR) in the surface of stem cells ($LKCD150^{+}CD48^{-}CD34^{-}$) were monitored by making use of a specific IFNAR antibody. Data are presented as mean ± SD with n ≥ 3. The significance was determined using an unpaired, two-tailed student's t-test (* $p < 0.05$).

3.1.2 Generation of mixed bone marrow chimeras

Due to the potential implications of these studies for the treatment of CML patients, we wanted to generate a mouse model that would more closely resemble the patient scenario. Whereas in the SCLtTA/BCR-ABL mice all the stem cells express BCR-ABL, in the patients there is a coexistence of both LSCs and healthy HSCs in the BM. Thus, we generated mixed BM chimeras harboring a mixture of both LSCs from the dtg mice as well as HSCs from WT mice (Fig. 3.5). Therefore, WT lethally irradiated recipients were transplanted with a mixture of 50% SCLtTA/BCR-ABL and 50% WT BM cells. These mice were always analyzed in comparison to control mixed BM chimeras generated from a mixture of 50% stg and 50% WT BM cells. Since the stg cells lack one of the transgenes, they are unable to express BCR-ABL.

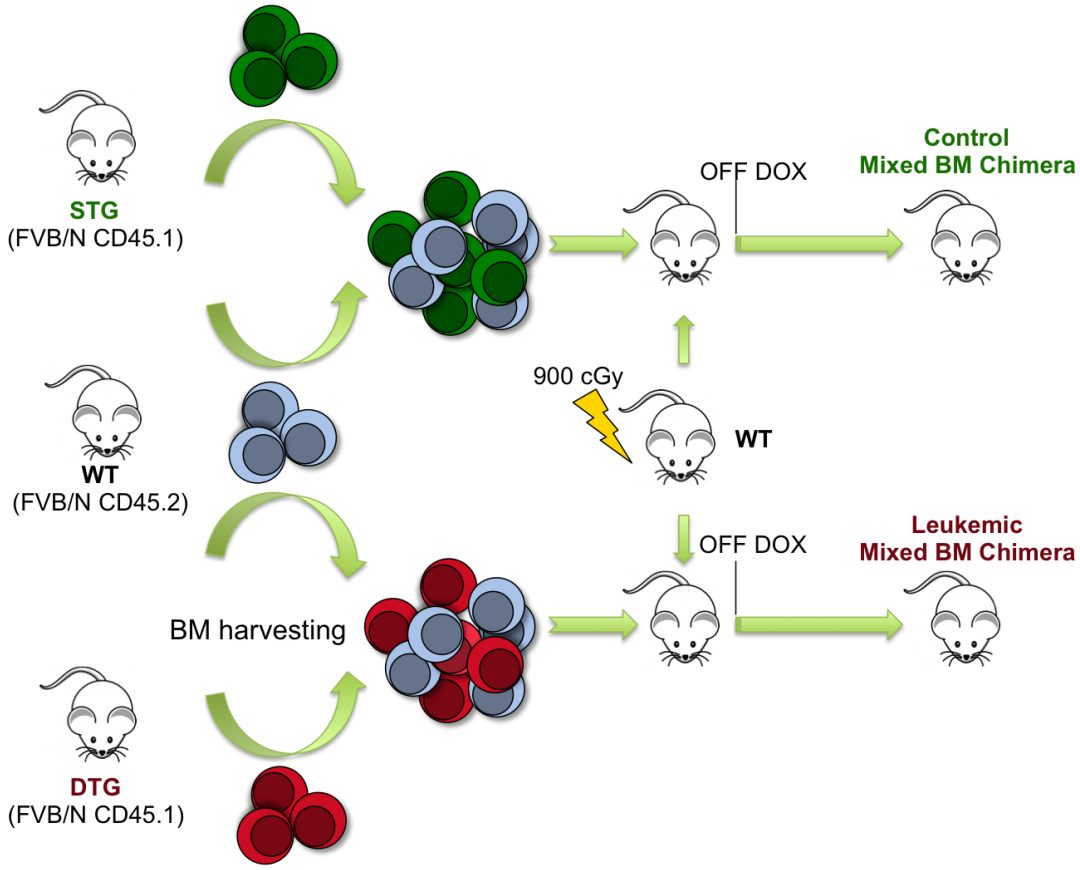

Figure 3.5: Mixed BM chimeras composed of cells derived from SCLtTA/BCR-ABL Tet-OFF mouse model and WT mice.
The mixed bone (BM) marrow chimeras were generated by transplanting a mixture of $5x10^6$ BM cells from both SCL-tTA/BCR-Abl double-transgenic (dtg) and WT mice in a 1:1 ratio into WT lethally irradiated recipients. As control, chimeras containing cells from single-transgenic (stg) mice (unable to express BCR-ABL due to lack of the other transgene) instead of dtg mice were generated.

3.1.2.1 Mixed BM chimeras develop a CML-like disease

In order to monitor the onset of leukemia, the mixed BM chimeras were checked for leukemic symptoms every two weeks following transplantation. Blood samples were taken and analyzed by Hemavet to ascertain the blood cell counts. Furthermore, the blood was stained for a panel of cell populations and analyzed by flow cytometry. In the course of time, the dtg chimeras developed a statistically significant increase in the white blood cell (WBC) counts as compared to the control stg chimeras (Fig. 3.6 A). Into more detail, the monocytes (MO) (Fig. 3.6 B) and neutrophils (NE) (Fig. 3.6 C) counts were specifically increased, whereas no statistically significant difference in the eosinophils (EO) (Fig. 3.6 D) or lymphocytes (LY) counts was observed (Fig. 3.6 E). Moreover, an expansion of both the mature ($CD11b^{+}Gr1^{high}$) (Fig. 3.6 F) and immature ($CD11b^{+}Gr1^{low}$) (Fig. 3.6 G) granulocyte populations could be observed in the dtg chimeras through flow cytometry analysis.

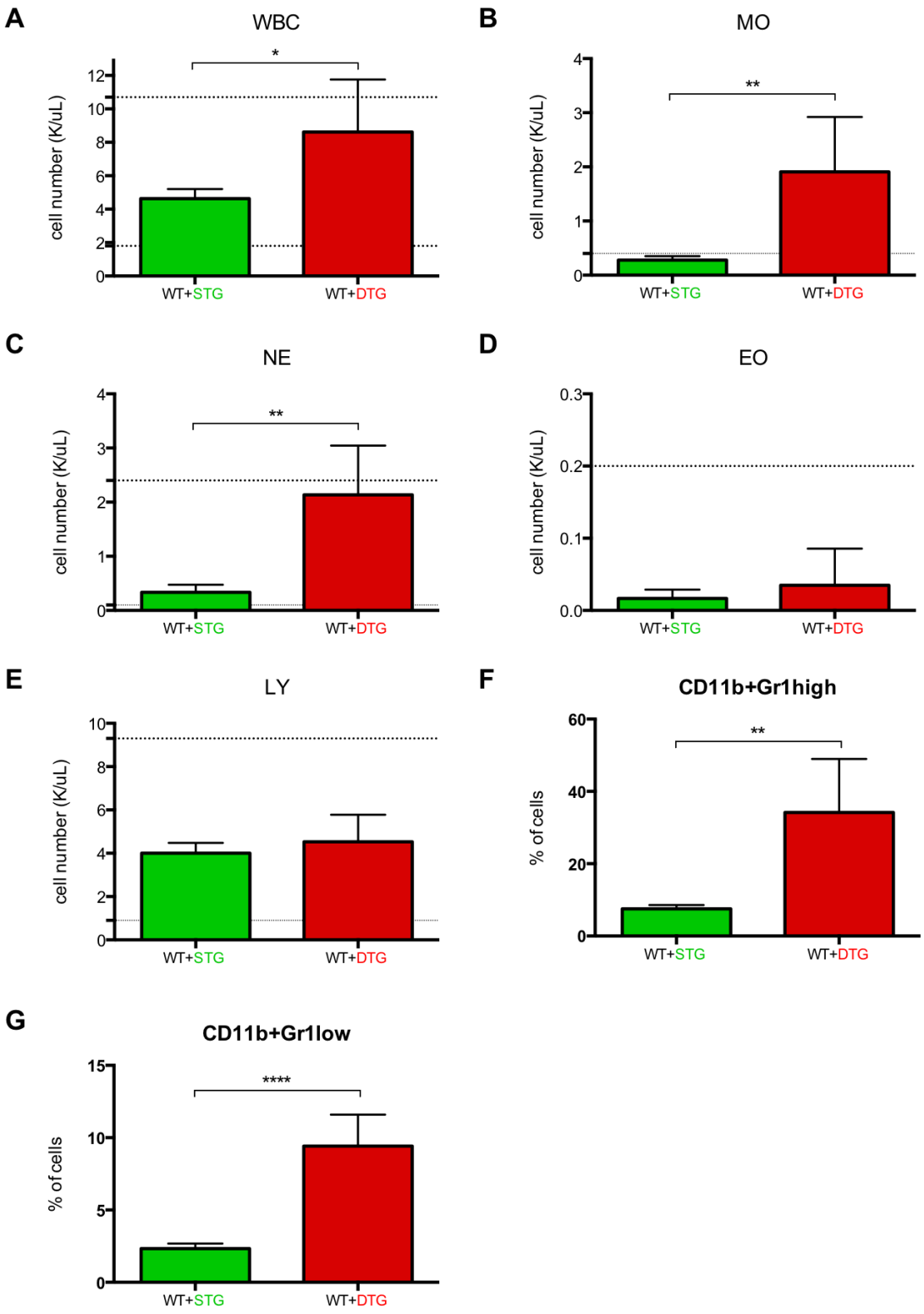

Figure 3.6: Mixed BM chimeras develop increased blood cell counts and an expansion of the granulocyte population.
The SCLtTA/BCR-ABL double-transgenic (dtg) mixed BM chimeras and control single-transgenic (stg) mixed BM chimeras were analyzed 22 weeks after bone marrow transplantation. The number of white blood cells (A), monocytes (B), neutrophils (C), eosinophils (D) and lymphocytes (E) in the blood were monitored by HEMAVET. (F) The blood mature granulocytes ($CD11b^{+}Gr1^{high}$) were examined by flow cytometry. (G) The immature granulocytes ($CD11b^{+}Gr1^{low}$) from the blood were monitored through flow cytometry. The dashed lines delineate the normal range of the blood cell counts. Data are presented as mean ± SD with n ≥ 3. The significance was determined using an unpaired, two-tailed student's t-test (* $p < 0.05$, ** $p < 0.01$, *** $p < 0.001$).

In addition, a decrease in the body weight of the dtg chimeras could be detected whereas the stg chimeras retained regular body weight values (Fig. 3.7 A). Upon further analysis, the dtg chimeras revealed the presence of enlarged spleens, whereas the stg chimeras presented normal spleen size (Fig. 3.7 B). Moreover, the spleens of dtg chimeras showed an increase in the mature (Fig. 3.7 C) and immature granulocyte populations as compared to the control stg chimeras (Fig. 3.7 D). On the other hand, the spleen of the dtg chimeras showed a decrease in the B cell population (Fig. 3.7 E).

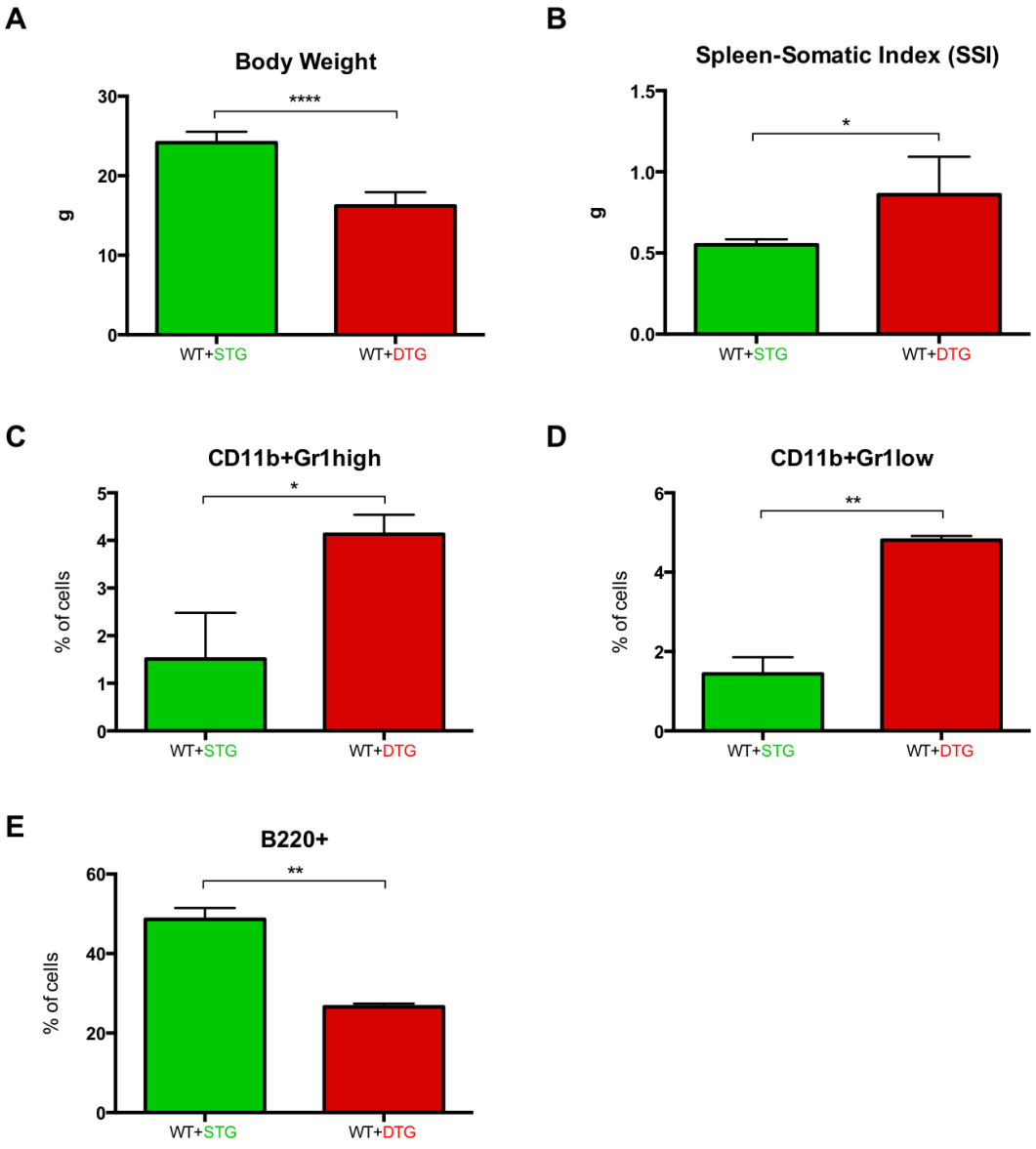

Figure 3.7: Spleen analysis of the mixed BM chimeras.
The SCLtTA/BCR-ABL double-transgenic (dtg) mixed BM chimeras and control single-transgenic (stg) mixed BM chimeras were analyzed 22 weeks after bone marrow transplantation. (A) The mice body weight was monitored. (B) The spleen was isolated and the formula (g spleen mass/g mouse mass)×100 was used to calculate the spleen-somatic index (SSI). (C) The spleen mature granulocytes ($CD11b^{+}Gr1^{high}$) were examined by flow cytometry. (D) The immature granulocytes ($CD11b^{+}Gr1^{low}$) from the spleen were monitored through flow cytometry. (E) The B cells (B220+) from the spleen were analyzed by flow cytometry. Data are presented as mean ± SD with n ≥ 3. The significance was determined using an unpaired, two-tailed student's t-test (* $p < 0.05$, ** $p < 0.01$, *** $p < 0.001$).

When analyzing the mature BM cells, an expansion of the granulocyte population (Fig. 3.8 A) and a decrease in the B cell population (Fig. 3.8 B) were detected in the dtg chimeras as compared to the stg chimeras. Upon examination of the committed progenitor cells, an expansion of the granulocyte-macrophage progenitor (GMP) population (Fig. 3.8 C) and a decrease in the megakaryocyte-erythrocyte progenitor (MEP) population (Fig. 3.8 D) were observed in the dtg chimeras.

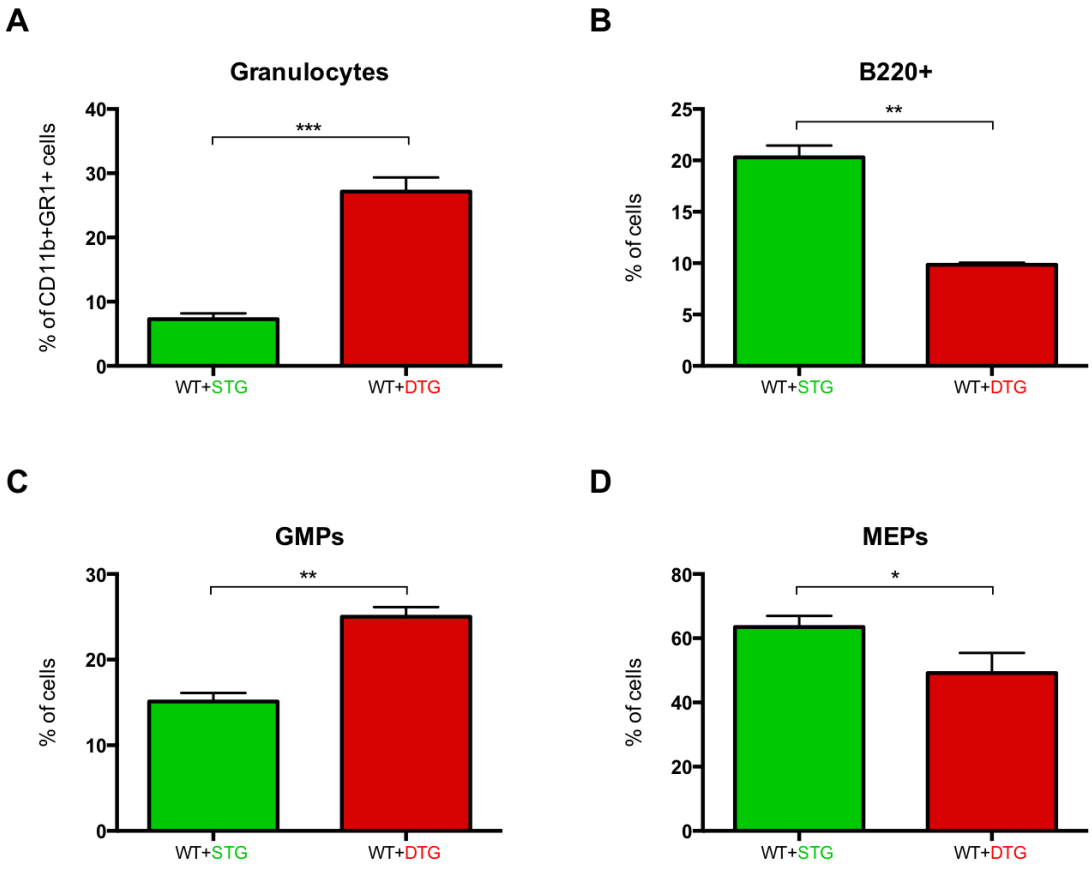

Figure 3.8: Bone marrow analysis of the mixed BM chimeras.
The SCLtTA/BCR-ABL double-transgenic (dtg) mixed bone marrow (BM) chimeras and control single-transgenic (stg) mixed BM chimeras were analyzed 22 weeks after BM transplantation. (A) The BM granulocytes ($CD11b^{+}Gr1^{+}$) were examined by flow cytometry. (B) The B cells ($B220^{+}$) from the BM were monitored through flow cytometry. (C) The granulocyte-macrophage progenitors (GMPs) from the BM (Lin^{-} $CD117^{+}$ $Sca\text{-}1^{-}$ $CD16/32^{high}$ $CD34^{+}$) were analyzed by flow cytometry. (D) The megakaryocyte-erythrocyte progenitors (MEPs) from the BM (Lin^{-} $CD117^{+}$ $Sca\text{-}1^{-}$ $CD16/32^{low}$ $CD34^{-}$) were investigated by flow cytometry. Data are presented as mean ± SD with $n \geq 3$. The significance was determined using an unpaired, two-tailed student's t-test (* $p < 0.05$, ** $p < 0.01$, *** $p < 0.001$).

In summary, the mixed BM chimeras transplanted with a mixture of dtg and WT BM cells develop a chronic myeloproliferative disorder resembling human chronic-phase CML. On the other hand, the control chimeras, which received a mixture of WT and stg cells (instead of the dtg cells), do not develop any of the disease signs.

3.1.3 Activation of quiescent leukemic stem cells by Interferon-alpha

It has been previously demonstrated by our group that IFNα induces quiescent HSCs to enter an active cell cycle in a manner dependent on IFNAR and STAT1 (Essers et al., 2009). However, it has remained unknown whether IFNα could have a similar effect in quiescent LSCs. Thus, we made use of our mixed BM chimera CML model that closely resembles the real patient scenario to investigate the effect of IFNα on LSCs. In order to challenge the chimeras with IFNα, we made use of the synthetic analog of dsRNA, pIC, which leads to the production of IFNα. Both leukemic dtg chimeras and healthy stg chimeras were treated with PBS or pIC for 20h followed by analysis of the BM stem cells. To ascertain the cell cycle status of the stem cells in the BM, the intracellular Ki67/Hoechst staining was performed followed by flow cytometry analysis. Through the combination of Ki67, a marker of active cycling cells, together with the DNA dye Hoechst33342, it is possible to distinguish between quiescent cells in G_0 ($Ki67^-Hoechst^{low}$) and cycling cells in G_1 ($Ki67^+Hoechst^{low}$) or S, G_2 and M phase ($Ki67^+Hoechst^{high}$). As expected, when the control healthy chimeras were challenged with IFNα, the HSCs were induced to exit G_0 phase and enter the active G_1 and $S/G_2/M$ phases of the cell cycle (Fig. 3.9 A). Interestingly, upon IFNα challenge, the LSCs in the leukemic dtg chimeras were also induced to enter an active cell cycle by exiting G_0 and entering the active G_1 and $S/G_2/M$ phases, to a similar extend as the healthy HSCs in the control stg chimeras (Fig. 3.9 A). To further assess the proliferation state of the stem cells we made use of the thymidine analogue BrdU. When cells are actively proliferating, they incorporate BrdU, and the levels of BrdU incorporation can be correlated with the proliferation rate. The chimeras were treated with PBS or pIC for 20h together with BrdU for the last 14h. Indeed, as expected, the stem cells in the control stg chimeras were induced to proliferate and incorporate BrdU upon IFNα challenging (Fig. 3.9 B). Interestingly, in the leukemic dtg chimeras the LSCs were also induced to proliferate when challenged with IFNα and furthermore, the levels of BrdU incorporation were similar to the ones observed in HSCs (Fig. 3.9 B).

Additionally, apart from the alteration in the cell cycle and proliferation status, we were also interested in investigating the direct effect of IFNα on the stem cells in terms of signaling. Thus, after treating control stg chimeras and leukemic dtg chimeras with PBS or pIC for 20 hours, we sorted the stem cells out of the BM and extracted the RNA in order to monitor changes in the expression of the INFα inducible gene ISG15 through qRT-PCR. From this, we could observe a similar

induction of the expression of ISG15 in the LSCs in comparison to healthy HSCs (Fig. 3.9 C).

It was recently suggested that BCR-ABL might lead to the degradation of the interferon-α/β receptor (IFNAR) (Bhattacharya et al., 2011). However the study was mainly conducted in cell lines and thus it required further *in vivo* validation. In order to address this, we quantified the levels of IFNAR in both LSCs from the dtg chimeras and HSCs from the stg chimeras by making use of a specific IFNAR antibody and flow cytometry analysis. In line with our previous results, the levels of IFNAR were similar between the LSCs and HSCs at steady state (Fig. 3.9 D). Additionally, after IFNα stimulation, the IFNAR levels of both HSCs and LSCs decreased to the same extend (Fig 3.9 D).

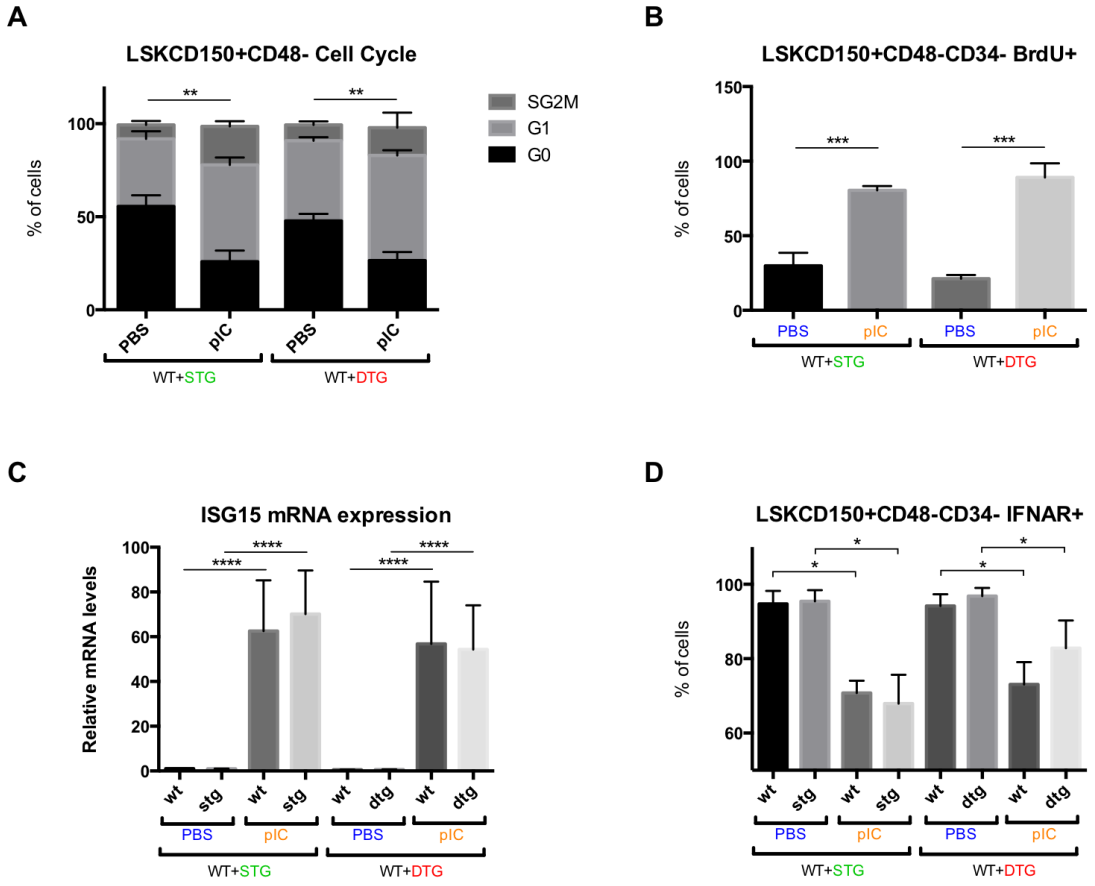

Figure 3.9: IFNα drives LSCs out of quiescence into an active cell cycle.
The SCLtTA/BCR-ABL double-transgenic (dtg) mixed BM chimeras and control single-transgenic (stg) mixed BM chimeras were analyzed 22 weeks after bone marrow transplantation. Mice were injected with a single dose of pIC (5mg/kg) or PBS and 20 hours later the stem cells from the bone marrow were isolated, stained, fixed, permeabilized and analyzed by flow cytometry. (A) The cell cycle status of stem cells ($LSKCD150^+CD48^-CD34^-$) was determined by Ki67/Hoechst intracellular staining (G_0: $Ki67^-$ $Hoechst^{low}$; G_1: $Ki67^+Hoechst^{low}$; SG_2M: $Ki67^+Hoechst^{high}$). (B) Mice were treated with BrdU, 14 hours before analysis, followed by analysis of the incorporation levels in the stem cells ($LSKCD150^+CD48^-CD34^-$). (C) Quantification of the mRNA expression of the IFNα inducible gene ISG15 relative to the house keeping gene Sdha (succinate dehydrogenase complex subunit A) by qRT-PCR in HSCs ($LKCD150^+CD48^-$) sorted from the bone marrow by FACS. (D) The levels of the interferon-α/β receptor (IFNAR) on the surface of stem cells ($LSKCD150^+CD48^-CD34^-$) were monitored with a specific IFNAR antibody by flow cytometry. Data are presented as mean ± SD with n ≥ 3. The significance was determined using an unpaired, two-tailed student's t-test (* $p < 0.05$, ** $p < 0.01$, *** $p < 0.001$).

In conclusion, we demonstrated that upon exposure to IFNα, the LSCs are induced to exit quiescence, enter an active cell cycle and proliferate to a similar extend as healthy HSCs. Accordingly, the levels of IFNAR and the induction of ISG15 were comparable between HSCs and LSCs. This finding paves the way for exploitation of the potential synergistic effect of IFNα and TKI in the treatment of CML.

3.1.4 Retroviral transduction of HSCs

Taking into consideration that the development of leukemia in our mixed BM chimeras was taking a considerable long time, we also set up an alternative CML mouse model with a faster onset of disease. For that purpose, we made use of retroviruses to introduce BCR-ABL into the FACS sorted HSC enriched population Lineage$^-$ Sca-1$^+$ c-Kit$^+$, followed by transplantation into WT lethally irradiated recipients (Fig. 3.10). Since the BCR-ABL open reading frame is attached to a GFP gene by an internal ribosome entry site, we were able to easily follow the leukemic cells through GFP detection.

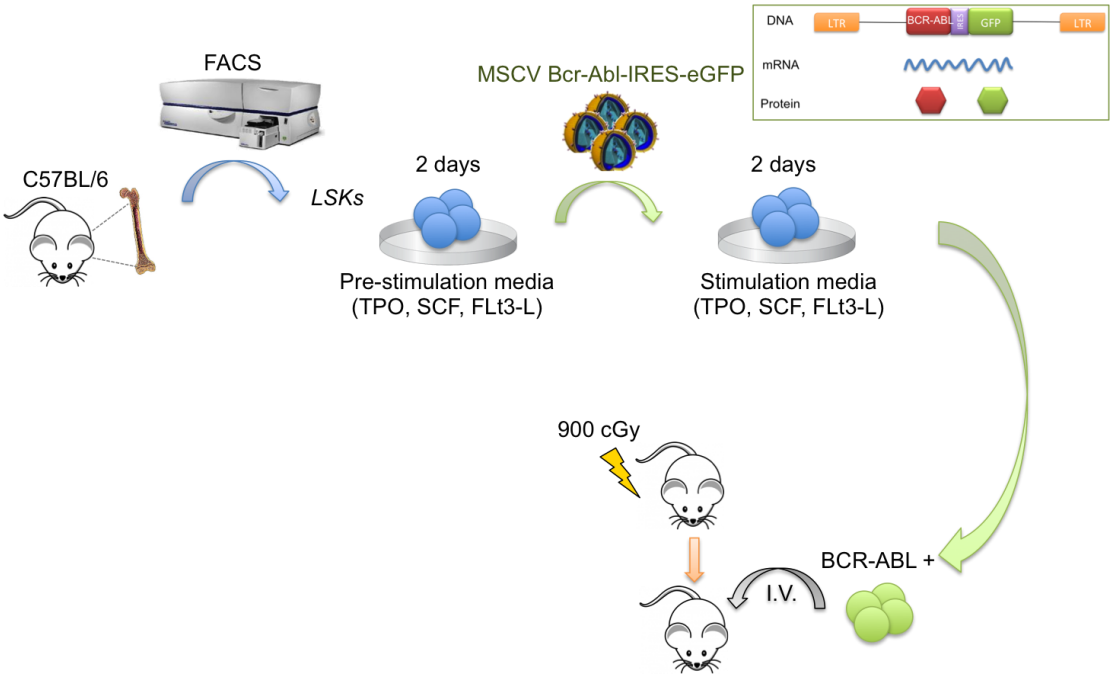

Figure 3.10: Transplantation of BCR-ABL transduced LSKs.
The HSC enriched population LSK (Lineage$^-$ Sca-1$^+$ c-Kit$^+$) from C57BL/6 mice were sorted out of the bone marrow by FACS and cultured for 2 days in HSC media supplemented with TPO, SCF and FLt3-L, followed by retroviral transduction with BCR-ABL by making use of the MSCV BCR-ABL-IRES-eGFP vector. As control, cells were transduced with the empty-vector (without BCR-ABL). Two days after transduction, the BCR-ABL+/GFP+ or control empty-vector/GFP+ cells were sorted by FACS and transplanted intravenously into C57BL/6 WT lethally irradiated recipients.

3.1.4.1 Transduced stem cells lead to the development of a CML-like disease

The mice transplanted with BCR-ABL+/GFP+ transduced HSCs were always compared to mice transplanted with control empty-vector GFP+ transduced HSCs. Every week following bone marrow transplantation (BMT), the blood cell counts were monitored through Hemavet and the distribution of the leukemic GFP+ cells as well as the mature blood cell populations were analyzed by flow cytometry. Already at 3 weeks after BMT, the BCR-ABL mice presented white blood cell (WBC) counts above the healthy threshold whereas the control empty-vector mice had normal counts (Fig. 3.11 A). Elevated counts of monocytes (MO) (Fig. 3.11 B) and neutrophils (NE) (Fig. 3.11 C) above the healthy threshold were also detected in the BCR-ABL mice but not in the control empty-vector mice. Furthermore, a statistically significant increase in the granulocytes was observed in the BCR-ABL mice as compared to the control empty-vector mice through flow cytometry analysis (Fig. 3.11 D).

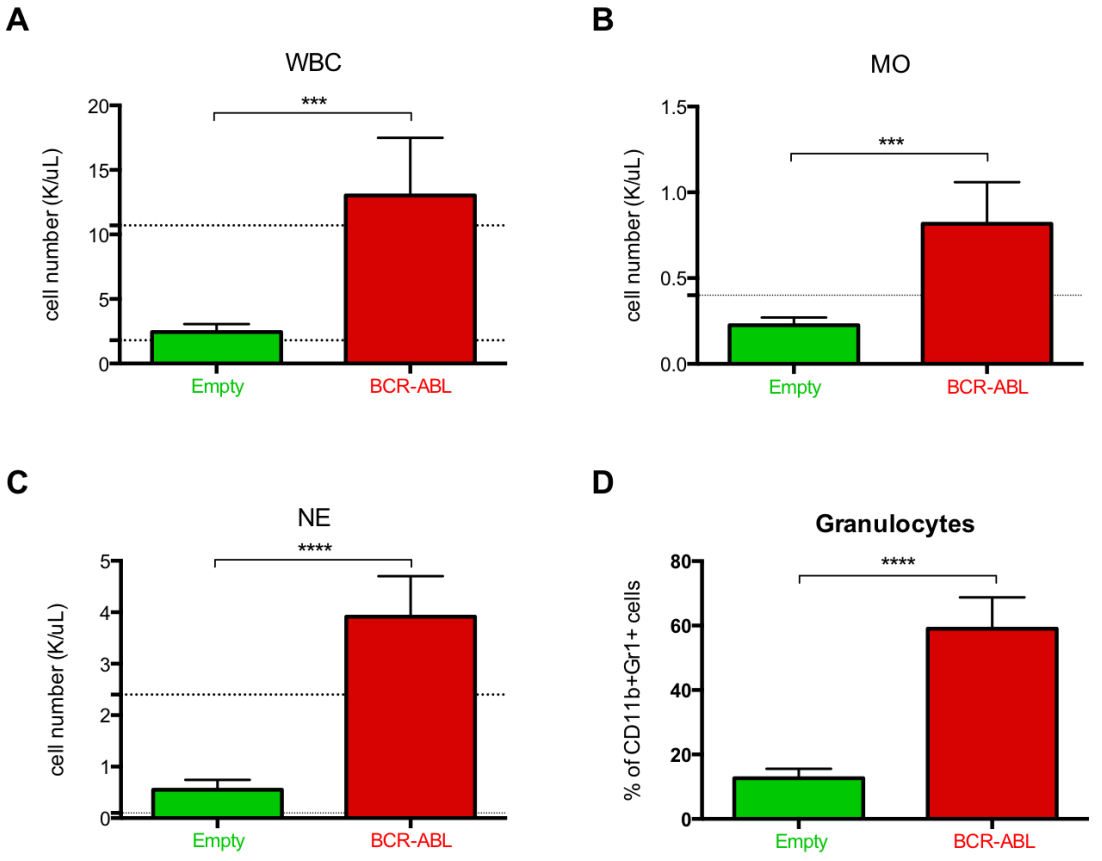

Figure 3.11: The blood of BCR-ABL mice presents increased cell counts and an expansion of the granulocyte population
The BCR-ABL mice and control empty-vector mice were analyzed 3 weeks after bone marrow transplantation. The number of white blood cells (A), monocytes (B) and neutrophils (C) in the blood were monitored by HEMAVET. (D) The blood cells were stained and the granulocyte population ($CD11b^{+}Gr1^{+}$) was investigated by flow cytometry. The dashed lines delineate the normal range of the blood cell counts. Data are presented as mean ± SD with n ≥ 3. The significance was determined using an unpaired, two-tailed student's t-test (* $p < 0.05$, ** $p < 0.01$, *** $p < 0.001$).

Additionally, the BCR-ABL mice presented with marked splenomegaly, while the control empty-vector mice maintained a normal spleen size (Fig. 3.12 A+B).

The survival of the BCR-ABL mice was markedly affected and by the 6th week after BMT all mice were dead whereas the control empty-vector mice remained alive during the complete course of the survival analysis (Fig. 3.12 C).

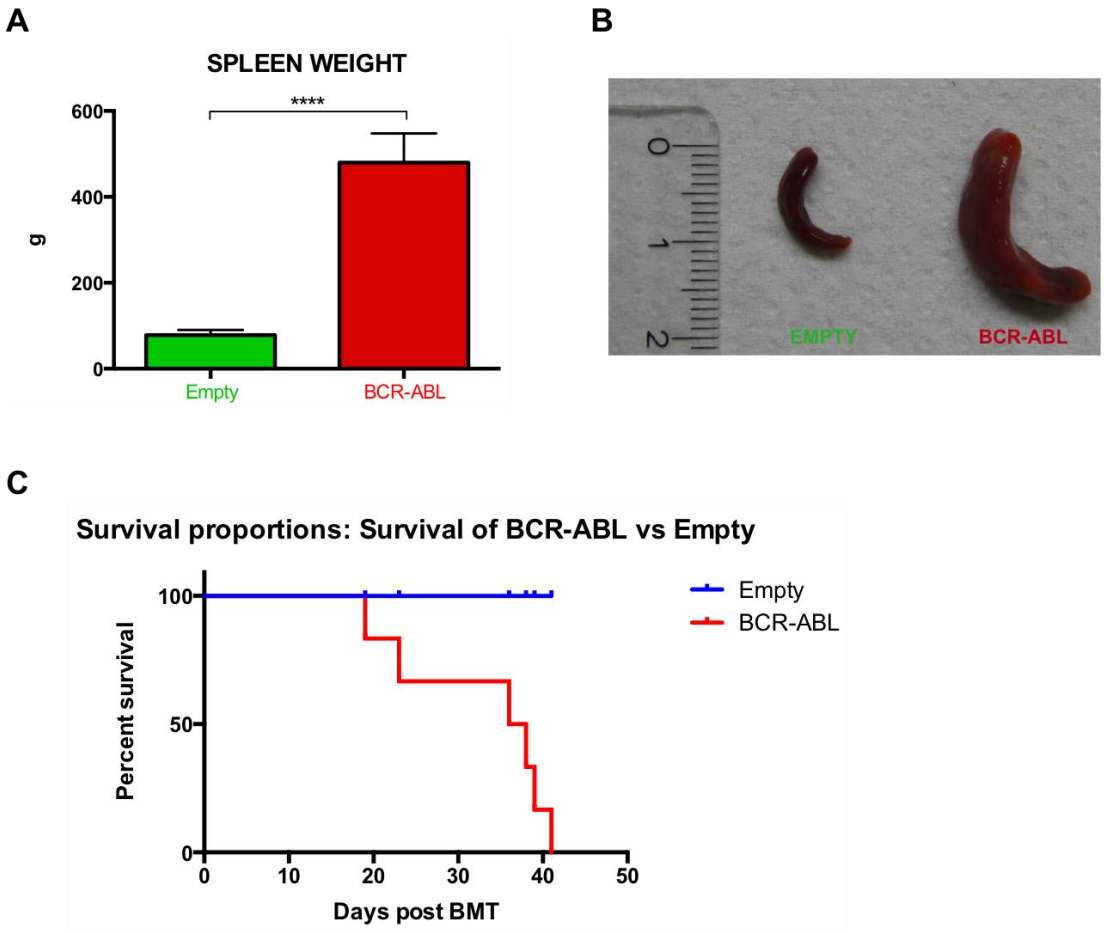

Figure 3.12: BCR-ABL mice develop splenomegaly and have an impaired survival.
(A) The spleen of BCR-ABL and control empty-vector mice was isolated 3 weeks after bone marrow transplantation and analyzed. (B) Representative picture of the macroscopic appearance of the spleen of BCR-ABL and control empty-vector mice. (C) Survival curve of the BCR-ABL and control empty-vector following bone marrow transplantation (BMT) with $6x10^4$ cells. Data are presented as mean ± SD with n ≥ 3. The significance was determined using an unpaired, two-tailed student's t-test (* $p < 0.05$, ** $p < 0.01$, *** $p < 0.001$).

In conclusion, the mice transplanted with BCR-ABL transduced HSCs develop a myeloproliferative disease that resembled human CML. In contrast, none of the recipients of control empty-vector transduced HSCs develop any signs of the disease.

3.1.5 Combinatorial treatment: IFNα + Imatinib

Since we could show that treatment with IFNα activates quiescent LSCs into an active cell cycle, we now wanted to test whether a combined treatment strategy with

TKI would be beneficial to eliminate not only the bulk of the tumor but also the LSCs. Through IFNα treatment the LSCs would first be activated, followed by TKI targeted therapy. Assuming that activated LSCs become susceptible to TKI treatment, this two-step treatment protocol would not only get rid of the leukemic clone but also of the LSCs, preventing relapse of the disease.

Interestingly, through a mathematical modeling approach, the persistence of CML leukemic cells following TKI treatment could be explained by a selective effect of the TKI exclusively in proliferative leukemic cells (Roeder et al., 2006). Furthermore, in the same study, the mathemetical model suggests that the combination of a cell cycle stimulating drug together with TKI would lead to the complete eradication of the CML cells. One of the crucial aspects of this combinatorial treatment approach is to determine the appropriate time points between each step. Recently, Glauche et al. have used a mathematical model to predict the potential effect of combining INFα with TKI administration (Glauche et al., 2012). Interestingly, the predicted more favourable combination would consist of a pulsed INFα treatment together with continuous TKI administration.

Using our CML mouse model in which BCR-ABL expression is targeted to the HSC population, we tested different combined treatment schemes running over a maximum span of 9 days by using Imatinib as a TKI and pIC as a way to challenge the mice with INFα. In the optimized protocol, mice were first challenged with INFα at day 1 followed by daily Imatinib administration for 9 days except on day 5 when the mice were re-challenged with INFα to ensure that LSCs that remained or returned to quiescence could be activated (Fig. 3.13 A).

In our studies, mice under combined treatment were compared to mice under imatinib-only treatment, pIC-only treatment and PBS treatment. Since the BCR-ABL leukemic cells expressed GFP, their presence could be measured through flow cytometry. In the PBS treatment group the leukemic clone expanded whereas in the pIC-only group there were no significant changes and in the imatinib-only group there was a slight decrease of the leukemic burden (Fig. 3.13 B). Interestingly, the combined treatment group had a deeper reduction in the leukemic burden as compared to any of the other groups (Fig. 3.13 B).

As shown before, the CML mice markedly develop splenomegaly. Although both the imatinib-only and the combined-treatment groups led to a decrease in splenomegaly as compared to the untreated group, the combined treatment led to a significant deeper reduction (Fig. 3.13 C). Furthermore, preliminary studies indicate a survival advantage conferred by the combined treatment (Fig. 3.13 D).

In conclusion, this combined-treatment protocol led to a deeper reduction of the

leukemic burden as compared to the PBS treated, pIC-only treated or imatinib-only treated CML mice. Additionally, the splenomegaly was markedly abrogated by the combined treatment to significant reduced levels than any of the other groups. Moreover, our data suggests that the combined treatment induces prolonged survival.

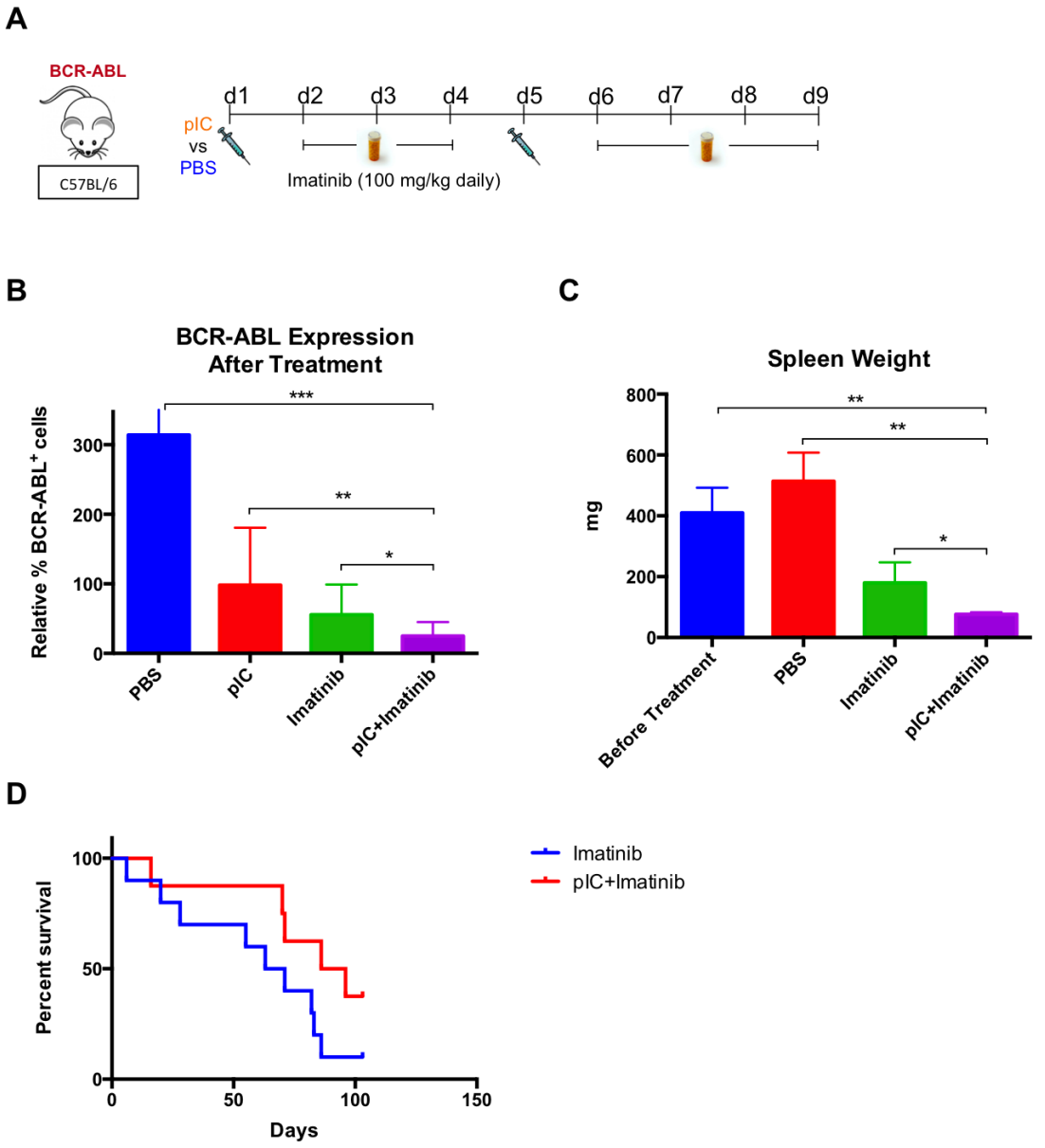

Figure 3.13: Combined treatment leads to a deeper reduction of the leukemic burden and restores spleen regular size.
(A) The BCR-ABL mice were daily treated with Imatinib (100mg/kg) for 9 days except on the 1st and 5th day when they were challenged with INFα through pIC injection. Apart from the combined treatment group, BCR-ABL mice were also treated with pIC-only, imatinib-only or left untreated. Following one day after finishing treatment, the mice were analyzed. (B) The levels of leukemic BCR-ABL+/GFP+ cells were monitored through flow cytometry and normalized to the the values before treatment initiation. (C) The spleen of mice was isolated and analyzed. (D) Survival curve of the BCR-ABL mice following treatment. Data are presented as mean ± SD with n ≥ 3. The significance was determined using an unpaired, two-tailed student's t-test (* $p < 0.05$, ** $p < 0.01$, *** $p < 0.001$).

3.1.6 Effect of the treatment in the T cell compartment

In order to investigate if the combined treatment was inducing an expansion of the T cell pool, which could also contribute to its beneficial effect, the blood of the leukemic BCR-ABL mice was analyzed one day after treatment through flow cytometry. No significant changes were detected in the total T cell population ($CD4/8^+$) between the PBS, pIC-only, imatinib-only or combined treatment groups (Fig. 3.14 B). We then specifically monitored the cytotoxic T cell compartment ($CD8^+$) and also no significant changes were detected when comparing the PBS, pIC-only, imatinib-only or combined treated mice (Fig. 3.14 C).

Overall, neither pIC-only, imatinib-only nor combined treatment led to a significant change in the distribution of the $CD4^+$ or $CD8^+$ T cell populations immediately after the treatment window.

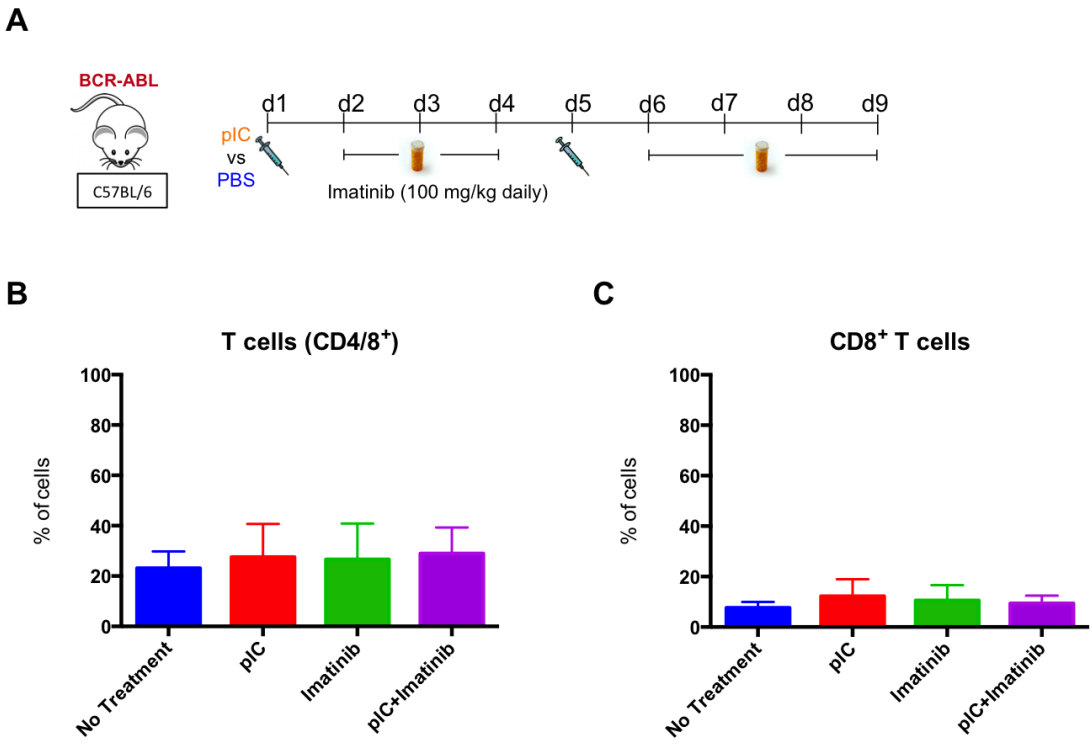

Figure 3.14: Analysis of the T cell pool of BCR-ABL mice following treatment
(A) The BCR-ABL mice were daily treated with Imatinib (100mg/kg) for 9 days except on the 1st and 5th day when they were challenged with INFα through pIC injection. Apart from the combined treatment group, BCR-ABL mice were also treated with pIC-only, imatinib-only or left untreated. Following one day after treatment, the mice were analyzed. (B) The blood cells were stained and the total T cell population ($CD4/8^+$) was investigated by flow cytometry. (C) The cytotoxic T cell population ($CD8^+$) in the blood was examined through flow cytometry. Data are presented as mean ± SD with n ≥ 3. The significance was determined using an unpaired, two-tailed student's t-test (* $p < 0.05$, ** $p < 0.01$, *** $p < 0.001$).

3.2 Influence of leukemic cells on the behavior of wild-type cells in mixed bone marrow chimeras

In our mixed BM chimera model, both a leukemic and healthy population of hematopoietic cells coexist inside the same organism, resembling the patient scenario. Furthermore, since the transgenic and wt cells have a different cell surface marker, namely CD45.1 and CD45.2 respectively, they can be easily distinguished through flow cytometry. Therefore we made use of this CML model to investigate interactions between leukemic and healthy cells.

Interestingly, we unexpectedly observed that the wt cells that coexist with the leukemic dtg cells behave differently to the wt cells from healthy chimeras.

3.2.1 The differences between the bone marrow dtg and stg mature cells are mimicked by the wt cells in the mixed BM chimeras

As previously described, when analyzing the total BM mature cell populations of the mixed BM chimeras, an expansion of the granulocyte population in the leukemic chimeras as compared to the healthy control chimeras was detected (Fig 3.15 A). However, since the transgenic and wt cells can be distinguished through the CD45 cell surface marker, instead of analyzing the bulk of cells, the analysis can be exclusively focused on either the transgenic or wt cells. As expected, when directly comparing the dtg cells inside the leukemic chimeras versus the stg cells inside the healthy chimeras, the expected increase in granulocytes could be detected (Fig. 3.15 A). Surprisingly, when exclusively comparing the wt cells inside the leukemic chimeras versus the wt cells inside the healthy chimeras, also an increase in the granulocyte population could be observed (Fig 3.15 A).

Furthermore, the decrease in the B cell population detected in the BM of the leukemic chimeras could be observed not only the dtg leukemic cells but also in the wt cells (Fig. 3.15 B).

In conclusion, the increase in the granulocytes and decrease in the B cells detected in the BM of leukemic chimeras was observed not only in the dtg cells but also mimicked in the wt cells.

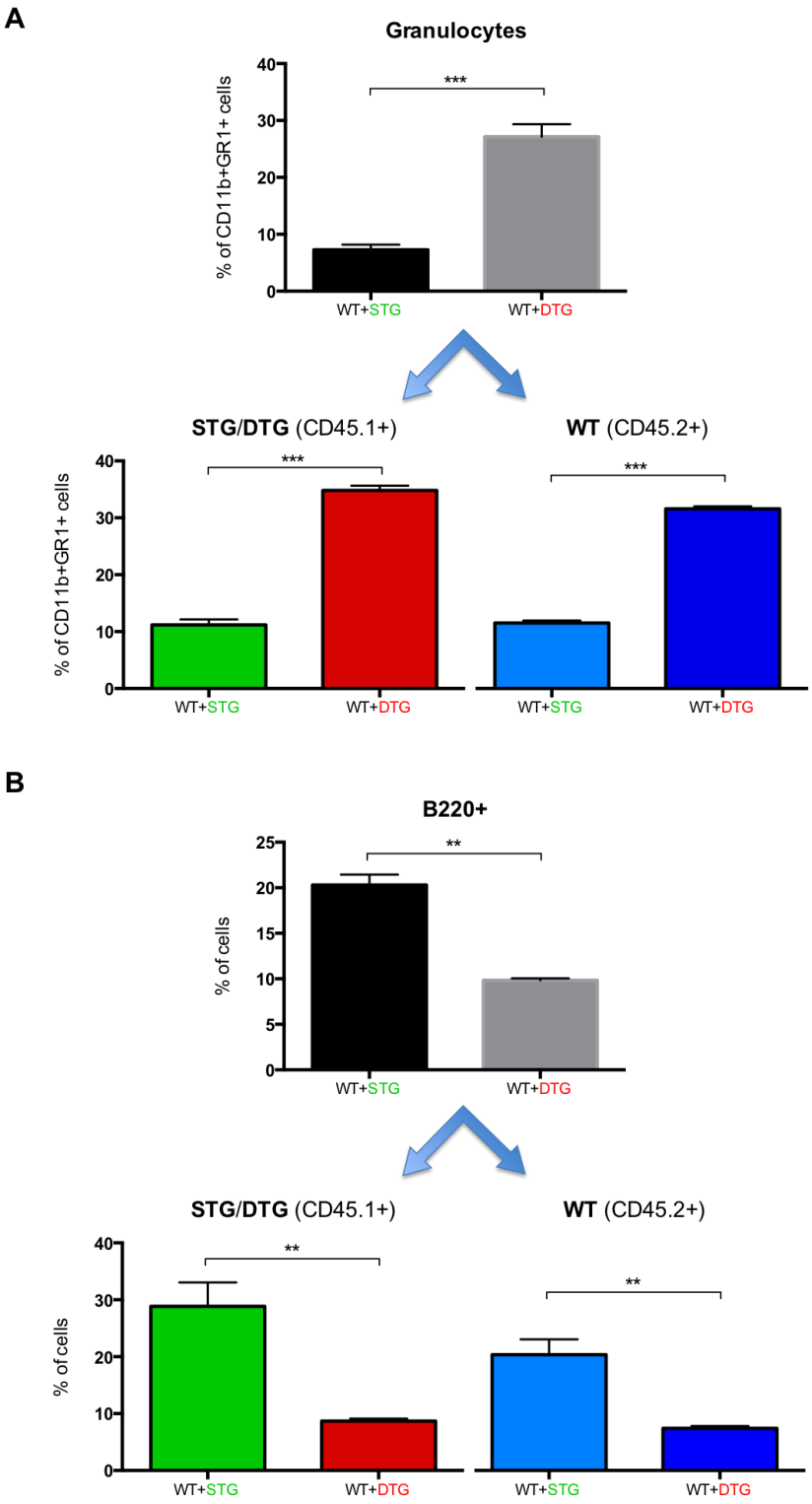

Figure 3.15: The changes in the bone marrow mature cell populations in the leukemic chimeras are detected in both dtg and WT cells.
The SCLtTA/BCR-ABL double-transgenic (dtg) mixed BM chimeras and control single-transgenic (stg) mixed BM chimeras were analyzed 22 weeks after bone marrow transplantation. By making use of the cell surface CD45 marker, the transgenic ($CD45.1^+$) and WT ($CD45.2^+$) cells within the same mouse can be distinguished through flow cytometry. Therefore, apart from the total population, the transgenic or WT cells exclusively can be directly compared between the leukemic dtg and control stg mixed BM chimeras. (A) The bone marrow granulocytes ($CD11b^+Gr1^+$) were examined by flow cytometry. (B) The B cells ($B220^+$) from the bone marrow were monitored through flow cytometry. Data are presented as mean ± SD with n ≥ 3. The significance was determined using an unpaired, two-tailed student's t-test (* $p < 0.05$, ** $p < 0.01$, *** $p < 0.001$).

3.2.2 Changes in the committed progenitor cell populations inside leukemic chimeras detected in both dtg and wt cells

The increase in GMPs detected in the BM of leukemic chimeras was investigated again but with an exclusive focus on either $CD45.1^+$ transgenic or $CD45.2^+$ wt cells. First, as expected, the increase in GMPs was observed when comparing the dtg cells from the leukemic chimeras with the stg cells from the control healthy chimeras (Fig. 3.16 A). Surprisingly, the same increase in GMPs was detected in the wt cells inside the leukemic chimeras as compared to the wt cells inside the control healthy chimeras (Fig. 3.16 A).

Moreover, the decrease in MEPs identified in the BM of leukemic chimeras was assessed purely in transgenic or wt cells. Interestingly, not only the dtg but also the wt cells from the leukemic chimeras showed the decrease in MEPs (Fig. 3.16 B).

Taken together, the changes in the distribution of the committed progenitor cell populations inside the leukemic chimeras are detected not only in the dtg cells but also mimicked in the wt cells.

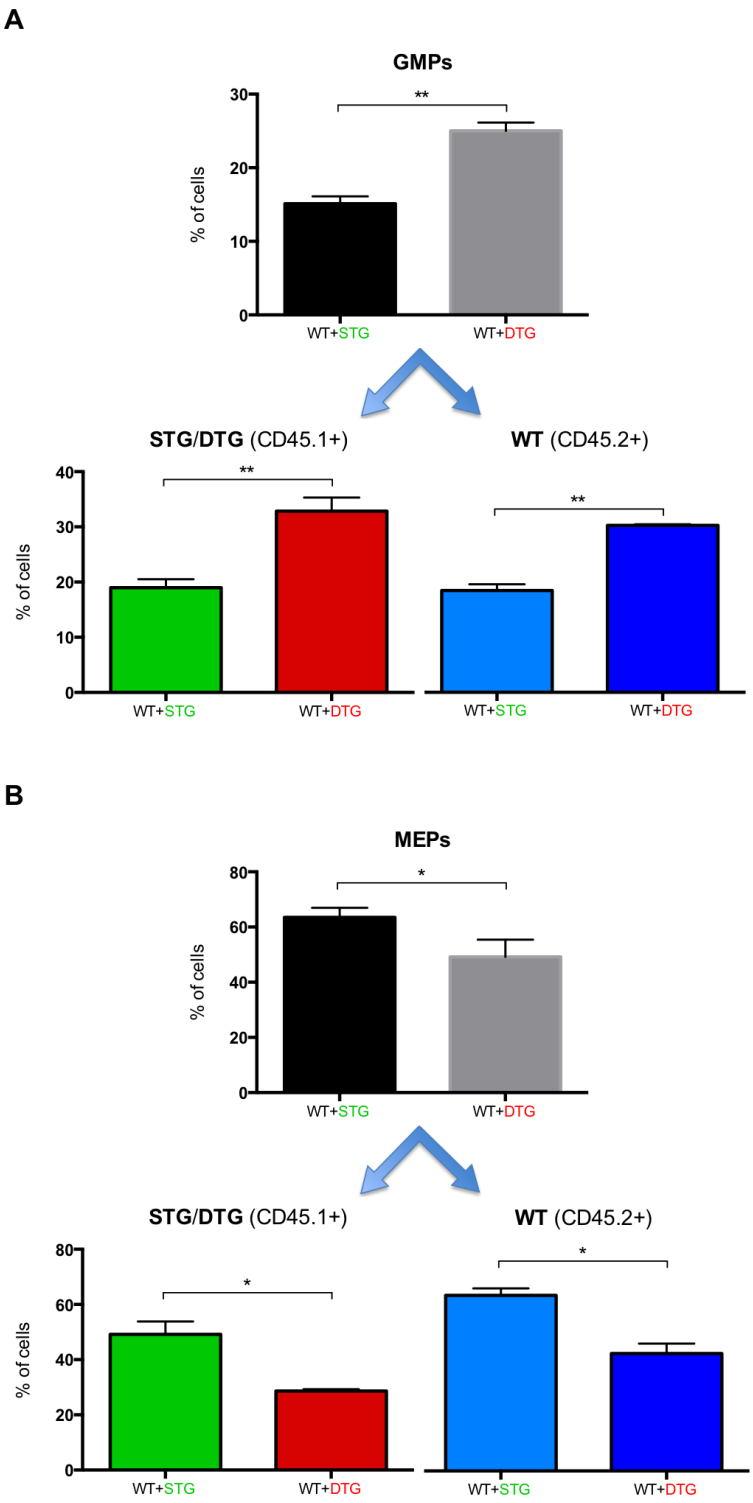

Figure 3.16: The differences between the bone marrow dtg and stg committed progenitor cells are mimicked by the WT cells in the mixed BM chimeras.
The SCLtTA/BCR-ABL double-transgenic (dtg) mixed BM chimeras and control single-transgenic (stg) mixed BM chimeras were analyzed 22 weeks after bone marrow transplantation. By making use of the cell surface CD45 marker, the transgenic ($CD45.1^+$) and WT ($CD45.2^+$) cells within the same mouse can be distinguished through flow cytometry. Therefore, apart from the total population, the transgenic or WT cells exclusively can be directly compared between the leukemic dtg and control stg mixed BM chimeras. (A) The granulocyte-macrophage progenitors (GMPs) from the bone marrow (Lin^- $CD117^+$ $Sca\text{-}1^-$ $CD16/32^{high}$ $CD34^+$) were analyzed by flow cytometry. (B) The megakaryocyte-erythrocyte progenitors (MEPs) from the bone marrow (Lin^- $CD117^+$ $Sca\text{-}1^-$ $CD16/32^{low}$ $CD34^-$) were investigated by flow cytometry. Data are presented as mean ± SD with n ≥ 3. The significance was determined using an unpaired, two-tailed student's t-test (* $p < 0.05$, ** $p < 0.01$).

3.2.3 The differences between the spleen dtg and stg mature cells are mimicked by the wt cells in the mixed BM chimeras

The expansion in the mature and immature granulocyte populations detected in the spleen of the leukemic chimeras was re-examined in either the purified CD45.1$^+$ transgenic or CD45.2$^+$ wt cell populations. When performing a CD45.1$^+$ exclusive comparison between the leukemic and control healthy chimeras, an increase in both mature and immature granulocytes was detected in the dtg versus stg cells (Fig 3.17 A+B). Interestingly, in a CD45.2$^+$ purified analysis, an increase in the mature and immature granulocytes was unveiled in the wt cells inside the leukemic chimeras as compared to the wt cells inside the control healthy chimeras (Fig 3.17 A+B). Additionally, when reassessing the decrease in the B cell compartment in the spleen of leukemic chimeras, not only was it confirmed when comparing the dtg to the stg cells but also in the wt cells in the leukemic chimeras versus the wt cells in the control healthy chimeras (Fig 3.17 C).

In summary, the changes in the mature cell populations observed in the spleen of the leukemic chimeras are not only detected in the dtg cells but also mimicked in the wt cells.

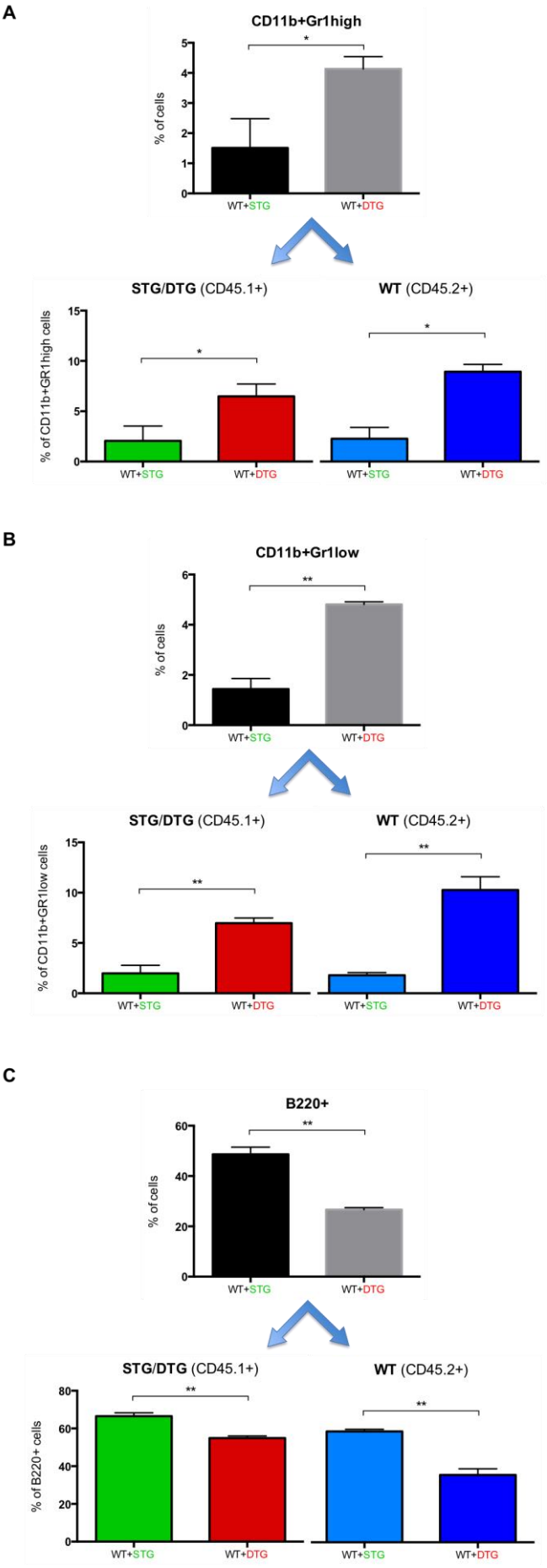
A
CD11b+Gr1high
% of cells
WT+STG
WT+DTG
STG/DTG (CD45.1+)
WT (CD45.2+)
% of CD11b+GR1high cells
B
CD11b+Gr1low
% of CD11b+GR1low cells
C
B220+
% of B220+ cells

Figure 3.17: The changes in the spleen mature cell populations in the leukemic chimeras are detected in both dtg and WT cells
The spleen of the SCLtTA/BCR-ABL double-transgenic (dtg) mixed BM chimeras and control single-transgenic (stg) mixed BM chimeras were analyzed 22 weeks after bone marrow transplantation. By making use of the cell surface CD45 marker, the transgenic ($CD45.1^+$) and WT ($CD45.2^+$) cells within the same mouse can be distinguished through flow cytometry. Therefore, apart from the total population, the transgenic or WT cells exclusively can be directly compared between the leukemic dtg and control stg mixed BM chimeras. (A) The spleen mature granulocytes ($CD11b^+Gr1^{high}$) were examined by flow cytometry. (B) The immature granulocytes ($CD11b^+Gr1^{low}$) from the spleen were monitored through flow cytometry. (C) The B cells ($B220^+$) from the spleen were analyzed by flow cytometry. Data are presented as mean ± SD with n ≥ 3. The significance was determined using an unpaired, two-tailed student's t-test (* $p < 0.05$, ** $p < 0.01$).

3.2.4 Cytokine expression profile of mixed BM chimeras

We hypothesized that the leukemic cells could affect the behavior of the wt cells through the production of secreted factors. In turn, these secreted factors could have a direct effect on the wt cells or induce the niche to produce other factors that would then affect both leukemic and wt cells. In order to detect these potential agents we performed a cytokine array on the BM supernatant of both the leukemic and healthy control chimeras (Fig. 3.18 A). Several clear differences between the leukemic versus healthy chimeras were observed, more precisely, a highly significant increase in the presence of IL-1α, IL-1β, IL-6, MIP-1α and MIP-1β and a marked decrease in CXCL9 (Fig. 3.18 B).

Subsequently, in order to validate the array results, ELISAs were performed on the BM supernatant of the mixed BM chimeras, which confirmed the increase in IL-1β, IL-6, MIP-1α and MIP-1β in the BM of the leukemic chimeras (Fig. 3.19 A-D).

Importantly, several of the obtained hits were also reported by other groups to be present in the BM of CML mouse models (Zhang et al., 2012), which further validates the quality of our array and mouse model. For some of these hits, like IL-6 (Reynaud et al., 2011), the functional importance and the molecular and cellular mechanisms through which they promote CML were already described but for the others it still remains unclear.

A

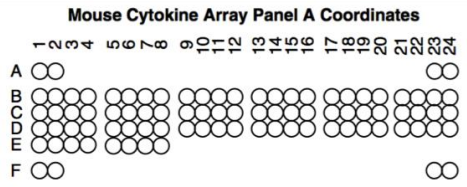

CXCL13/BLC/BCA-1	IL-5	M-CSF
C5a	IL-6	CCL2/JE/MCP-1
G-CSF	IL-7	CCL12/MCP-5
GM-CSF	IL-10	CXCL9/MIG
CCL1/I-309	IL-12 p70	CCL3/MIP-1 alpha
CCL11/Eotaxin	IL-13	CCL4/MIP-1 beta
ICAM-1	IL-16	CXCL2/MIP-2
IFN-gamma	IL-17	CCL5/RANTES
IL-1 alpha	IL-23	CXCL12/SDF-1
IL-1 beta	IL-27	CCL17/TARC
IL-1ra	CXCL10/IP-10	TIMP-1
IL-2	CXCL11/I-TAC	TNF-alpha
IL-3	CXCL1/KC	TREM-1
IL-4		

B

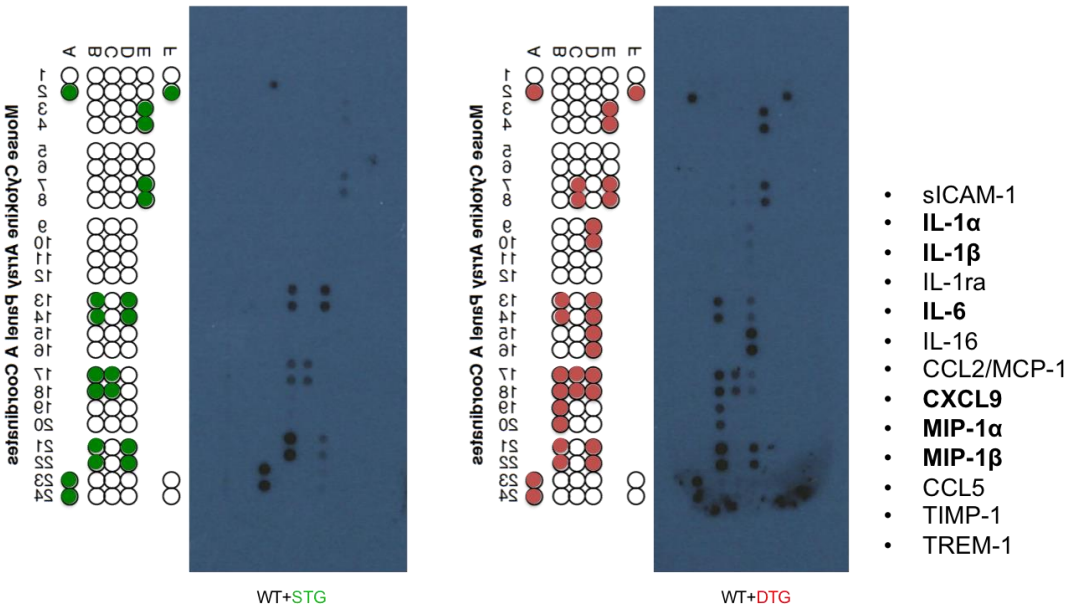

Figure 3.18: Cytokine array of the bone marrow supernatant of mixed BM chimeras.
The bone marrow supernatant of the SCLtTA/BCR-ABL double-transgenic (dtg) mixed BM chimeras and control single-transgenic (stg) mixed BM chimeras was analyzed 22 weeks after BM transplantation. (A) List of the cytokines examined in the bone marrow supernatant of the mixed BM chimeras by making use of the R&D Systems Mouse Cytokine Array, Panel A. (B) Cytokines detected in the bone marrow supernatant of the mixed BM chimeras and summary of the most prominently differentially expressed cytokines between dtg and stg chimeras.

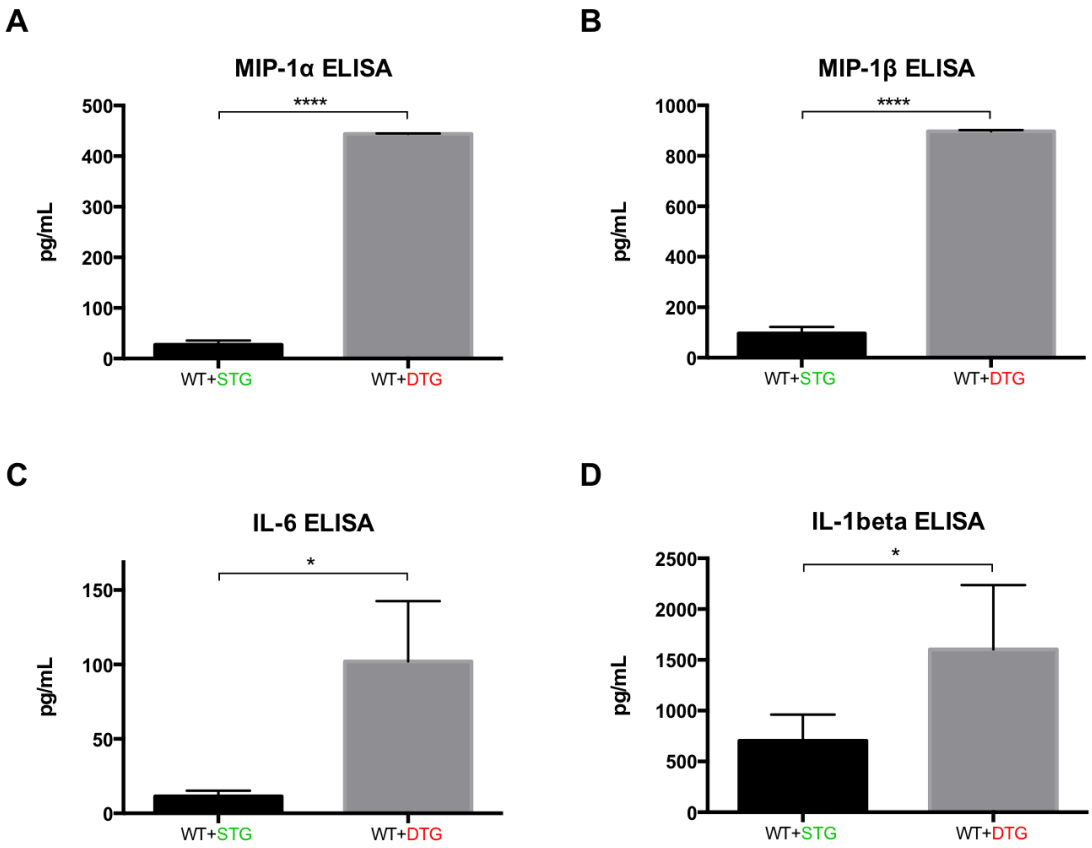

Figure 3.19: The bone marrow of SCLtTA/BCR-ABL dtg chimeras is enriched in MIP-1α, MIP-1β, IL-6 and IL-1β as compared to the control stg chimeras.
The bone marrow supernatant of the SCLtTA/BCR-ABL double-transgenic (dtg) mixed BM chimeras and control single-transgenic (stg) mixed BM chimeras was analyzed 22 weeks after bone marrow transplantation. (A) The concentration of MIP-1α in the bone marrow supernatant was determined by ELISA assay. (B) MIP-1β protein concentration was determined by ELISA of the bone marrow supernatant. (C) IL-6 protein concentration was determined by ELISA on the bone marrow supernatant. (D) IL-1β levels (ELISA) in the bone marrow supernatant. Data are presented as mean ± SD with n ≥ 3. The significance was determined using an unpaired, two-tailed student's t-test (* $p < 0.05$, ** $p < 0.01$, *** $p < 0.001$).

3.2.5 Effect of MIP-1α and MIP-1β in the cell cycle behavior of HSCs

It has been suggested that MIP-1 inhibits HSC proliferation and maintenance of these cells in a quiescent state (Dunlop et al., 1992). Although in these studies the HSC challenging was performed *in vivo* by injecting mice with MIP-1, their read-out consisted of CFUs *in vitro*. Therefore the population being addressed was actually mainly consisting of progenitors and not specifically the HSCs. To gain further insights, we challenged mice with PBS, MIP-1α (also known as CCL3) or MIP-1β (CCL4) for 20h and specifically analyzed the HSC population in the BM through flow cytometry. In order to assess the cell cycle status of the HSCs, we performed intracellular Ki67/Hoechst staining to determine the percentage of cells in G_0, G_1 and S, G_2 or M phases. The HSCs challenged with either MIP-1α or MIP-1β showed no significant differences in the cell cycle distribution as compared to the PBS control

group (Fig. 3.20 A). To analyze the proliferation levels of the treated HSCs we used an *in vivo* BrdU incorporation assay. For this, mice were treated with the base analog BrdU for 14h before the analysis of the incorporation rate in HSCs through flow cytometry. No significant differences in the incorporation levels of BrdU were detected in the HSCs treated with MIP-1α, MIP-1β or PBS (Fig. 3.20 B).

Although, at steady state, MIP-1α or MIP-1β showed no effect in the cell cycle or proliferation state of HSCs, we wondered whether in a stress condition, where stem cells are pushed into an active cell, MIP-1α/MIP-1β would then abrogate this activation. Hence we co-challenged mice with pIC together with MIP-1α or MIP-1β for 20 hours. Through Ki67/Hoechst analysis, no significant difference in the HSC cell cycle distribution was observed with MIP-1α or MIP-1β treatment (Fig. 3.20 C). In addition, there was no significant difference induced by either MIP-1α or MIP-1β in the incorporation levels of BrdU (Fig. 3.20 D).

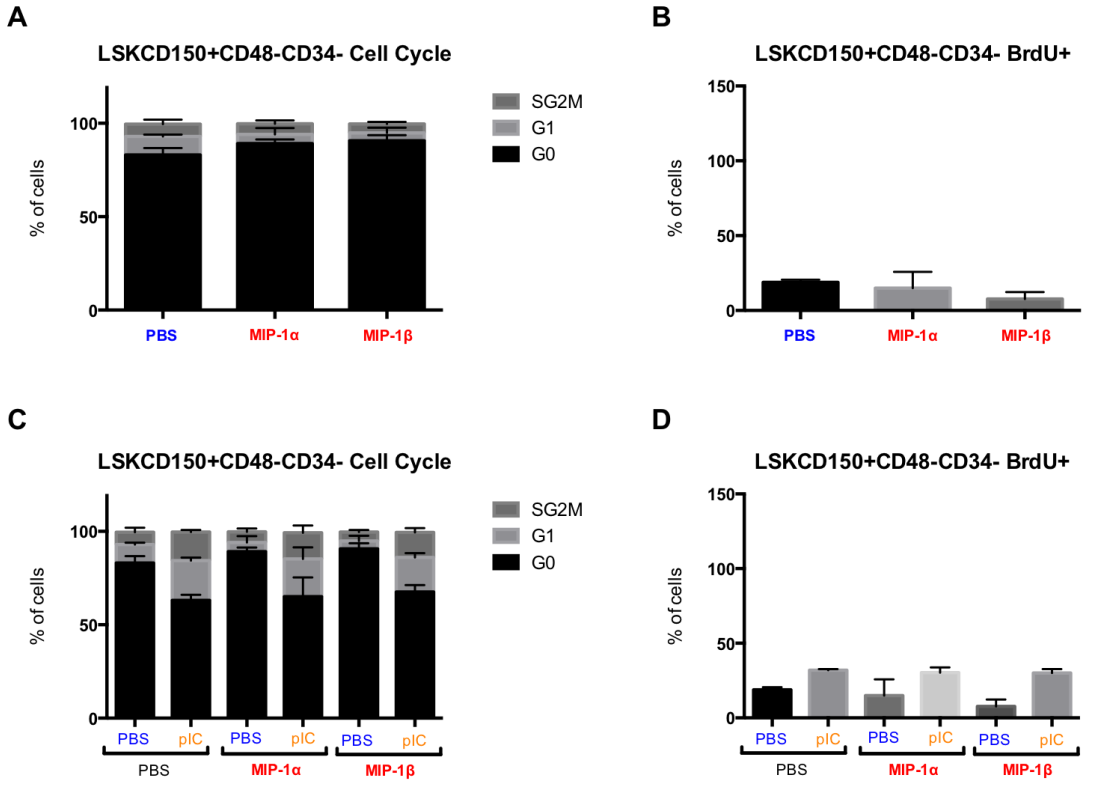

Figure 3.20: Influence of MIP-1α and MIP-1β on the cell cycle behavior of HSCs.
The wt mice were challenged with an intraperitoneal injection of PBS or 500 ng of MIP-1α / MIP-1β and 20 hours later the stem cells from the bone marrow were isolated, stained, fixed, permeabilized and analyzed by flow cytometry. (A) The cell cycle status of stem cells ($LSKCD150^{+}CD48^{-}CD34^{-}$) was determined by Ki67/Hoechst intracellular staining (G_0: $Ki67^{-}Hoechst^{low}$; G_1: $Ki67^{+}Hoechst^{low}$; SG_2M: $Ki67^{+}Hoechst^{high}$). (B) Mice were treated with BrdU, 14 hours before analysis, followed by analysis of the incorporation levels in the stem cells ($LSKCD150^{+}CD48^{-}CD34^{-}$). (C) Mice were co-challenged with MIP-1α / MIP-1β and a dose of pIC (5mg/kg) or PBS for 20 hours followed by analysis of the cell cycle status of stem cells ($LSKCD150^{+}CD48^{-}CD34^{-}$) through Ki67/Hoechst intracellular staining. (D) Mice were co-challenged with MIP-1α / MIP-1β and a dose of pIC (5mg/kg) or PBS for 20 hours followed by treatment with BrdU 14 hours before analysis, followed by analysis of the incorporation levels in the stem cells ($LSKCD150^{+}CD48^{-}CD34^{-}$). Data are presented as mean ± SD with n ≥ 3. The significance was determined using an unpaired, two-tailed student's t-test (* $p < 0.05$).

In order to exclude the possibility that no significant effect of MIP-1α or MIP-1β in the cell cycle distribution and proliferation status of HSCs was detected due to an insufficient amount of stimulus, we increased the dose given per mouse from 500 ng to 5 µg. Nonetheless, the percentage of HSCs in G_0, G_1 and S, G_2, or M phases was similar between PBS, MIP-1α or MIP-1β treated mice (Fig. 3.21 A). Furthermore, there was no significant difference in the levels of HSC proliferation in mice treated with MIP-1α, MIP-1β or PBS (Fig. 3.21 B).

The effect of a high dose of MIP-1α/MIP-1β (5 µg/mouse) together with a pIC co-challenge was then investigated. However, no significant differences in the cell cycle distribution were detected between the BM HSCs of MIP-1α, MIP-1β or PBS treated mice (Fig. 3.21 C). Moreover, no significant difference was observed in the HSC proliferation rate of mice treated with MIP-1α, MIP-1β or PBS (Fig. 3.21 D).

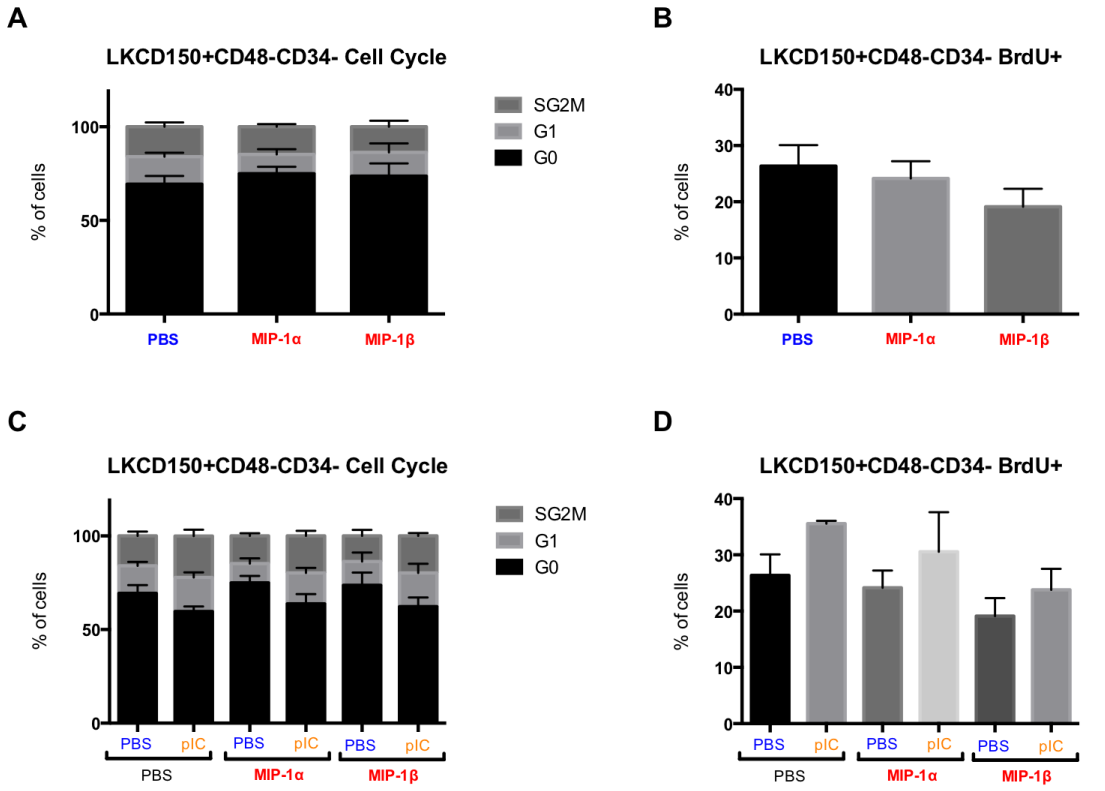

Figure 3.21: Effect of a high dose of MIP-1α and MIP-1β on the proliferation of HSCs.
The wt mice were challenged with an intraperitoneal injection of PBS or 5 µg of MIP-1α / MIP-1β and 20 hours later the stem cells from the bone marrow were isolated, stained, fixed, permeabilized and analyzed by flow cytometry. (A) The cell cycle status of stem cells ($LSKCD150^+CD48^-CD34^-$) was determined by Ki67/Hoechst intracellular staining (G_0: $Ki67^-Hoechst^{low}$; G_1: $Ki67^+Hoechst^{low}$; SG_2M: $Ki67^+Hoechst^{high}$). (B) Mice were treated with BrdU, 14 hours before analysis, followed by analysis of the incorporation levels in the stem cells ($LSKCD150^+CD48^-CD34^-$). (C) Mice were co-challenged with MIP-1α / MIP-1β and a dose of pIC (5mg/kg) or PBS for 20 hours followed by analysis of the cell cycle status of stem cells ($LSKCD150^+CD48^-CD34^-$) through Ki67/Hoechst intracellular staining. (D) Mice were co-challenged with MIP-1α / MIP-1β and a dose of pIC (5mg/kg) or PBS for 20 hours followed by treatment with BrdU 14 hours before analysis, followed by analysis of the incorporation levels in the stem cells ($LSKCD150^+CD48^-CD34^-$). Data are presented as mean ± SD with n ≥ 3. The significance was determined using an unpaired, two-tailed student's t-test (* $p < 0.05$).

Taken together, our data suggests that not only at the steady-state condition but also under an inflammatory setting, MIP-1α or MIP-1β have no impact in the cell cycle status or proliferation rate of HSCs.

3.2.6 Effect of the leukemic clone in the wt hematopoietic progenitor cells

We wanted to evaluate whether the function of the wt progenitor cells inside the leukemic chimeras was altered as compared to the wt progenitor cells inside the control healthy chimeras. Therefore, we sorted the BM wt cells ($CD45.2^+$) out of the leukemic and control healthy chimeras and performed an *in vitro* colony-forming unit (CFU) assay to evaluate the expansion and differentiation capacity of the progenitors. This method is based on the ability of progenitors to form colonies in a semi-solid methylcellulose medium supplemented with cytokines that induce differentiation of the progenitor cells. After 7 days of culture the total number of generated colonies per plate was determined. Interestingly, the wt progenitor cells that coexisted with the leukemic dtg cells showed a decreased potential to generate colonies as compared to the wt progenitor cells from the control healthy chimeras (Fig. 3.22).

Thus, these data indicate that the leukemic cells impair the function of the wt progenitor cells, leading to a decrease in their colony forming ability.

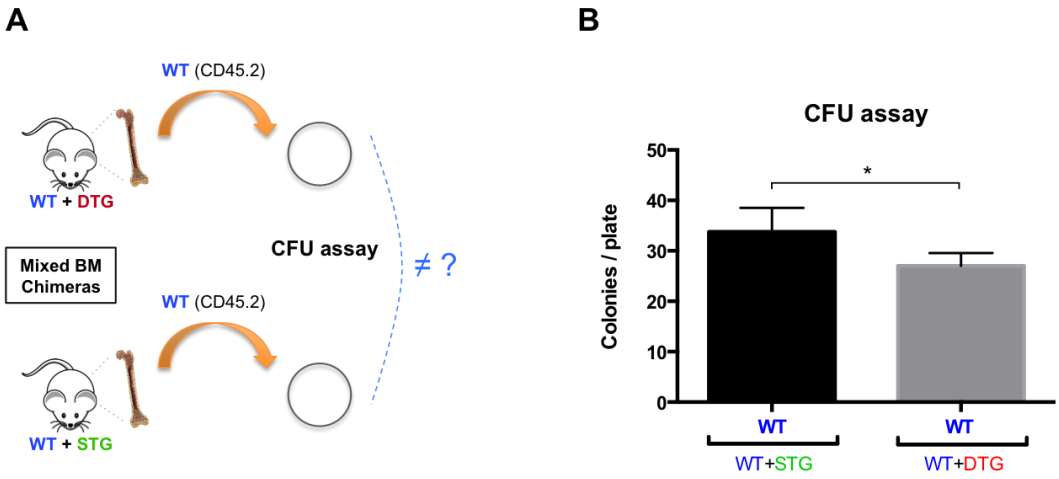

Figure 3.22: The WT committed progenitor cells that coexisted with the leukemic cells in the mixed BM chimeras have an impaired function.
The SCLtTA/BCR-ABL double-transgenic (dtg) mixed BM chimeras and control single-transgenic (stg) mixed BM chimeras were analyzed 22 weeks after bone marrow transplantation. (A) By making use of the cell surface CD45 marker, the bone marrow WT ($CD45.2^+$) cells were sorted apart from the the transgenic ($CD45.1^+$) cells and plated in a semi-solid methylcellulose medium supplemented with cytokines that induce differentiation of the progenitor cells. (B) After 7 days of culture in the colony-forming unit (CFU) assay specific medium, the colonies formed per plate were counted. Data are presented as mean ± SD with n ≥ 3. The significance was determined using an unpaired, two-tailed student's t-test (* $p < 0.05$).

3.2.7 The function of the wt HSCs is impaired by the leukemic cells

To investigate whether the effect of the leukemic cells on the wt cells was also taking place at the stem cell level we performed transplantation assays. The wt cells ($CD45.2^+$) from either leukemic or control healthy chimeras were sorted out of the BM by FACS and transplanted into $CD45.1^+$ wt lethally irradiated recipients. Later on, when analyzing the blood of the recipients, we could observe that the wt stem cells that once coexisted with the leukemic cells were impaired in their ability to generate mature cells as compared to the wt stem cells that coexisted with the control stg cells (Fig. 3.23). The contribution of the wt stem cells from the leukemic chimeras to the generation of granulocytes in the $CD45.1^+$ recipients was markedly decreased as compared to the wt cells from the control healthy chimeras (Fig. 3.23 B+C). While investigating the BM of the $CD45.1^+$ wt recipients, the same phenotype was detected. The wt stem cells from the leukemic chimeras were impaired in their potential to contribute to the generation of mature cells whereas the wt stem cells from the healthy control chimeras performed normally (Fig. 3.23 D). The ability of the wt stem cells that were sorted out of the leukemic chimeras to generate granulocytes was markedly decreased as compared to the wt cells sorted out of the healthy chimeras (Fig. 3.23 E).

In order to further validate the effect at the stem cell level, we performed similar transplantation experiments as described above, but instead of transplanting the bulk BM cells we specifically sorted and transplanted the HSC enriched population $lineage^-$ $Sca\text{-}1^+$ $c\text{-}Kit^+$ (LSK). Again, when analyzing the $CD45.1^+$ recipients, the wt HSCs that previously coexisted with the dtg leukemic cells showed a marked decreased contribution in the generation of mature cells as compared to the wt cells that coexisted with the control stg cells (Fig. 3.24).

Furthermore, we investigated whether the HSC impairment was caused by a defect of the cells to find their BM niche. Therefore, we transplanted LSK cells directly into the bone by intrafemoral injection, as opposed to intravenous transplantation. However, once more, the wt HSCs that coexisted with the dtg cells had an impaired ability to contribute to the generation of blood cells as compared to the wt cells from control stg chimeras (Fig. 3.24 D).

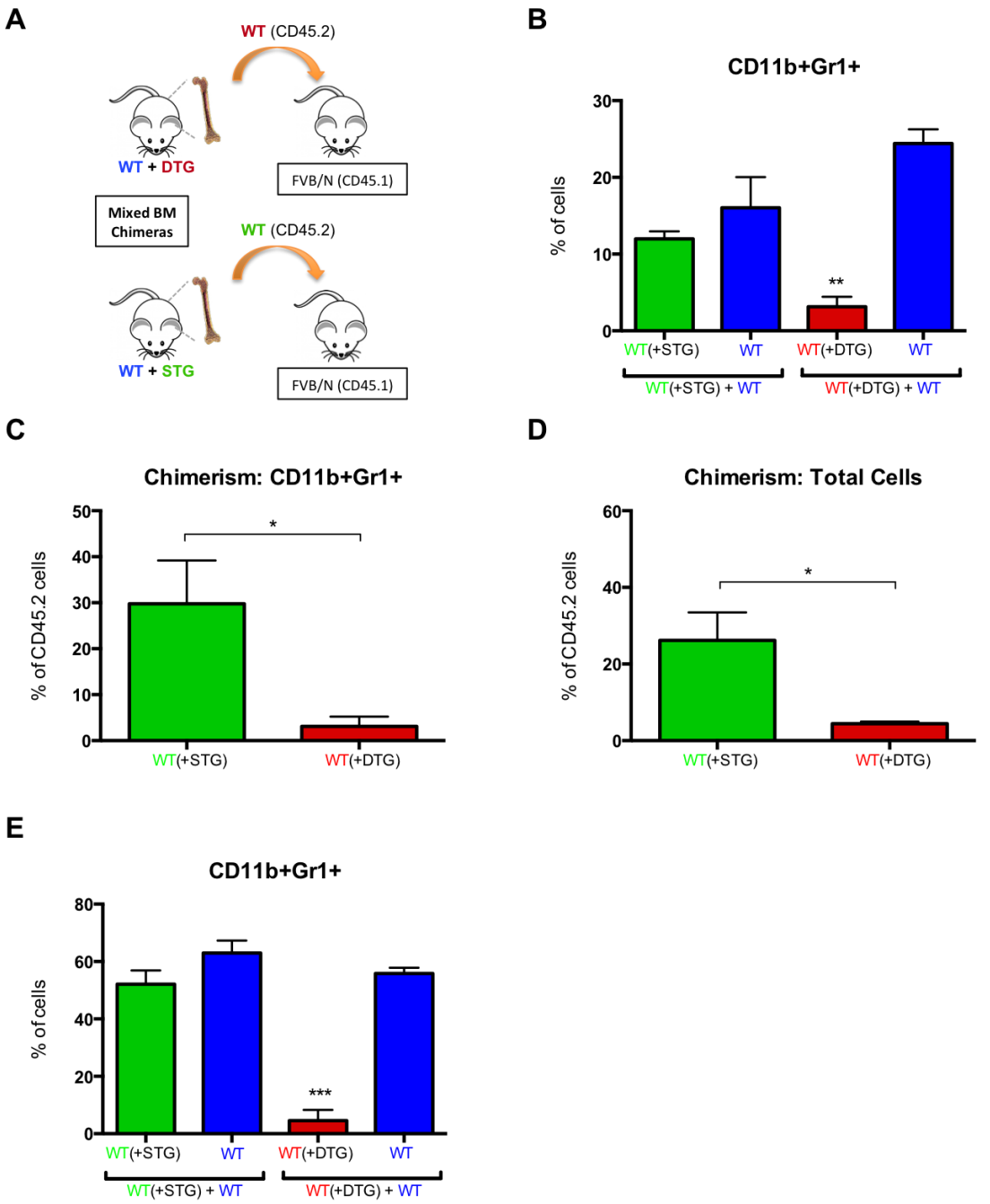

Figure 3.23: The engraftment potential of the WT cells that coexisted with leukemic cells in the mixed BM chimeras is impaired.
(A) By making use of the cell surface CD45 marker, the bone marrow WT ($CD45.2^+$) cells from either leukemic or control healthy chimeras (22 weeks after BMT) were sorted apart from the transgenic ($CD45.1^+$) cells by FACS and transplanted into $CD45.1^+$ WT lethally irradiated recipients. The blood and bone marrow of the recipients was analyzed 16 weeks after BMT. (B) The blood cells were stained and the granulocyte population ($CD11b^+Gr1^+$) was investigated by flow cytometry. (C) The contribution of the WT cells ($CD45.2^+$) that coexisted with the transgenic cells to the generation of blood granulocytes ($CD11b^+Gr1^+$) in the $CD45.1^+$ WT recipients was examined by flow cytometry. (D) The contribution of the WT cells ($CD45.2^+$) that coexisted with the transgenic cells to the generation of bone marrow mature cells in the CD45.1+ WT recipients was monitored through flow cytometry. (E) The bone marrow (BM) cells were stained and the granulocyte population ($CD11b^+Gr1^+$) was investigated by flow cytometry. Data are presented as mean ± SD with n ≥ 3. The significance was determined using an unpaired, two-tailed student's t-test (* $p < 0.05$, ** $p < 0.01$, *** $p < 0.001$).

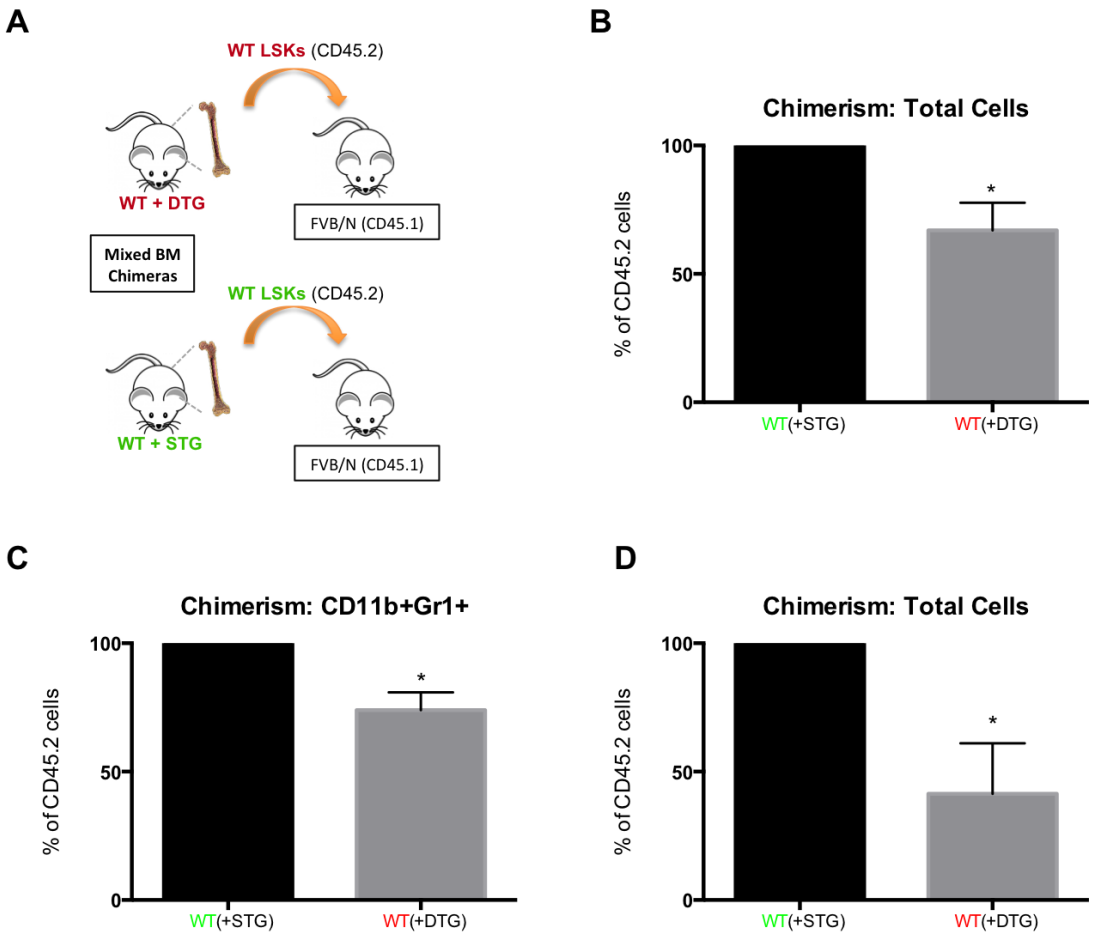

Figure 3.24: The WT HSCs that coexisted with the leukemic cells in the mixed BM chimeras have an impaired function.
(A) By making use of the cell surface CD45 marker, the bone marrow WT LSK (Lineage$^-$Sca-1$^+$c-Kit$^+$CD45.2$^+$) cells from either leukemic or control healthy chimeras (22 weeks after BMT) were sorted apart from the transgenic (CD45.1$^+$) cells by FACS and intravenously transplanted into CD45.1$^+$ WT lethally irradiated recipients. The blood and bone marrow of the recipients was analyzed 10 weeks after BMT. (B) The contribution of the WT cells (CD45.2$^+$) that coexisted with the transgenic cells to the generation of mature cells in the CD45.1$^+$ WT recipients was monitored through flow cytometry. (C) The contribution of the WT cells (CD45.2$^+$) that coexisted with the transgenic cells to the generation of granulocytes (CD11b$^+$Gr1$^+$) in the CD45.1$^+$ WT recipients was examined by flow cytometry. (D) The WT cells (CD45.2$^+$) that coexisted with the transgenic cells were transplanted intrafemorally into CD45.1$^+$ WT recipients, and the contribution to the generation of mature cells was monitored through flow cytometry. Data are presented as mean ± SD with n ≥ 3. The significance was determined using an unpaired, two-tailed student's t-test (* $p < 0.05$).

Interestingly, these data indicate that the wt HSCs that coexisted with the dtg cells in the leukemic chimeras were severely impaired in their engraftment ability whereas the ones interacting with the stg cells in the healthy control chimeras performed normally.

4. DISCUSSION

4.1 Combined treatment approach to target quiescent LSCs

The life-long blood production is maintained by HSCs, which reside at the apex of the hierarchically organized hematopoietic system (Kondo et al., 2003). The majority of adult HSCs are found in a quiescent state during homeostasis, nonetheless they have the potential to respond to external stimuli and rapidly enter an active cell cycle in order to meet the organism's requirements for blood cells (Wilson et al., 2008). Our group has previously demonstrated that one such stimulus is IFNα, which very efficiently drives HSCs out of quiescence into an active cell cycle (Essers et al., 2009). However, whether quiescent LSCs can also be pushed into an active cell cycle by IFNα has remained unknown. Given that quiescence has been proposed as one of the mechanisms through which LSCs are able to resist treatment, we investigated the activation potential of IFNα. More specifically, we focused on the LSCs from CML, which is one of the best-characterized malignancies and nowadays serves as a model disease for stem cell based malignancies. CML is driven by the constitutively active BCR-ABL tyrosine kinase, which arises as consequence of a reciprocal chromosomal translocation between chromosomes 9 and 22. By deregulating a wide range of signal transduction pathways, BCR-ABL induces leukemic cell growth, proliferation and survival. With the development of TKIs, which selectively target BCR-ABL, the treatment of patients was revolutionized and the rates of remission and survival were significantly increased. However, even after years of treatment with TKIs, residual LSCs remain present in most patients, which can lead to a relapse of the disease upon discontinuation of treatment, emphasizing the need for a curative approach that eradicates the LSCs.

For the first time, we have demonstrated that quiescent LSCs can also be pushed into an active cell cycle upon IFNα exposure, to a similar extend as HSCs. Furthermore, since quiescence has been proposed to confer treatment resistance in LSCs, we investigated the potential benefit of combining the activation capacity of IFNα with TKI to eradicate the leukemic cells. We could demonstrate that a combined treatment of IFNα short acute exposures together with continuous TKI administration is more advantageous than any of the agents alone, leading to a deeper decrease of the leukemic burden.

4.1.1 Establishment of experimental CML models

To unravel the *in vivo* effects of IFNα on LSCs and the potential synergistic effect of combination treatments with TKI, we employed CML mouse models in which BCR-ABL expression is mainly targeted to the HSC population. Such studies could not be carried out *in vitro* since HSCs need to be in their BM niche microenvironment in order to be activated by IFNα. When isolated HSCs are exposed to IFNα *in vitro* no activation is detected.

In our studies we initially made use of the dtg SCLtTA/BCR-ABL Tet-OFF mouse model, in which HSCs inducible and reversible express BCR-ABL in a DOX dependent manner (Fig. 3.1). However, a disadvantage of this mouse model is that all the stem cells express BCR-ABL. In contrast, there is a coexistence of both healthy and leukemic cells in CML patients. Therefore, in order to more closely mimic the patient scenario, we generated mixed BM chimeras by co-transplanting a mixture of HSCs and LSCs into wt recipients (Fig. 3.5). In the course of time, the dtg mixed BM chimeras developed signs of a CML-like disease whereas the control stg chimeras remained healthy. Such signs included enlarged spleen size, increased blood cell counts, decreased body weight and an expansion of the mature and immature granulocyte population in the blood, spleen and BM (Fig 3.6 - 3.8).

Although, initial studies were performed in the SCLtTA/BCR-ABL mice, they were then recapitulated and further explored in the mixed BM chimeras. In order to distinguish the leukemic from the healthy population we made use of wt mice that express CD45.2 in the surface of hematopoietic cells, whereas the transgenic cells posses the CD45.1 isoform. Of note, the onset of leukemia in the mixed BM chimeras took a considerable amount of time. Therefore, we additionally set up a CML mouse model with a faster onset of leukemia by making use of retroviruses to introduce BCR-ABL into the HSC enriched population Lineage$^-$ Sca-1$^+$ c-Kit$^+$ (LSK), followed by transplantation into wt recipients (Fig. 3.10). Since a GFP gene is attached to the BCR-ABL open reading through an IRES sequence, the leukemic cells can be easily followed by GFP detection. This retroviral vector has been typically used to transduce BM cells from mice serially treated with 5-Fluoro-Uracil (5-FU) as way to eliminate mature blood cells and enrich the BM for stem and progenitor cells. However, in order to target a more precise HSC enriched population we made use of FACS to transduce sorted LSK cells. Furthermore, through this approach, the stress caused on the HSCs by the 5-FU chemotherapy is avoided. Following transplantation of the transduced LSKs, the recipient mice develop signs of leukemia within weeks rather than months (Fig. 3.11 - 3.12). Although, this model is

advantageous from a logistic point of view, particularly taking into account the time constraints of these studies, the levels of BCR-ABL induced by the retroviral vector are supraphysiological and consequently the fast development of disease does not adequately recapitulates the chronic phase of CML. In contrast, the slow onset of leukemia in the mixed BM chimeras more physiologically mimics the natural course of the disease in patients.

As a way to get further closer to the patient scenario, similar experiments to the ones previously described could be carried out in human cells. To date, the activation potential of IFNα has not been demonstrated for neither human HSCs nor LSCs. Such experiments are not feasible to be carried out *in vitro*, since the stem cells need to be in their BM niche in order to be activated, and no effect is detected *in vitro*. Therefore, xenotransplantation mouse models could be established by making use of immunocompromised mice. However CP-CML human samples have been shown quite difficult to engraft in mice. A possible way to circumvent this issue and improve the efficacy of transplantation could be through the co-transplantaion of human MSCs together with the human primary hematopoietic cells. This approach has been recently shown to significantly improve the efficacy of transplantation of primary myelodysplastic syndrome (MDS) samples, which had also been known to poorly engraft in mice (Medyouf et al., 2014).

Apart from the engraftment hurdle, the human primary hematopoietic cells would reside in a mouse specific environment and thus they might lack essential cues provided by the human niche. As a possible way to overcome this potential issue, the primary hematopoietic cells could be transplanted in combination with human niche cells in an effort to humanize the mouse BM niche environment.

In order to explore the activation potential of IFNα *in vitro*, the niche might have to be reconstructed *in vitro*. In such complex effort, not only the different components would have to be added but also their spatial distribution might have to be considered. Furthermore, the culture conditions should take into account the BM environment characteristics such as the low concentration of oxygen. When such approach would enable the activation of HSCs *in vitro*, it would be interesting to selectively remove or add different elements of the niche and investigate which ones are crucial for the IFNα effect.

4.1.2 Activation of quiescent LSCs into an active cell cycle through IFNα

One of the crucial questions to address for a potential combined treatment with IFNα and TKI was whether quiescent LSCs could be activated by IFNα and how comparable would this effect be to healthy HSCs. In order to challenge the mice with

IFNα, we made use of pIC, a synthetic analogue of dsRNA that ultimately leads to the production of INFα. Through cell cycle analysis and proliferation assays, we demonstrated that upon exposure to IFNα, the LSCs were induced to exit G_0, enter an active cell cycle and proliferate to a similar extend as the HSCs (Fig. 3.9 A+B). In addition, by making use of qRT-PCR we observed an induction of the expression of the INFα inducible gene ISG15 in the LSCs to the same levels as in the healthy HSCs (Fig. 3.9 C).

A previous study has suggested that BCR-ABL leads to the degradation of the interferon-α/β receptor (IFNAR) and consequently impairs the response to INFα (Bhattacharya et al., 2011). However the majority of the study was carried out using cell lines and all the assays were performed *in vitro*. Therefore whether such effect would occur in the *in vivo* setting has remained unclear. Although we did not detect impairment in the response to INFα in the CML mouse model, we quantified the level of IFNAR expressed on the surface of LSCs as compared to healthy HSCs. In accordance with our previous studies, the levels of IFNAR, and therefore the potential to respond to IFNα, were comparable between HSCs and LSCs, both at steady state and after stimulation with IFNα (Fig. 3.9 D).

In summary our data indicate that IFNα exposure induces LSCs to exit quiescence, enter an active cell cycle and proliferate to a similar extend as healthy HSCs. This finding paves the way for exploitation of the potential synergistic effect of IFNα and TKI in the treatment of CML.

4.1.3 Combinatorial treatment: IFNα + Imatinib

Once we demonstrated that quiescent LSCs could be pushed into an active cell cycle through IFNα exposure, we then investigated the potential beneficial effect of a combined treatment strategy with imatinib for the treatment of CML. The quiescent LSCs would first be activated into an active cell cycle by IFNα, followed by imatinib targeted therapy. Assuming that cycling LSCs become susceptible to the cytotoxic effect of imatinib, the combined therapy would target not only the bulk of the tumor but also the LSCs, avoiding relapse of the disease (Fig. 4.1).

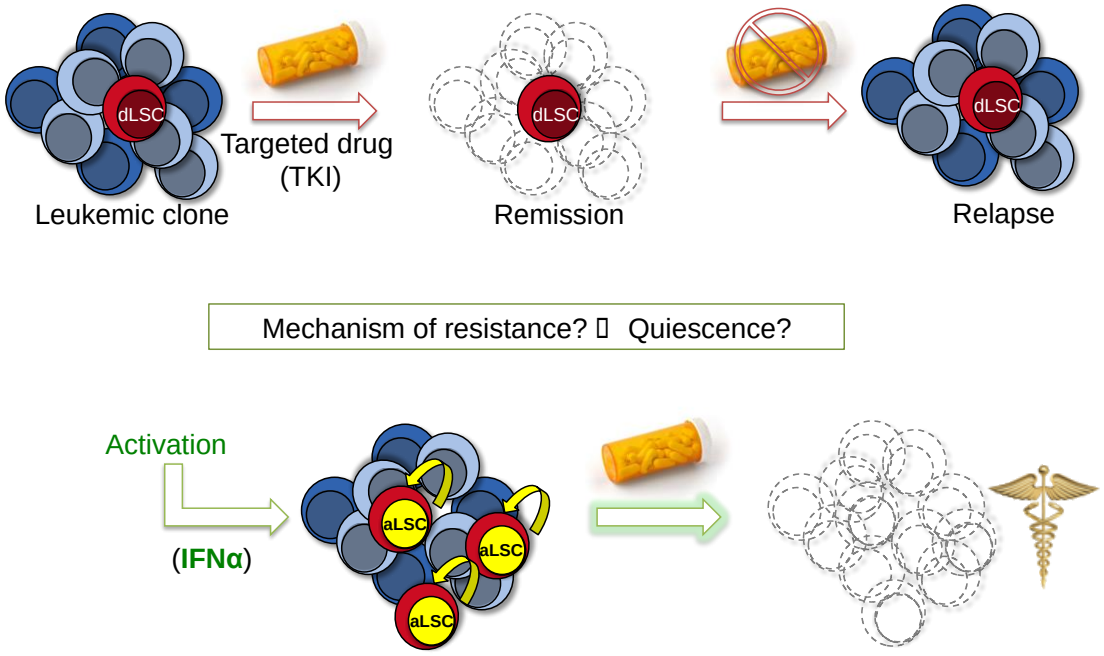

Figure 4.1: Combined treatment strategy to target and eliminate the quiescent LSCs.
Since quiescence has been proposed to render LSCs resistant against TKI treatment, then activating the LSCs might be a way to make them susceptible to TKI treatment and therefore lead to the eradication not only of the bulk of leukemia but also the LSCs, avoiding relapse of the disease.

The cause for the resistance of LSCs to imatinib has been highly debated, and several mechanisms have been proposed. Since LSCs have been reported to express higher levels of BCR-ABL than the more differentiated leukemic cells (Jiang et al., 2007), the same concentration of imatinib could possibly inhibit BCR-ABL in the bulk of the leukemia whereas it would be inefficient within the LSCs. Additionally, LSCs where shown to express decreased levels of the uptake transporter OCT1 and higher levels of the efflux transporters ABCB1 and ABCG2, which could actively reduce the amount of imatinib within LSCs and further contribute to an insufficient inhibition of BCR-ABL (Engler et al., 2010; Jiang et al., 2007). Challenging the hypothesis of an inefficient inhibition of the BCR-ABL kinase activity within LSCs, when primary human CML samples where subjected to high doses of TKI together with BCR-ABL knockdown *in vitro*, although maximal pharmacological inhibition was achieved, the LSCs were still able to survive (Hamilton et al., 2012). Interestingly, when BCR-ABL inhibition was discontinued, the LSCs were able to proliferate. Additionally, similar results were replicated in a CML mouse model (Hamilton et al., 2012). Altogether, these results suggest that LSC survival is independent of BCR-ABL kinase activity.

Several lines of evidence correlate LSC treatment resistance to quiescence, as further discussed below (section 4.1.4). In addition, the location or interaction of the stem cells with the bone marrow niche have been suggested for playing a role in the

resistance, which, interestingly, have been shown to be linked to quiescence in normal HSCs. So, if quiescence and the localization in the bone marrow niche prevent imatinib from targeting the LSCs, then activating the LSCs might be a way to make them susceptible to imatinib treatment.

In support of this concept, mathematical modelling of the imatinib effect on CML cells suggested that the persistence of LSCs following treatment could be explained by a selective effect of imatinib exclusively on proliferative leukemic cells (Roeder et al., 2006). Additionally, the same mathematical modelling approach suggests that the combination of a cell cycle stimulating drug together with imatinib would lead to the complete eradication of the CML cells. The determination of the appropriate time points between each step is one of the crucial aspects of this combinatorial treatment. Recently, another study employing mathematical modeling to investigate the potential effect of combining IFNα with imatinib predicted that the more favorable combination would consist of a pulsed INFα treatment together with continuous TKI administration (Glauche et al., 2012).

We employed our CML mouse model, in which BCR-ABL expression is targeted to the HSC population, to investigate the in vivo outcome of several treatment schemes lasting up to 9 days. The optimized combined treatment begins with IFNα stimulation followed by continuous imatinib administration in the following days, except on the 5^{th} day on which IFNα re-stimulation is performed. The idea was to initiate the treatment with the activation of the quiescent LSCs into an active cell cycle so that the TKI treatment could then affect all CML cells. Moreover, in the middle of the treatment window, a re-stimulation with IFNα would ensure that LSCs that remained or returned to quiescence could be activated.

The combined treatment was analyzed in comparison to either of the agents alone as well as to the absence of both. Interestingly, the combined treatment led to a significant deeper reduction of the leukemic burden as compared to any of the other groups (Fig. 3.13 B). Furthermore, the combined treatment led to a reversion of splenomegaly to significant levels as compared to any of the other groups (Fig. 3.13 C). Additionally, our preliminary studies indicate a survival advantage conferred by the combined treatment (Fig. 3.13 D).

Altogether, our data indicate that a combined treatment approach with IFNα and imatinib is more effective for the treatment of CML as compared to any of the agents alone. Although the combined treatment was shown to be advantageous, it was not surprising that it did not let to the complete elimination of leukemic cells, since the mice were only subjected to a short treatment window of 9 days. To investigate whether the surviving leukemic cells were able to resist due to permanence in a

quiescent state a characterization of their cell cycle status could be performed. Furthermore, it would be interesting to investigate whether the reiteration of several continuous cycles of our optimized combined treatment scheme would further enhance the eradication of leukemic cells.

Of note, although pIC has been commonly used as cost effective way to challenge mice with IFNα, it can also induce the production of other cytokines and therefore it would be interesting to test the direct administration of purified IFNα. Also it should be noted the IFNα could possibly contribute to the beneficial effect of the combined treatment through additional mechanisms apart from the activation of LSCs into cell cycle, such as the activation of the immune system against the cancer cells (further discussed in 4.1.5). In order to further correlate the benefit of the combined treatment to the activation of quiescent LSCs, alternative cell-cycle-stimulation agents could be tested. By showing that alternative ways of stem cell activation enhance imatinib efficacy, a strong indication that activated LSCs become susceptible to imatinib would be made. More specifically, it would be particularly interesting to explore the potential effect of TPO, since in this approach the stem cell activation is detached from an inflammatory setting (Yoshihara et al., 2007).

4.1.4 Quiescence as a mechanism for LSC treatment resistance

A similar concept, correlating drug resistance to quiescence, has been demonstrated for healthy HSCs. While quiescent HSCs are resistant to the chemotherapy drug 5-FU, they become vulnerable when activated into cell cycle by IFNα (Essers et al., 2009). The combined treatment depletes the HSC pool, leading to a severe pancytopenia and ultimately death of mice (Essers et al., 2009).

Furthermore, similar rationales have been explored in CML LSCs. Previous work has demonstrated that the promyelocytic leukaemia tumour-suppressor protein (PML) contributes to the regulation of quiescence in HSCs and LSCs (Ito et al., 2008). The genetic deletion of PML or its pharmacological inhibition with arsenic trioxide (As_2O_3) in CML mouse models induces an increase in actively cycling LSCs. The combination of As_2O_3 with the chemotherapeutic drug cytaribine led to an increased eradication of LSCs in a CML mouse model as well as in primary human CML samples in vitro (Ito et al., 2008). It should be noted that As_2O_3 was also shown to activate HSCs and therefore they might also be affected by the combined treatment. However the effect appeared to be stronger in LSCs, opening the possibility for a therapeutic window. Nonetheless, since both agents do not specifically target only the leukemic cells, a careful and precise determination of the ideal doses and time-points have to be investigated in such a way that the effect on

leukemic cells would be considerable greater than on the healthy cells.

Several studies have also explored the potential benefit of G-CSF, which has also been shown to induce quiescent HSCs into an active cell cycle (Morrison et al., 1997b; Wright et al., 2001). The *in vitro* treatment of CML primary human samples with G-CSF was shown to induce activation of LSCs and make them more susceptible to imatinib (Jorgensen et al., 2006). However, when the efficacy of a combined treatment with G-CSF and imatinib was accessed in a clinical trial, no significant advantage in eradicating the leukemic cells was detected in the 2-year follow up (Drummond et al., 2009). Interestingly, in the 5-year follow up analysis, a deeper reduction of the BCR-ABL levels was reported in the combined treatment group as compared to the group of patients under continuous imatinib administration, suggesting a potential benefit for the combined treatment in the long-term (Gallipoli et al., 2013b). It should be noted that this clinical trial was conducted on a relatively small number of patients and therefore larger studies are needed to provide a more definitive insight into the efficacy of this combined treatment.

The LSC resistance has also been associated with quiescence in other types of leukemia such as acute myeloid leukemia (AML). By making use of an AML xenotransplantation model, G-CSF treatment was shown to induce quiescent LSCs to enter an active cell cycle and to render them more susceptible to the chemotherapy drug cytarabine (Saito et al., 2010). The combined treatment led to a significant reduction of the LSCs and increased survival of the mice, however it was not able to completely eradicate the disease. The mouse HSCs were not affected by the combined treatment, nevertheless the effect on human HSCs was not elucidated. Since both agents have the potential to also act on HSCs, a detailed evaluation of the ideal doses and administration timing would be necessary to determine an adequate therapeutic window.

A most recent study suggests that the PPARγ receptor regulates quiescence in LSCs through a pathway involving STAT5, HIF2α and CITED2 (Prost et al., 2015). Interestingly, the pharmacologically activation of PPARγ with pioglitazone, which induces LSCs to exit quiescence, in combination with TKI had a synergistic effect in inducing death of LSCs (Prost et al., 2015).

Altogether, several independent studies point towards the importance of LSC quiescence for treatment resistance, further strengthening the rationale explored here for combining IFNα and imatinib for the treatment of CML. Others have also explored alternative ways of cell cycle stimulation, such as the previously described experiments with G-CSF. However, G-CSF is also known to induce mobilization of HSCs out of the BM, which puts them under an additional stress situation. In contrast

to G-CSF induced activation, IFNα does not induce mobilization of HSCs to the periphery. Additionally, IFNα may contribute to the elimination of leukemic cells trough additional mechanisms such as immunomodulatory effects.

4.1.5 Pleiotropic effects of IFNα

Interferon-α has been known for its role in resistance to viral infections, anti-proliferative effects, and enhancing innate and adaptive immune responses (Belardelli et al., 2002; Stark et al., 1998). The pleiotropic effects of IFNα can be explained by its role in regulating the transcription of more than 300 IFN-stimulated genes (ISGs), encoding antiviral, host defense, immunomodulatory, apoptotic, cell cycle, and transcription factor proteins (de Veer et al., 2001).

Although IFNα has been recently shown to induce quiescent HSCs into proliferation (Essers et al., 2009), in the past it has been demonstrated to have an anti-proliferative effect against many cell types *in vitro* (Borden et al., 2007), indicating that IFNα signals are perceived differently depending on the cell context.

Aside from pushing quiescent LSCs into an active cell cycle, IFNα could also contribute to the combined treatment enhanced eradication of leukemic cells through additional mechanisms. Since IFNα has been implicated in the activation of the immune system, we wondered whether such mechanism was also responsible for the improved efficacy of the combined treatment. In order to investigate the potential role of IFNα in activating T cells we examined the distribution of the T cell compartment immediately after the treatment window. However no significant changes were detected in the combined treatment as compared to the other groups (Fig 3.14 A). Additionally, instead of examining the distribution of the total T cell compartment, we specifically investigated the $CD8^+$ cytotoxic T cells (Fig. 3.14 B). Actually, IFNα has been shown to induce proliferation, expansion, and long-term survival of mouse and human cytotoxic T cells (Hervas-Stubbs et al., 2010). Nonetheless, the combined treatment did not led to significant alterations.

It should be kept in mind, that the changes in the T cell populations were exclusively analyzed 1 day after the treatment window and therefore the analysis of additional time-points could give a better understating of the changes across time. Additionally, changes in the T cell activity could be investigated by analyzing alterations in the expression of markers associated with activated T cells. Also, since IFNα has been shown to enhance the activity of natural killer (NK) cells *in vitro* (Lee et al., 2000), and the NK cell antitumor response in mice (Swann et al., 2007), it is possible that such a mechanism could also contribute to the beneficial effect of the treatment.

It would be interesting to investigate whether the combined treatment would remain advantageous in the absence of T cells and NK cells. For that, disease could be induced in immunodeficient mice lacking those cell populations, such as the NSG mice, and the combined treatment could be evaluated in comparison to imatinib-alone.

4.1.6 From the bench to the clinic

Apart from preclinical studies, there is also accumulating evidence from clinical trials suggesting a beneficial effect for the combination TKI with IFNα. Interestingly, the discontinuation of TKI therapy seems to be more successful when patients were previously subjected to interferon treatment (Ross et al., 2013; Rousselot et al., 2007). Recently, the potential beneficial effect of combining a pegylated long lasting form of IFNα together with imatinib has been addressed in clinical trials, and the combination therapy seems to be more favorable than imatinib alone, leading to significantly higher rates of molecular response (Nicolini et al., 2011; Preudhomme et al., 2010; Simonsson et al., 2011). Altogether, the studies suggest that the combination of low doses of IFNα with TKI for at least 12 months can be beneficial in the achievement of remission. Currently, clinical trials testing the beneficial effect of second generation TKIs (nilotinib/dasatinib) in combination with IFNα are underway (NCT01657604; NCT01725204).

Of note, apart from the dose determination, also the adequate administration timing of each agent is crucial for maximal synergistic effect. Instead of long exposures to the pegylated forms of IFNα, it would be interesting to investigate the effect of periodic short acute exposures as a way to render the LSCs susceptible to continuous TKI administration.

4.1.7 Arms race for the treatment of CML

On a broader perspective, for the past two decades, CML treatment has mainly focused on the inhibition of BCR-ABL kinase activity through TKIs. However this approach has been continuously counteracted by the occurrence of mutations in the BCR-ABL kinase domain. Due to the inability of imatinib to target several BCR-ABL kinase domain mutants, second generation TKIs (nilotinib/dasatinib) were developed with a higher affinity to the kinase domain. In turn, these TKIs were able to target many of the imatinib-resistant mutants. However, the BCR-ABL^{T315I} mutant was shown to be resistant even to these TKIs. The arms race continued and the third generation TKI ponatinib was developed and shown to overcome the BCR-ABL^{T315I} resistance. Nevertheless, the combination of different mutations in the BCR-ABL

kinase domain was shown to confer resistance against ponatinib. Therefore, new approaches that focus on alternative targets than the kinase domain may benefit the treatment of CML patients. As an example, a recent studied focused on the interference with the BCR-ABL oligomerization, which is crucial for its activity (Woessner et al., 2015). The inhibition of this event led to inhibition of proliferation and induction of apoptosis of BCR-ABL-expressing cell lines in vitro, irrespective of the kinase domain mutation status (including compound mutants resistant to ponatinib). Furthermore, through the same approach, the colony formation ability was inhibited in human primary CML samples, including a sample with the BCR-ABL^{T315I} mutation. Although, this was still a very preliminary study carried out only *in vitro* and mainly on cell lines and on a few number of patient samples, it serves as an example of potential alternatives to the direct kinase inhibition. Alternatively, therapeutic approaches could also focus on the microenvironmental agents that promote leukemia development as well as on the modulation of the immune system against the leukemic cells.

4.2 Impact of leukemic cells on the behavior of wt cells

4.1.1 Leukemia-induced alteration of the wt cell population distribution and BM cytokine repertoire

Using our mixed BM chimera model, which mimics the coexistence of leukemic and healthy cells that occurs in CML patients, we investigated the interplay between both populations. More precisely, we wanted to shed light on the impact of leukemic cells on the healthy hematopoietic cells. Since in the mixed BM chimeras, the leukemic and wt healthy hematopoietic cells have a different CD45 surface marker, they can be easily distinguished.

We have shown that the alterations of the mature cell populations in the spleen and BM of leukemic chimeras occurred not only in the leukemic compartment but also in the wt cells. More precisely, the expansion of the granulocyte population and the decrease of the B cell population observed in leukemic chimeras were detected in both the leukemic and wt cells (Fig 3.15 + 3.17). Additionally, the modifications in the committed progenitor cell populations that unfold in the leukemic chimera BM, such as the expansion of GMPs and decrease in MEPs, were detected not only in the leukemic cells but also in their wt counterpart (Fig 3.16).

We then investigated possible mechanisms through which the leukemic cells could influence the behavior of wt cells. We hypothesized that such effect could be mediated by secreted agents from the leukemic clone that could directly affect the wt cells or induce changes in the niche that in turn would impact the wt cells. In order to detect such potential agents, we performed a cytokine array in the BM supernatant of the mixed BM chimeras (Fig 3.18). Several differences were detected, however the most prominent and clear hits were a significant increase in IL-1α, IL-1β, MIP-1α, MIP-1β and decrease in CXCL9. The array results were then validated by ELISAs performed on the BM supernatant (Fig 3.19). Interestingly, some of the cytokines detected by our array have also been shown to be present in CML mouse models by other groups (Zhang et al., 2012), further validating the quality of our array and mouse model. For some of the hits, potential mechanisms through which they might contribute to disease progression have been elucidated whereas for others it remains unclear.

Using CML mouse models, BCR-ABL was shown to induce production of IL-6 in the expanded myeloid leukemic cells, which in turn blocks the differentiation of CML multipotent progenitors into the lymphoid lineage and redirects them into the myeloid lineage, creating a paracrine positive feedback loop for CML development (Reynaud et al., 2011).

Interestingly, using a $JAK2^{V617F}$ mouse model for myeloproliferative neoplasms, it has been recently shown that IL-1β secreted by mutated HSCs induces damage on the BM sympathetic nerve fibers and triggers apoptosis of Schwann cells and MSCs, contributing to disease development (Arranz et al., 2014).

In another study, MIP-1α was shown to be produced by leukemic cells and to contribute to the maintenance of LSCs. In the absence of MIP-1α, the LSCs become impaired in their ability to propagate disease. Similarly, LSCs have a reduced ability to populate the BM of mice lacking CCR1 or CCR5 (receptors through which MIP-1α signals). The authors hypothesize that MIP-1α confers a competitive growth advantage to the LSCs by displacing the wt cells from their niche and therefore making space for the leukemic cells. Of note, upon wt mice injection with MIP-1α, a mobilization of the $lineage^{-}$ $c\text{-}Kit^{+}$ progenitors was demonstrated, but not of a specific HSC population. The competitive advantage conferred by MIP-1α could also be possibly driven by inhibiting the growth of the wt cells. Actually, in the past it has been suggested that MIP-1 inhibits the proliferation of HSCs and induces them into quiescence. Although in these studies the stimulation with MIP-1 was performed *in vivo* by injecting mice, the read out consisted of *in vitro* CFU assays. Therefore, the population being addressed was mainly consisting of progenitors and not specifically

HSCs. Therefore we sought to investigate the *in vivo* effect of both MIP-1α and MIP-1β in the cell cycle behavior of the purified LSKCD150^{+}CD48^{-}CD34^{-} HSC population. For that, we challenged mice with either MIP-1α or MIP-1β and analyzed the cell cycle status and proliferation levels of HSCs. Neither agent induced a significant change in the HSC cell cycle or proliferation behavior (Fig. 3.20 A+B). Although no effect was detected when mice were under homeostatic conditions, we wondered whether in a stress condition where HSCs are induced to proliferate, MIP-1 would then interfere with such activation. Thus, we co-challenged mice with MIP-1α/MIP-1β and pIC. However, no significant changes were induced by either MIP-1 (Fig. 3.20 C+D). In order to discard the possibility that no effect of MIP-1α/MIP-1β was observed due to an insufficient amount of stimulus we performed the same experiments described above but instead of administrating 500 ng per mouse, a high dose of 5 µg was used. Nonetheless, even at the high dose of 5 µg, MIP-1α/MIP-1β did not have an impact in the HSC cell cycle and proliferation behavior, either at steady state or under an inflammatory setting (Fig. 3.21). Although no effect was detected, one should consider that we only tested a single acute exposure and no long-term exposures were examined.

When investigating the potential function of one of the array-acquired hits on the wt cell behavior, a long-term, instead of a momentary, stimulation or blockage might be required, since the phenotype observed in the mixed BM also develops through a considerable length of time. Furthermore, the phenotype could be induced by a combination of several cytokines.

In order to get further insights into the potential role of the array obtained hits in the influence of leukemic cells on the behavior of wt cells, mixed BM chimeras could be generated under specific KO backgrounds. More precisely, one could investigate whether the previously described influence would still occur when a particular cytokine gene is deleted from the leukemic cells. Conversely the mixed BM chimeras could also be evaluated when the cytokine receptor is KO from the wt cells. However, one should keep in mind that such effect could be driven not only by one but trough the combination of several agents.

4.1.2 Leukemic cells impair the function of wt hematopoietic progenitor and stem cells

Since we observed that the leukemic cells modify the distribution of the wt cell populations, we investigated whether the function of the wt committed progenitors was being altered. Therefore we evaluated the progenitor expansion and differentiation capacity of the wt cells from either leukemic or control chimeras

through CFU assays. Interestingly, the coexistence with leukemic cells led to an impairment of the wt committed progenitors ability to generate colonies (Fig. 3.22).

Following up on the observed decreased ability of wt committed progenitors to expand and differentiate as a result of interacting with leukemic cells, we sought to investigate whether the function of HSCs was also being altered. Thus we performed transplantation experiments and evaluated the HSC capacity to reconstruct the hematopoietic system of lethally irradiated recipients. Interestingly, the wt cells from leukemic chimeras showed a significantly reduced engraftment potential and ability to generate blood cells as compared to wt cells from control chimeras (Fig. 3.23). Since we transplanted total BM cells, we could not exclude the possibility that there was a reduced number of HSCs within the wt population of the leukemic versus control chimeras. Therefore, we performed additional transplantation experiments but instead of total wt BM cells we specifically transplanted the stem and progenitor enriched population LSK. Similarly, the wt cells that coexisted with leukemic cells showed a reduced ability to engraft and generate blood cells as compared to wt cells from control chimeras.

We wondered whether the wt HSCs from leukemic chimeras had a defective homing capacity. Therefore we examined whether the defective phenotype would still be observed when the cells are transplanted directly into the BM as opposed to intravenously.

In summary, we have shown an unexpected influence of the leukemic cells on the behavior of the wt healthy cells. More precisely, the coexistence with leukemic cells impairs the expansion and differentiation potential of wt progenitors as well as the function of HSCs.

To gain further insights, it would be interesting to conduct transplantation experiments with more precise and purer progenitor (for instance, differentiate between MPPs and other committed progenitors) and HSC populations (such as LSKCD150^{+}CD48^{-}C34^{-}) in order to differentiate the effect in each precise population. Additionally, limiting dilution transplantation assays could be performed in order to more precisely quantify the impact of leukemic cells in functional HSC frequency. Moreover, single cell HSC transplantation assays could elucidate the impact of leukemic cells in the HSC pool heterogeneity and differentiation bias.

To better understand the leukemia-induced changes on the wt cells, the gene expression profile of precise HSC and progenitor populations could be investigated and compared to the control healthy chimeras.

To implicate the array-obtained hits in the leukemia-induced effect on wt cells, one could investigate whether the genetic deletion or pharmacological inhibition of a

particular cytokine (on the leukemic cells) or the corresponding receptor (on the wt cells) would revert the phenotype. However, as previously mentioned, the effect might be driven by a combination of several agents and a long-term exposure (in the case of the pharmacological approach) might be required.

Importantly, the relevance and quality of our data have been strengthened by a most recent study, where leukemic cells were also shown to alter normal hematopoiesis and, interestingly, inhibiting IL-6 attenuated the effect (Welner et al., 2015).

Altogether, the present studies reveal for the first time the ability of INFα exposure to push LSCs out of quiescence, and underline the potential advantage of combining INFα with TKI for the treatment of CML patients. Such a combined treatment could potentially avoid relapse of the disease by rendering the otherwise resistant LSCs susceptible to TKI. Additionally, the present work sheds light on the detrimental impact of the leukemic cells on the function of wt progenitors and HSCs. By interfering with this process, the leukemic cells may lose competitive advantage and become impaired in their ability to propagate disease.

5. METHODS

5.1 Molecular Biology

5.1.1 Bacterial Work

5.1.1.1 Transformation of Eschericha Coli

Chemically competent E. Coli cells (Stbl3) were used for the amplification of plasmids by chemical transformation. Therefore, the cells were thawed on ice and incubated with a small amount of plasmid DNA for 30-40min on ice. After a short heat shock for 45sec at 42°C in a water bath and a cool down on ice for 2min, 200µl of S.O.C medium was added. The mix was then incubated at 37°C and slight shaking for another hour. Afterwards, some of cell suspension was spread on LB agar plates containing the required antibiotics. Plates were incubated at 37°C overnight for bacterial growth.

5.1.1.2 Bacterial liquid cultures

Single colonies were picked and transferred to 2ml of LB medium with ampicillin. These small-scale cultures were incubated over night at 37°C with shaking. For large-scale liquid cultures, the small-scale liquid cultures were transferred to 200ml of LB medium. Subsequently, the cultures were incubated over night at 37°C with shaking.

5.1.1.3 Preparation of plasmid DNA from Eschericha Coli

Plasmid preparation from large-scale bacterial liquid cultures was performed using the Qiaprep Plasmid Maxi Kit provided by Qiagen following the manufacturer's instruction. The DNA was eluted with 200µl 1x TE buffer and stored at -20°C.

5.1.2 DNA work

5.1.2.1 Preparation of genomic DNA for genotyping

PCR Tail Lysis reagent was added to a piece of mouse tail tip and incubated according to the manufacturer's instructions.

5.1.2.2 Genotyping PCR

Genomic DNA from mice was amplified by polymerase chain reactions using the Taq polymerase. The primers used are listed in the material part 6.4 and the reaction mix composed as followed:

BCR-ABL

Component	**Volume (total 25µl)**
H2O	18,95µl
Home-made buffer (10x)	2,5µl
BSA (10mg/ml)	0,25µl
dNTP's (10mM)	1µl
BCR/ABL s (10µM)	0,5µl
BCR/ABL as (10µM)	0,5µl
Home-made Taq polymerase	0,3µl
DNA	1µl

SCLtTA

Component	**Volume (total 25µl)**
H2O	15,55µl
Invitrogen buffer (10x)	2,5µl
MgCl2 (50mM)	0,75µl
DMSO	2,5µl
dNTP's (10mM)	1µl
Scl enh wt R (10µM)	0,5µl
Scl enh wt F (10µM)	0,5µl
tTA (10µM)	0,5µl
Invitrogen Taq polymerase	0,2µl
DNA	1µl

The reactions were as followed:

Transgene	**Amplification**	
BCR-ABL	95°C, 2min	
	94°C, 45sec	40x
	58°C, 1min	
	72°C, 1min	
	72°C, 5min	

SCLtTA	94°C, 5min	
	94°C, 40sec	40x
	59°C, 1min	
	72°C, 1min	
	72°C, 10min	

The amplified PCR products were analyzed by 1% agarose gel electrophoresis with expected results were as followed:

BCR-ABL	tg:	500 bp
SCLtTA	wt:	250 bp
	tg:	750 bp

5.1.3 RNA work

5.1.3.1 RNA isolation

For qPCR samples, RNA was isolated with the Arcutus PicoPure™ RNA Isolation Kit after FACS sorting the cells directly in 50µl extraction buffer delivered with the kit. All steps were carried out according to the manufacturer's protocol, including a DNA digestion step with RNAse-free DNAse.

5.1.3.2 cDNA Synthesis

RNA was reverse transcribed with the SuperScript VILO cDNA synthesis kit (Invitrogen) according to manufacturer's protocol. After completion, cDNA samples were diluted in RNAse-free water before use for quantitative real-time PCR.

5.1.3.3 Quantitative real-time PCR

Quantification of mRNA expression was performed using the ViiA™ 7 Real-Time PCR System (Applied Biosystems). Technical duplicates of all samples were performed in 384-well plates with primer concentrations of 0,5µM and a 2x DNA-polymerase-SYBR-Green master mix. RNA expression data were quantified according to the comparative ΔΔ-ct method and normalized to RNA levels of the house keeping genes *Sdha* and *Oaz1*.

The qPCR program was as followed:

Temperature	Time	
95°C	10min	
95°C	15sec	40x
60°C	60sec	

5.2 Cell and Virus Work

5.2.1 Cell culture conditions

All experiments with eukaryotic cells were performed under sterile conditions, and cells were cultivated at 37°C, 5% CO_2 and 95% humidity. All media and additives were warmed to 37°C prior to use. When the cells reached 80% confluency, they were splitted using trypsin-EDTA and distributed into new dishes containing fresh media. A list of the media used for cell culture experiments is shown below:

Cell line	Medium	FCS	Antibiotics	Further additives	Dish coating
Phoenix-GP	DMEM	10%	1% P/S	1% L-glutamine	0,1% gelatine
3T3	DMEM	10%	1% P/S	1% L-glutamine	-

5.2.2 Transient transfection of Phoenix-GP cells for virus production

For retrovirus production, the human embryonic kidney (HEK) cell line 293T-derived Phoenix-GP cells and the Calcium Phosphate Transfection Kit were used. The transient transfection was performed according to the manufacturer's instructions. In detail, on the day of transfection when the cells reached 70-80% confluence in 10cm cell culture dishes, the transfection mix was prepared (8µg MSCV BCR-Alb-IRES-eGFP retroviral plasmid, 10µg Gag/Pol packaging plasmid, 3µg envelope plasmid and 2M CaCl2 in sterile water at a final volume of 300µl), mixed thoroughly with 300µl 2x HEPES Buffered Saline (HBS, provided with the kit) and added to the cells. The incubation time was 45min at room temperature, during which the medium of the cells was replaced with fresh DMEM containing 25µM of chloroquine to increase the transfection efficiency. Afterwards, the transfection mixture was added drop-wise to the cells, which then were incubated overnight. The next morning, the culture medium was replaced by fresh medium. On the evening of the same day, the culture medium was switched to collection media (normal growth medium containing 1% HEPES buffer and having a pH of 7,8 – 7,9).

5.2.3 Retrovirus harvest

The retroviral supernatant was collected 48 hours post transfection, stored at 4°C and fresh collection medium was added to the cells for another 6-8 hours. Both harvests were combined and filtered through a 0,45µm filter. The virus particles were concentrated by ultracentrifugation (17.000 x g, 4°C overnight), and stored at -80°C after resuspension in IMDM.

5.2.4 Virus Titration

In order to assess the efficiency of the retrovirus production and to calculate the infectious units received within the process, a limiting dilution transduction series with murine 3T3 cells was conducted. Therefore, the cells were cultured as described in section 5.2.1 and seeded in 6-well plates with a concentration of 100000 cells per well. The next day, cells of two wells were collected, combined and counted to estimate the average number of cells to be transduced. A limiting dilution series of the retrovirus was prepared in growth medium containing 8µg/ml polybrene, and added to the wells. The next morning, this transduction medium was switched to fresh growth medium lacking polybrene. After an incubation time of 36-48 hours, the transduced cells were harvested and re-suspended in PBS containing 2% FCS for analysis using flow cytometry (see section 5.3.5). The dilution factor (DF), the frequency of transduced cells, the count noted on the day of transduction and the total volume were needed to calculate the infectious units (IU) as followed:

$$\left(\frac{\text{DF x frequency of transduced cells x counted cells}}{\text{volume}}\right) = \text{IU/ml}$$

5.2.5 Transduction of murine LSK cells

FACS-isolated LSK cells were pre-stimulated in serum-free StemPro 34 medium containing StemPro supplement, 1% L-glutamine, 1% P/S, 50ng/ml murine SCF, 50ng/ml murine TPO, and 50ng/ml murine Flt3-L for 48h on suspension culture plates, followed by retroviral transduction in 6-well cell culture plates pre-coated with 4µg/cm^2 retronectin. In detail, approximately 5 x 10^6 IU/well of virus was mixed with pre-stimulation medium, added to the wells and spinned down for 45min at 2500rpm, 24°C, to immobilize the virus on the pre-coated plates. Afterwards, appropriate volumes of thoroughly re-suspended cells were added onto each well of the virus-coated plate. 8h later, a second transduction round was conducted, wherein the same amount of virus was added to each well. Cells were harvested two days after

transduction, and live GFP+ cells were isolated by FACS sorting and used in transplantation experiments.

5.3 Animal experiments

5.3.1 General procedures and housing

All mice were housed in individually ventilated cages under specific pathogen-free conditions at the German Cancer Research Center (DKFZ, Heidelberg) according to international standard conditions with a 12 hours dark, 12 hours light cycle with free access to water and food. Animal handling and experimentation was performed in agreement with National Institute of Health (NIH) guidelines and approved by local authorities (Regierungspräsidium Karlsruhe).

5.3.2 Mouse strains

The SCLtTA;BCR/ABL mice were obtained from the laboratory of Dr. Steffen Koschmieder and kept on a FVB/N background (Koschmieder et al., 2005). The transgenic mice were kept on DOX in the drinking water (2 g/L) from the moment they were born until they reached adulthood (8-10 weeks old). The FVB/N wt mice were used as recipients for the generation of mixed BM chimeras. For the generation and transplantation of BCR-ABL transduced cells, C57Bl/6 mice were used.

5.3.3 Treatment

For the activation of quiescent HSCs, 5mg/kg pIC was diluted in PBS and injected intraperitoneally (i.p.) 20h before analysis. For proliferation assays, mice were injected i.p. with BrdU (18mg/kg) 14h prior to analysis. For Imatinib treatment, mice were injected i.p. with a dose of 100mg/kg daily (diluted in PBS). For all treatments, control mice received an equal volume of PBS. For the combined treatment, mice were daily treated with Imatinib for 9 days except on the 1st and 5th day when they were injected i.p. with pIC. The treatment was initiated 26 days after BM transplantation.

5.3.4 Preparation of bone marrow, spleen and peripheral blood serum

Mice were sacrificed by cervical dislocation and tibiae, femura, sternum, coxae and vertebral column were collected as source for bone marrow cells. The bones were cleaned and crushed in ice-cold RPMI-1640 medium supplemented with 2%

FCS, after which the cells were filtered through a 40µm nylon filter. Also the spleen was disintegrated in RPMI-1640 medium supplemented with 2% FCS, the cells resuspended by pipetting up and down and filtered through a 40µm nylon filter. Viability and number of bone marrow and spleen cells was assessed with the Vi-Cell Automated Cell Viability Analyzer.

For lineage depletion, bone marrow cells were incubated for 30 minutes on ice with lineage antibodies against CD4, CD8, CD11b, B220, Gr-1 and TER119 diluted in RPMI-1640 medium with 2% FCS. Afterwards, the cell suspension was washed with PBS/2%FCS, centrifuged for 5min at 16000 rpm, 4 °C, and the lineage positive cells were removed with Dynabeads® Magnetic Beads.

Peripheral blood was collected from the vena facialis into EDTA coated tubes. The blood cells were counted using the Hemavet 950 or used for FACS analysis. Therefore, the erythrocytes were lysed in 1ml of ACK buffer according to the manufacture's protocol, washed and stained as described in section 5.3.5.

5.3.5 Fluorescence activated cell staining and sorting (FACS)

All antibodies for cell staining and sorting were titrated with whole bone marrow before using them in experiments. In general, the antibodies were diluted in a mixture of 50% PBS (with 2% FCS) and 50% 24G2 hybridoma cell line supernatant to prevent unspecific binding. Only for analysis of CD16/32 expression the respective antibody was diluted only in PBS/FCS. Cells were incubated with antibody dilution for 30min on ice. Incubation with biotin-coupled antibodies was followed by an additional incubation step of 20min on ice with streptavidin conjugates.

All cell suspensions were filtered through a 70 µm nylon mesh filter prior to FACS analysis, which was performed using the BD LSRII or BD LSR Fortessa with 350 nm, 405 nm, 488 nm, 561 nm, and 640 nm lasers. For cell sorting, the BD Aria I, Aria II and Aria III were used. For all flow cytometeric applications, compensation using OneComp eBeads stained with single antibodies and the auto-compensation tool of the BD FACSDiva software was performed. Data were analyzed with the FlowJo software.

5.3.6 Transplantation

For the generation of mixed BM chimeras, FVB/N recipient mice were lethally irradiated (2 x 475 rad) before intravenously (i.v.) receiving 5 x 10^6 bone marrow cells (diluted in 200µl of PBS) with a 1:1 ratio of each genotype. A FACS analysis of the injected cells was performed in order to assess the input ratio, and the mixed blood chimerism was monitored every two weeks by FACS analysis. During the first three

weeks after transplantation, all mice received antibiotic (Cotrim) containing water. Transgenic and wt cells were distinguished by using mice with different CD45 isoforms, CD45.1 and CD45.2, respectively. For the BCR-ABL transduced cells, C57BL/6J mice with the CD45.1 isoform were used for transduction whereas C57BL/6J mice with the CD45.2 isoform were used as wt. In this case, C57BL/6J (CD45.2) lethally irradiated recipients (2 x 475 rad) were i.v. injected with 1.5 x 10^4 LSK cells, unless stated otherwise.

5.3.7 Cell Cycle and Proliferation Analysis

Assessment of the cell cycle activity and proliferation profile of HSCs was performed by cell surface staining as described in section 5.3.5, combined with intracellular DNA Ki67-Hoechst staining or BrdU incorporation assays, respectively.
For the Ki67-Hoechst analysis, cells were fixed with Cytofix/Cytoperm buffer after cell surface staining, then washed with 1x Permwash and subsequently stained with anti-Ki67-FITC or anti-Ki67-APC at 4°C overnight. Cells were co-incubated with 25µg/ml of Hoechst 33342 10min before analysis.

For the BrdU analysis, mice were injected i.p. with 18mg/kg BrdU 14h before sacrifice. Bone marrow cells were isolated and stained as described in section 5.3.5. Fixation, DNAse I treatment and intra-cellular BrdU staining of the cells were performed according to the manufacturer's protocol of the BD Pharmigen™ FITC or APC BrdU Flow Kit.

5.3.8 Cytokine Array & ELISA

Femura and tibiae were crushed in 450µl RPMI, and the BM supernatant was used for the cytokine array or ELISAs according to manufacturer's instructions (see material section 6.2). The SpectraMax M5 Microplate Reader from Molecular Devices was used to measure the absorbance.

5.3.9 Colony-forming assay

Bone marrow cells were prepared and stained as described in section 5.3.5. 500 LSK sorted cells were plated in 1ml of Methocult 3434® into 35mm tissue culture dishes as duplicates and incubated in a humidified atmosphere at 37°C and 5% CO2. After 7d, colonies were counted using an inverted microscope.

5.4 Statistical Analysis

Data plotted in figures are mean ± standard deviation (SD) generated with the GraphPad Prism® software. Statistical analyses were performed using unpaired two-tailed student's t-test. Statistical significance is indicated by *$p < 0.05$, **$p < 0.01$, ***$p < 0.001$.

6. MATERIAL

6.1 Antibodies

Antigen	Clone	Label	Distributor
B220	RA3-6B2	PECy5, PECy7	eBioscience
B220	RA3-6B2	Biotin	BioLegend
CD4	GK1.5	PECy7	eBioscience
CD4	GK1.5	Biotin	BioLegend
CD8a	53-6.7	PECy7	eBioscience
CD8a	53-6.7	Biotin	BioLegend
CD11b	M1/70	PECy7	eBioscience
CD11b	M1/70	Biotin	BioLegend
CD34	RAM34	FITC, Alexa700	eBioscience
CD45.1	A20.1	FITC	eBioscience
CD45.2	104	Pacific Blue	BioLegend
CD45.2	104	Alexa700	BD Pharmingen
CD48	HM48-1	PE	eBioscience
CD48	HM48-1	Pacific Blue	BioLegend
CD150	TC15-12F12.2	PECy5, APC	BioLegend
CD117 (c-Kit)	2B8	PE, APC	eBioscience
Gr-1 (Ly6G)	RB6-8C5	PE, PECy7	eBioscience
Gr-1	RB6-8C5	Biotin	BioLegend
Ki67	B56	FITC, APC	BD Pharmingen
Sca-1	D7	APC-Cy7	BD Pharmingen
Streptavidine	-	PETexasRed	BD Pharmingen
TER-119	TER-119	PECy7, APC-Cy7	eBioscience
TER-119	TER-119	Biotin	BioLegend

6.2 Kits

Kit	Distributor
ABI Power SYBR Green Master Mix	Applied Biosciences
APC BrdU Flow Kit	BD Pharmingen
Arcturus® PicoPure® RNA Isolation Kit	Life Technologies
Calcium Phosphate Kit	Invitrogen

DNAse Set, RNAse-free	Qiagen
FITC BrdU Flow Kit	BD Pharmingen
Mouse IL-6 ELISA Kit	R&D Systems
Mouse IL-1 beta/Il-1F2 Quantikine ELISA Kit	R&D Systems
Mouse MIP-1 alpha Quantikine ELISA Kit	R&D Systems
Mouse MIP 1 beta Quantikine ELISA Kit	R&D Systems
Mouse Cytokine Antibody Array, Panel A	R&D Systems
QIAGEN Plasmid Mega Kit	Qiagen
SuperScript® VILOTM cDNA Synthesis Kit	Life Technologies

6.3 Oligonucleotides for genotyping

Product	Primer	Sequence (5‘ → 3‘)
BCR-ABL	Sense	GAGCGTGCAGAGTGGAGGGAGAAC
	Anti-sense	GGTACCAGGAGTGTTTCTCCAGACTG
SCLtTA	SCLenh wt R	AGAACAGAATTCAGGGTCTTCCTT
	SCLenh wt F	GGGCAGTTGATGTGTTTGTG
	tTA5 F	TTTCGATCTGGACATGTTGG

6.4 qRT-PCR primers

Gene	Direction	Sequence (5‘ → 3‘)
Isg15	fwd	TCCTTAATTCCAGGGGACCTA
Isg15	rev	ACCGTCATGGAGTTAGTCACG
Oaz1	fwd	TTTCAGCTAGCATCCTGTACTCC
Oaz1	rev	GACCCTGGTCTTGTCGTTAGA
Sdha	fwd	AAGTTGAGATTTGCCGATGC
Sdha	rev	TGGTTCTGCATCGACTTCTG

6.5 Cell lines

Cell line	Distributor
Phoenix-GP (HEK 293T-derived) cell line	ATCC
3T3 (murine embryonic fibroblast) cell line	ATCC
E. coli Stbl3 Chemically Competent Cells	Life Technologies

6.6 Mice

Mouse	Distributor
C57Bl6/J	Harlan Laboratories
FVB/N	Charles River
SCLtTA/BCR-Abl	Dr. Steffen Koschmieder

6.7 Enzymes

Enzyme	Distributor
DNase I	Qiagen
Proteinase K	Thermo Scientific
Taq Polymerase	Invitrogen

6.8 Reagents and Consumables

Chemical/Reagent	Distributor
6-well cell culture plates	Corning
ACK buffer	Life Technologies
Chloroquine	AppliChem
Cytox/CytopermTM Buffer	BD Biosciences
Dulbecco's modified Eagle's medium (DMEM)	Sigma
Dynabeads® Magnetic beads	Invitrogen
Fetal calf serum (FCS)	Invitrogen
Filters (0.45 µm)	Millipore
Gelatine-coated (0,1%) tissue culture dishes	Sigma
HEPES buffer	Life Technologies
Hoechst 33342	Molecular Probes
Imatinib Mesylate	Selleckchem
Iscove's modified Dulbecco's medium (IMDM)	Life Technologies
LB-Agar	Merck
LB medium	Merck
L-Glutamine	Invitrogen
Methocult 3434	Stem Cell Technologies
Murine Flt3-L	PeproTech
Murine TPO	PeproTech,

Murine SCF	PeproTech
Nylon filter (40 µm)	BD Biosciences
Nylon filter (70 µm)	BD Biosciences
OneComp eBeads	eBioscience
PCR Tail Lysis Reagent	Peqlab
Penicillin / Streptomycin (P/S)	Invitrogen
Polybrene	Sigma
Retronectin	TaKaRa
RPMI-1640 medium	Sigma
S.O.C medium	Invitrogen
StemPro 34 medium	Invitrogen
StemPro supplement	Invitrogen
Suspension culture plates	Cellstar
Tissue culture dishes (35 mm)	Stem Cell Technologies
Trypsin-EDTA solution	Life Technologies

6.9 Instruments

Equipment	**Distributor**
Aria I, Aria II, Aria III	BD Biosciences
Centrifuge (5810R)	Eppendorf
Hemavet 950	Drew Scientific
LSRII and LSR Fortessa	BD Biosciences
SpectraMax M5 Microplate Reader	Molecular Devices
Vi-Cell Automated Cell Viability Analyzer	Beckmann
ViiA^{TM} 7 Real-Time PCR System	Applied Biosystems

6.10 Software

Software	**Distributor**
Endnote	Thomson
FlowJo	Tree Star
GraphPad Prism®	GraphPad Software Inc.
Pubmed	http://www.pubmedcentral.nih.gov

7. APPENDIX

7.1 List of figures

7.2 Abbreviations

2G	Second generation
ABL	Abelson murine leukemia viral oncogene homolog
BL6	C57BL/6 mice
AKT	Protein kinase B (PKB)
AlloSCT	Allogeneic stem cell transplantation
APC	Allophycocyanine
APC-Cy7	Allophycocyanine-cyanine 7
BC	Blast crisis
BCR	Breakpoint cluster region
BM	Bone marrow
BMT	Bone marrow transplantation
BrdU	5-bromo-2-deoxyuridine
CCyR	Complete cytogenetic response
CD	Cluster of differentiation
CFU	Colony forming unit
CHR	Complete hematological response
c-Kit	V-kit Hardy-Zuckerman 4 feline sarcoma cellular homologue
CLP	Common lymphoid progenitor

CML	Chronic myeloid leukemia
CMP	Common myeloid progenitor
CP	Chronic phase
CSC	Cancer stem cells
DC	Dendritic cells
DNA	Deoxyribonucleic acid
DOX	Doxycycline
dsRNA	Double-stranded RNA
dtg	Double-transgenic
ECs	Endothelial cells
ELISA	Enzyme-linked immunosorbent assay
ELN	European Leukemia Net
EO	Eosinophils
ERK	Extracellular-signal-regulated kinase
FACS	Fluorescence-activated cell sorting
Flt-3	Fms-like tyrosine kinase 3
FGF2	Fibroblast growth factor 2
FISH	Fluorescent in situ hybridization
FITC	Fluorescein isothiocyanate
GFP	Green fluorescent protein
GMP	Granulocyte-macrophage progenitor
HSC	Hematopoietic stem cell
i.f.	Intrafemoral
i.p.	Intraperitoneal
i.v.	Intravenous
IFN	Interferon
IFNAR	Interferon-α/β receptor
IFNα	Interferon-alpha
IL	Interleukin
ISG	Interferon-alpha inducible genes
IVC	Individually ventilated cage
JAK	Janus kinase
LSC	Leukemic stem cell
LT-HSC	Long term hematopoietic stem cell

LY	Lymphocytes
MEK	Mitogen-activated protein kinase kinase (MAP2K, MAPKK)
MEP	Megakaryocyte-erythrocyte progenitor
MIP	Macrophage inflammatory protein
MkP	Megakaryocyte progenitor
MMR	Major molecular response
MO	Monocytes
MPP	Multipotent progenitor
mRNA	Messenger RNA
MSC	Mesenchymal stem cell
mTOR	Mammalian target of rapamycin
NE	Neutrophils
OBs	Osteoblasts
PB	Pacific blue
PBS	Phosphate buffered saline
PCR	Polymerase chain reaction
PE	Phycoerythrin
PE-Cy5	Phycoerythrin-cyanine 5
Ph	Philadelphia chromosome
PI3K	Phosphoinositide 3-kinase
pIC	Polyinosinic-polycytidylic acid
qRT-PCR	Quantitative real-time polymerase chain reaction
RAF	Rapidly accelerated fibrosarcoma
RAS	Rat sarcoma
RBCs	Red blood cell
ROS	Reactive oxygen species
RT-PCR	Reverse transcriptase-polymerase chain reaction
Sca-1	Stem cell antigen 1
SCF	Stem cell factor
SCL	Stem cell leukemia
SDHA	Succinate dehydrogenase complex subunit A
SLAM	Signaling lymphocytic activation molecule
STAT1	Signal transducer and activator of transcription 1
stg	Single-transgenic

ST-HSC	Short term hematopoietic stem cell
TKI	Tyrosine kinase inhibitor
TPO	Thrombopoietin
TRE	Tetracycline Response Element
tTA	Tetracycline transactivator
UMRD	Undetectable minimal residual disease
USA	United States of America
WBC	White blood cells
WT	Wild-type

7.3 Acknowledgements

First of all I would like to thank **Marieke Essers** and **Andreas Trumpp** for giving me the opportunity to perform my PhD studies in HI-STEM.

I would like to further thank **Marieke Essers** for all the supervision, advice and support across my PhD studies.

I would like to thank all **members of the Essers Lab** for critical discussions, feedback and exchange of technical knowledge.

I would like to thank all **members of HI-STEM** for exchange of ideas and technical expertise.

I would like to thank **Sandra Blaszkiewicz** and **Andrea Kuck** for all the technical support, including bone marrow isolation, bleeding of mice and genotyping.

I would like to thank **Mick Milsom** for providing me with the retroviral vector. Also I would like to thank him and all his group members for critical discussion during our joint group meetings.

I would like to thank **Simon** for the translation of my abstract into German.

I would like to thank **Corinna** for taking care of the ordering.

I would like to thank my TAC members **Andreas Trumpp**, **Martin Müller** and **Alwin Krämer** for taking the time to attend my TAC meetings and providing new insights for the further development of my project.

I would like to thank all of my examiners, **Andreas Trumpp**, **Alwin Krämer**, **Matthias Mayer** and **Karin Müller-Decker** for accepting to be part of my PhD defense examination committee and taking the time to read and evaluate my thesis.

I would like to thank all the **FACS facility members** for performing the sorts and maintaining the instruments.

I would like to thank our **animal caretakers** for the maintenance of our mouse facility and the irradiation of mice.

8. BIBLIOGRAPHY

(1997). Interferon alfa versus chemotherapy for chronic myeloid leukemia: a meta-analysis of seven randomized trials: Chronic Myeloid Leukemia Trialists' Collaborative Group. J Natl Cancer Inst *89*, 1616-1620.

(2013). The price of drugs for chronic myeloid leukemia (CML) is a reflection of the unsustainable prices of cancer drugs: from the perspective of a large group of CML experts. Blood *121*, 4439-4442.

Abramson, S., Miller, R. G., and Phillips, R. A. (1977). The identification in adult bone marrow of pluripotent and restricted stem cells of the myeloid and lymphoid systems. J Exp Med *145*, 1567-1579.

Adolfsson, J., Mansson, R., Buza-Vidas, N., Hultquist, A., Liuba, K., Jensen, C. T., Bryder, D., Yang, L., Borge, O. J., Thoren, L. A.*, et al.* (2005). Identification of Flt3+ lympho-myeloid stem cells lacking erythro-megakaryocytic potential a revised road map for adult blood lineage commitment. Cell *121*, 295-306.

Akashi, K., Traver, D., Miyamoto, T., and Weissman, I. L. (2000). A clonogenic common myeloid progenitor that gives rise to all myeloid lineages. Nature *404*, 193-197.

Arranz, L., Sanchez-Aguilera, A., Martin-Perez, D., Isern, J., Langa, X., Tzankov, A., Lundberg, P., Muntion, S., Tzeng, Y. S., Lai, D. M.*, et al.* (2014). Neuropathy of haematopoietic stem cell niche is essential for myeloproliferative neoplasms. Nature *512*, 78-81.

Baccarani, M., Deininger, M. W., Rosti, G., Hochhaus, A., Soverini, S., Apperley, J. F., Cervantes, F., Clark, R. E., Cortes, J. E., Guilhot, F.*, et al.* (2013). European LeukemiaNet recommendations for the management of chronic myeloid leukemia: 2013. Blood *122*, 872-884.

Bakker, S. T., and Passegue, E. (2013). Resilient and resourceful: genome maintenance strategies in hematopoietic stem cells. Exp Hematol *41*, 915-923.

Balazs, A. B., Fabian, A. J., Esmon, C. T., and Mulligan, R. C. (2006). Endothelial protein C receptor (CD201) explicitly identifies hematopoietic stem cells in murine bone marrow. Blood *107*, 2317-2321.

Baldridge, M. T., King, K. Y., Boles, N. C., Weksberg, D. C., and Goodell, M. A. (2010). Quiescent haematopoietic stem cells are activated by IFN-gamma in response to chronic infection. Nature *465*, 793-797.

Becker, A. J., Mc, C. E., and Till, J. E. (1963). Cytological demonstration of the clonal nature of spleen colonies derived from transplanted mouse marrow cells. Nature *197*, 452-454.

Belardelli, F., Ferrantini, M., Proietti, E., and Kirkwood, J. M. (2002). Interferon-alpha in tumor immunity and immunotherapy. Cytokine Growth Factor Rev *13*, 119-134.

Benz, C., Copley, M. R., Kent, D. G., Wohrer, S., Cortes, A., Aghaeepour, N., Ma, E., Mader, H., Rowe, K., Day, C.*, et al.* (2012). Hematopoietic stem cell subtypes expand differentially during development and display distinct lymphopoietic programs. Cell Stem Cell *10*, 273-283.

Bhattacharya, S., Zheng, H., Tzimas, C., Carroll, M., Baker, D. P., and Fuchs, S. Y. (2011). Bcr-abl signals to desensitize chronic myeloid leukemia cells to IFNalpha via accelerating the degradation of its receptor. Blood *118*, 4179-4187.

Bolton-Gillespie, E., Schemionek, M., Klein, H. U., Flis, S., Hoser, G., Lange, T., Nieborowska-Skorska, M., Maier, J., Kerstiens, L., Koptyra, M.*, et al.* (2013). Genomic instability may originate from imatinib-refractory chronic myeloid leukemia stem cells. Blood *121*, 4175-4183.

Bonnet, D., and Dick, J. E. (1997). Human acute myeloid leukemia is organized as a hierarchy that originates from a primitive hematopoietic cell. Nat Med *3*, 730-737.

Borden, E. C., Sen, G. C., Uze, G., Silverman, R. H., Ransohoff, R. M., Foster, G. R., and Stark, G. R. (2007). Interferons at age 50: past, current and future impact on biomedicine. Nat Rev Drug Discov *6*, 975-990.

Brazma, D., Grace, C., Howard, J., Melo, J. V., Holyoke, T., Apperley, J. F., and Nacheva, E. P. (2007). Genomic profile of chronic myelogenous leukemia: Imbalances associated with disease progression. Genes Chromosomes Cancer *46*, 1039-1050.

Cassuto, O., Dufies, M., Jacquel, A., Robert, G., Ginet, C., Dubois, A., Hamouda, A., Puissant, A., Luciano, F., Karsenti, J. M.*, et al.* (2012). All tyrosine kinase inhibitor-resistant chronic myelogenous cells are highly sensitive to ponatinib. Oncotarget *3*, 1557-1565.

Cedar, H., and Bergman, Y. (2011). Epigenetics of haematopoietic cell development. Nat Rev Immunol *11*, 478-488.

Cheshier, S. H., Prohaska, S. S., and Weissman, I. L. (2007). The effect of bleeding on hematopoietic stem cell cycling and self-renewal. Stem Cells Dev *16*, 707-717.

Cho, R. W., and Clarke, M. F. (2008). Recent advances in cancer stem cells. Curr Opin Genet Dev *18*, 48-53.

Chomel, J. C., Bonnet, M. L., Sorel, N., Bertrand, A., Meunier, M. C., Fichelson, S., Melkus, M., Bennaceur-Griscelli, A., Guilhot, F., and Turhan, A. G. (2011). Leukemic stem cell persistence in chronic myeloid leukemia patients with sustained undetectable molecular residual disease. Blood *118*, 3657-3660.

Chomel, J. C., and Turhan, A. G. (2011). Chronic myeloid leukemia stem cells in the era of targeted therapies: resistance, persistence and long-term dormancy. Oncotarget *2*, 713-727.

Chu, S., McDonald, T., Lin, A., Chakraborty, S., Huang, Q., Snyder, D. S., and Bhatia, R. (2011). Persistence of leukemia stem cells in chronic myelogenous leukemia patients in prolonged remission with imatinib treatment. Blood *118*, 5565-5572.

Corbin, A. S., Agarwal, A., Loriaux, M., Cortes, J., Deininger, M. W., and Druker, B. J. (2011). Human chronic myeloid leukemia stem cells are insensitive to imatinib despite inhibition of BCR-ABL activity. J Clin Invest *121*, 396-409.

Cortes, J. (2004). Natural history and staging of chronic myelogenous leukemia. Hematol Oncol Clin North Am *18*, 569-584, viii.

Cortes, J. E., Kantarjian, H., Shah, N. P., Bixby, D., Mauro, M. J., Flinn, I., O'Hare, T., Hu, S., Narasimhan, N. I., Rivera, V. M.*, et al.* (2012). Ponatinib in refractory Philadelphia chromosome-positive leukemias. N Engl J Med *367*, 2075-2088.

Cortes, J. E., Kim, D. W., Pinilla-Ibarz, J., le Coutre, P., Paquette, R., Chuah, C., Nicolini, F. E., Apperley, J. F., Khoury, H. J., Talpaz, M.*, et al.* (2013). A phase 2 trial of ponatinib in Philadelphia chromosome-positive leukemias. N Engl J Med *369*, 1783-1796.

Cortes, J. E., Talpaz, M., and Kantarjian, H. (2014). Ponatinib in Philadelphia chromosome-positive leukemias. N Engl J Med *370*, 577.

Dai, Y., Rahmani, M., Corey, S. J., Dent, P., and Grant, S. (2004). A Bcr/Abl-independent, Lyn-dependent form of imatinib mesylate (STI-571) resistance is associated with altered expression of Bcl-2. J Biol Chem *279*, 34227-34239.

de Veer, M. J., Holko, M., Frevel, M., Walker, E., Der, S., Paranjape, J. M., Silverman, R. H., and Williams, B. R. (2001). Functional classification of interferon-stimulated genes identified using microarrays. J Leukoc Biol *69*, 912-920.

Deininger, M. W., Goldman, J. M., and Melo, J. V. (2000). The molecular biology of chronic myeloid leukemia. Blood *96*, 3343-3356.

Dick, J. E. (2008). Stem cell concepts renew cancer research. Blood *112*, 4793-4807.

Donato, N. J., Wu, J. Y., Stapley, J., Gallick, G., Lin, H., Arlinghaus, R., and Talpaz, M. (2003). BCR-ABL independence and LYN kinase overexpression in chronic myelogenous leukemia cells selected for resistance to STI571. Blood *101*, 690-698.

Druker, B. J., Guilhot, F., O'Brien, S. G., Gathmann, I., Kantarjian, H., Gattermann, N., Deininger, M. W. N., Silver, R. T., Goldman, J. M., Stone, R. M.*, et al.* (2006). Five-year follow-up of patients receiving imatinib for chronic myeloid leukemia. New Engl J Med *355*, 2408-2417.

Druker, B. J., and Lydon, N. B. (2000). Lessons learned from the development of an Abl tyrosine kinase inhibitor for chronic myelogenous leukemia. Journal of Clinical Investigation *105*, 3-7.

Drummond, M. W., Heaney, N., Kaeda, J., Nicolini, F. E., Clark, R. E., Wilson, G., Shepherd, P., Tighe, J., McLintock, L., Hughes, T., and Holyoake, T. L. (2009). A pilot study of continuous imatinib vs pulsed imatinib with or without G-CSF in CML patients who have achieved a complete cytogenetic response. Leukemia *23*, 1199-1201.

Dunlop, D. J., Wright, E. G., Lorimore, S., Graham, G. J., Holyoake, T., Kerr, D. J., Wolpe, S. D., and Pragnell, I. B. (1992). Demonstration of stem cell inhibition and myeloprotective effects of SCI/rhMIP1 alpha in vivo. Blood *79*, 2221-2225.

Dykstra, B., Kent, D., Bowie, M., McCaffrey, L., Hamilton, M., Lyons, K., Lee, S. J., Brinkman, R., and Eaves, C. (2007). Long-term propagation of distinct hematopoietic differentiation programs in vivo. Cell Stem Cell *1*, 218-229.

Efficace, F., Baccarani, M., Breccia, M., Alimena, G., Rosti, G., Cottone, F., Deliliers, G. L., Barate, C., Rossi, A. R., Fioritoni, G.*, et al.* (2011). Health-related quality of life in chronic myeloid leukemia patients receiving long-term therapy with imatinib compared with the general population. Blood *118*, 4554-4560.

Ema, H., Morita, Y., and Suda, T. (2014). Heterogeneity and hierarchy of hematopoietic stem cells. Exp Hematol *42*, 74-82 e72.

Engler, J. R., Frede, A., Saunders, V. A., Zannettino, A. C., Hughes, T. P., and White, D. L. (2010). Chronic myeloid leukemia CD34+ cells have reduced uptake of imatinib due to low OCT-1 activity. Leukemia *24*, 765-770.

Eppert, K., Takenaka, K., Lechman, E. R., Waldron, L., Nilsson, B., van Galen, P., Metzeler, K. H., Poeppl, A., Ling, V., Beyene, J.*, et al.* (2011). Stem cell gene expression programs influence clinical outcome in human leukemia. Nat Med *17*, 1086-1093.

Essers, M. A., Offner, S., Blanco-Bose, W. E., Waibler, Z., Kalinke, U., Duchosal, M. A., and Trumpp, A. (2009). IFNalpha activates dormant haematopoietic stem cells in vivo. Nature *458*, 904-908.

Fava, C., Rege-Cambrin, G., and Saglio, G. (2015). The choice of first-line chronic myelogenous leukemia treatment. Ann Hematol *94 Suppl 2*, S123-131.

Fitzgerald-Bocarsly, P., Dai, J., and Singh, S. (2008). Plasmacytoid dendritic cells and type I IFN: 50 years of convergent history. Cytokine Growth Factor Rev *19*, 3-19.

Fleischman, A. G., Aichberger, K. J., Luty, S. B., Bumm, T. G., Petersen, C. L., Doratotaj, S., Vasudevan, K. B., LaTocha, D. H., Yang, F., Press, R. D.*, et al.* (2011). TNFalpha facilitates clonal expansion of JAK2V617F positive cells in myeloproliferative neoplasms. Blood *118*, 6392-6398.

Ford, C. E., Hamerton, J. L., Barnes, D. W., and Loutit, J. F. (1956). Cytological identification of radiation-chimaeras. Nature *177*, 452-454.

Gallipoli, P., Pellicano, F., Morrison, H., Laidlaw, K., Allan, E. K., Bhatia, R., Copland, M., Jorgensen, H. G., and Holyoake, T. L. (2013a). Autocrine TNF-alpha production supports CML stem and progenitor cell survival and enhances their proliferation. Blood *122*, 3335-3339.

Gallipoli, P., Stobo, J., Heaney, N., Nicolini, F. E., Clark, R., Wilson, G., Tighe, J., McLintock, L., Hughes, T., Michor, F.*, et al.* (2013b). Safety and efficacy of pulsed imatinib with or without G-CSF versus continuous imatinib in chronic phase chronic myeloid leukaemia patients at 5 years follow-up. Br J Haematol *163*, 674-676.

Gekas, C., and Graf, T. (2013). CD41 expression marks myeloid-biased adult hematopoietic stem cells and increases with age. Blood *121*, 4463-4472.

Glauche, I., Horn, K., Horn, M., Thielecke, L., Essers, M. A., Trumpp, A., and Roeder, I. (2012). Therapy of chronic myeloid leukaemia can benefit from the activation of stem cells: simulation studies of different treatment combinations. Br J Cancer *106*, 1742-1752.

Goardon, N., Marchi, E., Atzberger, A., Quek, L., Schuh, A., Soneji, S., Woll, P., Mead, A., Alford, K. A., Rout, R.*, et al.* (2011). Coexistence of LMPP-like and GMP-like leukemia stem cells in acute myeloid leukemia. Cancer Cell *19*, 138-152.

Golas, J. M., Arndt, K., Etienne, C., Lucas, J., Nardin, D., Gibbons, J., Frost, P., Ye, F., Boschelli, D. H., and Boschelli, F. (2003). SKI-606, a 4-anilino-3-quinolinecarbonitrile dual inhibitor of Src and Abl kinases, is a potent antiproliferative agent against chronic myelogenous leukemia cells in culture and causes regression of K562 xenografts in nude mice. Cancer Res *63*, 375-381.

Goldman, J. M. (2009). Treatment strategies for CML. Best Pract Res Clin Haematol *22*, 303-313.

Goldman, J. M., and Melo, J. V. (2001). Targeting the BCR-ABL tyrosine kinase in chronic myeloid leukemia. New Engl J Med *344*, 1084-1086.

Grassinger, J., Haylock, D. N., Williams, B., Olsen, G. H., and Nilsson, S. K. (2010). Phenotypically identical hemopoietic stem cells isolated from different regions of bone marrow have different biologic potential. Blood *116*, 3185-3196.

Groffen, J., Stephenson, J. R., Heisterkamp, N., de Klein, A., Bartram, C. R., and Grosveld, G. (1984). Philadelphia chromosomal breakpoints are clustered within a limited region, bcr, on chromosome 22. Cell *36*, 93-99.

Grossmann, V., Kohlmann, A., Zenger, M., Schindela, S., Eder, C., Weissmann, S., Schnittger, S., Kern, W., Muller, M. C., Hochhaus, A.*, et al.* (2011). A deep-sequencing study of chronic myeloid leukemia patients in blast crisis (BC-CML) detects mutations in 76.9% of cases. Leukemia *25*, 557-560.

Grosso, S., Puissant, A., Dufies, M., Colosetti, P., Jacquel, A., Lebrigand, K., Barbry, P., Deckert, M., Cassuto, J. P., Mari, B., and Auberger, P. (2009). Gene expression profiling of imatinib and PD166326-resistant CML cell lines identifies Fyn as a gene associated with resistance to BCR-ABL inhibitors. Mol Cancer Ther *8*, 1924-1933.

Guzman, M. L., and Allan, J. N. (2014). Concise review: Leukemia stem cells in personalized medicine. Stem Cells *32*, 844-851.

Haas, S., Hansson, J., Klimmeck, D., Loeffler, D., Velten, L., Uckelmann, H., Wurzer, S., Prendergast, A. M., Schnell, A., Hexel, K.*, et al.* (2015). Inflammation-Induced Emergency Megakaryopoiesis Driven by Hematopoietic Stem Cell-like Megakaryocyte Progenitors. Cell Stem Cell *17*, 422-434.

Hamilton, A., Helgason, G. V., Schemionek, M., Zhang, B., Myssina, S., Allan, E. K., Nicolini, F. E., Muller-Tidow, C., Bhatia, R., Brunton, V. G.*, et al.* (2012). Chronic myeloid leukemia stem cells are not dependent on Bcr-Abl kinase activity for their survival. Blood *119*, 1501-1510.

Hehlmann, R., Lauseker, M., Jung-Munkwitz, S., Leitner, A., Muller, M. C., Pletsch, N., Proetel, U., Haferlach, C., Schlegelberger, B., Balleisen, L.*, et al.* (2011). Tolerability-adapted imatinib 800 mg/d versus 400 mg/d versus 400 mg/d plus interferon-alpha in newly diagnosed chronic myeloid leukemia. J Clin Oncol *29*, 1634-1642.

Hervas-Stubbs, S., Riezu-Boj, J. I., Gonzalez, I., Mancheno, U., Dubrot, J., Azpilicueta, A., Gabari, I., Palazon, A., Aranguren, A., Ruiz, J.*, et al.* (2010). Effects of IFN-alpha as a signal-3 cytokine on human naive and antigen-experienced CD8(+) T cells. Eur J Immunol *40*, 3389-3402.

Hochhaus, A., O'Brien, S. G., Guilhot, F., Druker, B. J., Branford, S., Foroni, L., Goldman, J. M., Muller, M. C., Radich, J. P., Rudoltz, M.*, et al.* (2009). Six-year follow-up of patients receiving imatinib for the first-line treatment of chronic myeloid leukemia. Leukemia *23*, 1054-1061.

Huang, X., Cortes, J., and Kantarjian, H. (2012). Estimations of the increasing prevalence and plateau prevalence of chronic myeloid leukemia in the era of tyrosine kinase inhibitor therapy. Cancer *118*, 3123-3127.

Ito, K., Bernardi, R., Morotti, A., Matsuoka, S., Saglio, G., Ikeda, Y., Rosenblatt, J., Avigan, D. E., Teruya-Feldstein, J., and Pandolfi, P. P. (2008). PML targeting eradicates quiescent leukaemia-initiating cells. Nature *453*, 1072-1078.

Jabbour, E., and Kantarjian, H. (2014). Chronic myeloid leukemia: 2014 update on diagnosis, monitoring, and management. Am J Hematol *89*, 547-556.

Jamieson, C. H., Ailles, L. E., Dylla, S. J., Muijtjens, M., Jones, C., Zehnder, J. L., Gotlib, J., Li, K., Manz, M. G., Keating, A.*, et al.* (2004). Granulocyte-macrophage progenitors as candidate leukemic stem cells in blast-crisis CML. N Engl J Med *351*, 657-667.

Jemal, A., Siegel, R., Xu, J., and Ward, E. (2010). Cancer statistics, 2010. CA Cancer J Clin *60*, 277-300.

Jiang, X., Zhao, Y., Smith, C., Gasparetto, M., Turhan, A., Eaves, A., and Eaves, C. (2007). Chronic myeloid leukemia stem cells possess multiple unique features of resistance to BCR-ABL targeted therapies. Leukemia *21*, 926-935.

Jin, L., Tabe, Y., Konoplev, S., Xu, Y., Leysath, C. E., Lu, H., Kimura, S., Ohsaka, A., Rios, M. B., Calvert, L.*, et al.* (2008). CXCR4 up-regulation by imatinib induces chronic myelogenous leukemia (CML) cell migration to bone marrow stroma and promotes survival of quiescent CML cells. Mol Cancer Ther *7*, 48-58.

Jorgensen, H. G., Copland, M., Allan, E. K., Jiang, X., Eaves, A., Eaves, C., and Holyoake, T. L. (2006). Intermittent exposure of primitive quiescent chronic myeloid leukemia cells to granulocyte-colony stimulating factor in vitro promotes their elimination by imatinib mesylate. Clin Cancer Res *12*, 626-633.

Kantarjian, H., and Cortes, J. (2011). Considerations in the management of patients with Philadelphia chromosome-positive chronic myeloid leukemia receiving tyrosine kinase inhibitor therapy. J Clin Oncol *29*, 1512-1516.

Kantarjian, H. M., Shan, J., Jones, D., O'Brien, S., Rios, M. B., Jabbour, E., and Cortes, J. (2009). Significance of increasing levels of minimal residual disease in

patients with Philadelphia chromosome-positive chronic myelogenous leukemia in complete cytogenetic response. J Clin Oncol *27*, 3659-3663.

Kharas, N. G., and Fruman, D. A. (2005). ABL oncogenes and phosphoinositide 3-kinase: Mechanism of activation and downstream effectors. Cancer Res *65*, 2047-2053.

Khorashad, J. S., Kelley, T. W., Szankasi, P., Mason, C. C., Soverini, S., Adrian, L. T., Eide, C. A., Zabriskie, M. S., Lange, T., Estrada, J. C*., et al.* (2013). BCR-ABL1 compound mutations in tyrosine kinase inhibitor-resistant CML: frequency and clonal relationships. Blood *121*, 489-498.

Kiel, M. J., and Morrison, S. J. (2008). Uncertainty in the niches that maintain haematopoietic stem cells. Nat Rev Immunol *8*, 290-301.

Kiel, M. J., Yilmaz, O. H., Iwashita, T., Terhorst, C., and Morrison, S. J. (2005). SLAM family receptors distinguish hematopoietic stem and progenitor cells and reveal endothelial niches for stem cells. Cell *121*, 1109-1121.

Kondo, M., Wagers, A. J., Manz, M. G., Prohaska, S. S., Scherer, D. C., Beilhack, G. F., Shizuru, J. A., and Weissman, I. L. (2003). Biology of hematopoietic stem cells and progenitors: implications for clinical application. Annu Rev Immunol *21*, 759-806.

Kondo, M., Weissman, I. L., and Akashi, K. (1997). Identification of clonogenic common lymphoid progenitors in mouse bone marrow. Cell *91*, 661-672.

Koschmieder, S., Gottgens, B., Zhang, P., Iwasaki-Arai, J., Akashi, K., Kutok, J. L., Dayaram, T., Geary, K., Green, A. R., Tenen, D. G., and Huettner, C. S. (2005). Inducible chronic phase of myeloid leukemia with expansion of hematopoietic stem cells in a transgenic model of BCR-ABL leukemogenesis. Blood *105*, 324-334.

Krivtsov, A. V., Twomey, D., Feng, Z., Stubbs, M. C., Wang, Y., Faber, J., Levine, J. E., Wang, J., Hahn, W. C., Gilliland, D. G*., et al.* (2006). Transformation from committed progenitor to leukaemia stem cell initiated by MLL-AF9. Nature *442*, 818-822.

Kunisaki, Y., Bruns, I., Scheiermann, C., Ahmed, J., Pinho, S., Zhang, D., Mizoguchi, T., Wei, Q., Lucas, D., Ito, K*., et al.* (2013). Arteriolar niches maintain haematopoietic stem cell quiescence. Nature *502*, 637-643.

Lange, R. D., Moloney, W. C., and Yamawaki, T. (1954). Leukemia in atomic bomb survivors. I. General observations. Blood *9*, 574-585.

Lapidot, T., Sirard, C., Vormoor, J., Murdoch, B., Hoang, T., Caceres-Cortes, J., Minden, M., Paterson, B., Caligiuri, M. A., and Dick, J. E. (1994). A cell initiating human acute myeloid leukaemia after transplantation into SCID mice. Nature *367*, 645-648.

Lee, C. K., Rao, D. T., Gertner, R., Gimeno, R., Frey, A. B., and Levy, D. E. (2000). Distinct requirements for IFNs and STAT1 in NK cell function. J Immunol *165*, 3571-3577.

Legros, L., Rousselot, P., Giraudier, S., Tulliez, M., Huguet, F., Nicolini, F. E., and Mahon, F. X. (2012). Second attempt to discontinue imatinib in CP-CML patients with a second sustained complete molecular response. Blood *120*, 1959-1960.

Lombardo, L. J., Lee, F. Y., Chen, P., Norris, D., Barrish, J. C., Behnia, K., Castaneda, S., Cornelius, L. A., Das, J., Doweyko, A. M.*, et al.* (2004). Discovery of N-(2-chloro-6-methyl- phenyl)-2-(6-(4-(2-hydroxyethyl)- piperazin-1-yl)-2-methylpyrimidin-4- ylamino)thiazole-5-carboxamide (BMS-354825), a dual Src/Abl kinase inhibitor with potent antitumor activity in preclinical assays. J Med Chem *47*, 6658-6661.

Lydon, N. (2009). Attacking cancer at its foundation. Nat Med *15*, 1153-1157.

Mahon, F. X., Hayette, S., Lagarde, V., Belloc, F., Turcq, B., Nicolini, F., Belanger, C., Manley, P. W., Leroy, C., Etienne, G.*, et al.* (2008). Evidence that resistance to nilotinib may be due to BCR-ABL, Pgp, or Src kinase overexpression. Cancer Res *68*, 9809-9816.

Mahon, F. X., Rea, D., Guilhot, J., Guilhot, F., Huguet, F., Nicolini, F., Legros, L., Charbonnier, A., Guerci, A., Varet, B.*, et al.* (2010). Discontinuation of imatinib in patients with chronic myeloid leukaemia who have maintained complete molecular remission for at least 2 years: the prospective, multicentre Stop Imatinib (STIM) trial. Lancet Oncol *11*, 1029-1035.

Mandanas, R. A., Leibowitz, D. S., Gharehbaghi, K., Tauchi, T., Burgess, G. S., Miyazawa, K., Jayaram, H. N., and Boswell, H. S. (1993). Role of p21 RAS in p210 bcr-abl transformation of murine myeloid cells. Blood *82*, 1838-1847.

Marin, D., Bazeos, A., Mahon, F. X., Eliasson, L., Milojkovic, D., Bua, M., Apperley, J. F., Szydlo, R., Desai, R., Kozlowski, K.*, et al.* (2010). Adherence is the critical factor for achieving molecular responses in patients with chronic myeloid leukemia who achieve complete cytogenetic responses on imatinib. J Clin Oncol *28*, 2381-2388.

Medyouf, H., Mossner, M., Jann, J. C., Nolte, F., Raffel, S., Herrmann, C., Lier, A., Eisen, C., Nowak, V., Zens, B.*, et al.* (2014). Myelodysplastic cells in patients reprogram mesenchymal stromal cells to establish a transplantable stem cell niche disease unit. Cell Stem Cell *14*, 824-837.

Mendelson, A., and Frenette, P. S. (2014). Hematopoietic stem cell niche maintenance during homeostasis and regeneration. Nat Med *20*, 833-846.

Michor, F., Hughes, T. P., Iwasa, Y., Branford, S., Shah, N. P., Sawyers, C. L., and Nowak, M. A. (2005). Dynamics of chronic myeloid leukaemia. Nature *435*, 1267-1270.

Minami, Y., Stuart, S. A., Ikawa, T., Jiang, Y., Banno, A., Hunton, I. C., Young, D. J., Naoe, T., Murre, C., Jamieson, C. H., and Wang, J. Y. (2008). BCR-ABL-transformed GMP as myeloid leukemic stem cells. Proc Natl Acad Sci U S A *105*, 17967-17972.

Morita, Y., Ema, H., and Nakauchi, H. (2010). Heterogeneity and hierarchy within the most primitive hematopoietic stem cell compartment. J Exp Med *207*, 1173-1182.

Morrison, S. J., and Scadden, D. T. (2014). The bone marrow niche for haematopoietic stem cells. Nature *505*, 327-334.

Morrison, S. J., Wandycz, A. M., Hemmati, H. D., Wright, D. E., and Weissman, I. L. (1997a). Identification of a lineage of multipotent hematopoietic progenitors. Development *124*, 1929-1939.

Morrison, S. J., and Weissman, I. L. (1994). The long-term repopulating subset of hematopoietic stem cells is deterministic and isolatable by phenotype. Immunity *1*, 661-673.

Morrison, S. J., Wright, D. E., and Weissman, I. L. (1997b). Cyclophosphamide/granulocyte colony-stimulating factor induces hematopoietic stem cells to proliferate prior to mobilization. Proc Natl Acad Sci U S A *94*, 1908-1913.

Nicolini, F. E., Hayette, S., Legros, L., Rousselot, P., Maloisel, F., Tulliez, M., Guerci, A., Charbonnier, A., Prebet, T., Rigal-Huguet, F.*, et al.* (2011). Pegylated IFN-alpha2a combined to imatinib mesylate 600mg daily can induce complete cytogenetic and molecular responses in a subset of chronic phase CML patients refractory to IFN alone or to imatinib 600mg daily alone. Leuk Res *35*, 80-86.

Nieborowska-Skorska, M., Kopinski, P. K., Ray, R., Hoser, G., Ngaba, D., Flis, S., Cramer, K., Reddy, M. M., Koptyra, M., Penserga, T.*, et al.* (2012). Rac2-MRC-cIII-generated ROS cause genomic instability in chronic myeloid leukemia stem cells and primitive progenitors. Blood *119*, 4253-4263.

Noens, L., van Lierde, M. A., De Bock, R., Verhoef, G., Zachee, P., Berneman, Z., Martiat, P., Mineur, P., Van Eygen, K., MacDonald, K.*, et al.* (2009). Prevalence, determinants, and outcomes of nonadherence to imatinib therapy in patients with chronic myeloid leukemia: the ADAGIO study. Blood *113*, 5401-5411.

Nowell, P. C., Cole, L. J., Habermeyer, J. G., and Roan, P. L. (1956). Growth and continued function of rat marrow cells in x-radiated mice. Cancer Res *16*, 258-261.

O'Brien, S., Radich, J. P., Abboud, C. N., Akhtari, M., Altman, J. K., Berman, E., DeAngelo, D. J., Deininger, M., Devine, S., Fathi, A. T.*, et al.* (2013). Chronic Myelogenous Leukemia, Version 1.2014. J Natl Compr Canc Netw *11*, 1327-1340.

O'Brien, S. G., Guilhot, F., Larson, R. A., Gathmann, I., Baccarani, M., Cervantes, F., Cornelissen, J. J., Fischer, T., Hochhaus, A., Hughes, T.*, et al.* (2003). Imatinib compared with interferon and low-dose cytarabine for newly diagnosed chronic-phase chronic myeloid leukemia. N Engl J Med *348*, 994-1004.

O'Hare, T., Shakespeare, W. C., Zhu, X., Eide, C. A., Rivera, V. M., Wang, F., Adrian, L. T., Zhou, T., Huang, W. S., Xu, Q.*, et al.* (2009). AP24534, a pan-BCR-ABL inhibitor for chronic myeloid leukemia, potently inhibits the T315I mutant and overcomes mutation-based resistance. Cancer Cell *16*, 401-412.

O'Hare, T., Walters, D. K., Stoffregen, E. P., Jia, T., Manley, P. W., Mestan, J., Cowan-Jacob, S. W., Lee, F. Y., Heinrich, M. C., Deininger, M. W., and Druker, B. J. (2005). In vitro activity of Bcr-Abl inhibitors AMN107 and BMS-354825 against clinically relevant imatinib-resistant Abl kinase domain mutants. Cancer Res *65*, 4500-4505.

Oguro, H., Ding, L., and Morrison, S. J. (2013). SLAM family markers resolve functionally distinct subpopulations of hematopoietic stem cells and multipotent progenitors. Cell Stem Cell *13*, 102-116.

Osawa, M., Hanada, K., Hamada, H., and Nakauchi, H. (1996). Long-term lymphohematopoietic reconstitution by a single CD34-low/negative hematopoietic stem cell. Science *273*, 242-245.

Pang, W. W., Price, E. A., Sahoo, D., Beerman, I., Maloney, W. J., Rossi, D. J., Schrier, S. L., and Weissman, I. L. (2011). Human bone marrow hematopoietic stem cells are increased in frequency and myeloid-biased with age. Proc Natl Acad Sci U S A *108*, 20012-20017.

Passegue, E., Jamieson, C. H., Ailles, L. E., and Weissman, I. L. (2003). Normal and leukemic hematopoiesis: are leukemias a stem cell disorder or a reacquisition of stem cell characteristics? Proc Natl Acad Sci U S A *100 Suppl 1*, 11842-11849.

Pene-Dumitrescu, T., and Smithgall, T. E. (2010). Expression of a Src family kinase in chronic myelogenous leukemia cells induces resistance to imatinib in a kinase-dependent manner. J Biol Chem *285*, 21446-21457.

Pietras, E. M., Lakshminarasimhan, R., Techner, J. M., Fong, S., Flach, J., Binnewies, M., and Passegue, E. (2014). Re-entry into quiescence protects hematopoietic stem cells from the killing effect of chronic exposure to type I interferons. J Exp Med *211*, 245-262.

Pietras, E. M., Warr, M. R., and Passegue, E. (2011). Cell cycle regulation in hematopoietic stem cells. J Cell Biol *195*, 709-720.

Preston, D. L., Kusumi, S., Tomonaga, M., Izumi, S., Ron, E., Kuramoto, A., Kamada, N., Dohy, H., Matsuo, T., Matsui, T., and et al. (1994). Cancer incidence in atomic bomb survivors. Part III. Leukemia, lymphoma and multiple myeloma, 1950-1987. Radiat Res *137*, S68-97.

Preudhomme, C., Guilhot, J., Nicolini, F. E., Guerci-Bresler, A., Rigal-Huguet, F., Maloisel, F., Coiteux, V., Gardembas, M., Berthou, C., Vekhoff, A.*, et al.* (2010). Imatinib plus peginterferon alfa-2a in chronic myeloid leukemia. N Engl J Med *363*, 2511-2521.

Prost, S., Relouzat, F., Spentchian, M., Ouzegdouh, Y., Saliba, J., Massonnet, G., Beressi, J. P., Verhoeyen, E., Raggueneau, V., Maneglier, B.*, et al.* (2015). Erosion of the chronic myeloid leukaemia stem cell pool by PPARgamma agonists. Nature *525*, 380-383.

Quintas-Cardama, A. (2014). Ponatinib in Philadelphia chromosome-positive leukemias. N Engl J Med *370*, 577.

Ren, R. (2005). Mechanisms of BCR-ABL in the pathogenesis of chronic myelogenous leukaemia. Nat Rev Cancer *5*, 172-183.

Reya, T., Morrison, S. J., Clarke, M. F., and Weissman, I. L. (2001). Stem cells, cancer, and cancer stem cells. Nature *414*, 105-111.

Reynaud, D., Pietras, E., Barry-Holson, K., Mir, A., Binnewies, M., Jeanne, M., Sala-Torra, O., Radich, J. P., and Passegue, E. (2011). IL-6 controls leukemic

multipotent progenitor cell fate and contributes to chronic myelogenous leukemia development. Cancer Cell *20*, 661-673.

Ross, D. M., Branford, S., Seymour, J. F., Schwarer, A. P., Arthur, C., Yeung, D. T., Dang, P., Goyne, J. M., Slader, C., Filshie, R. J.*, et al.* (2013). Safety and efficacy of imatinib cessation for CML patients with stable undetectable minimal residual disease: results from the TWISTER study. Blood *122*, 515-522.

Rousselot, P., Charbonnier, A., Cony-Makhoul, P., Agape, P., Nicolini, F. E., Varet, B., Gardembas, M., Etienne, G., Rea, D., Roy, L.*, et al.* (2014). Loss of major molecular response as a trigger for restarting tyrosine kinase inhibitor therapy in patients with chronic-phase chronic myelogenous leukemia who have stopped imatinib after durable undetectable disease. J Clin Oncol *32*, 424-430.

Rousselot, P., Huguet, F., Rea, D., Legros, L., Cayuela, J. M., Maarek, O., Blanchet, O., Marit, G., Gluckman, E., Reiffers, J.*, et al.* (2007). Imatinib mesylate discontinuation in patients with chronic myelogenous leukemia in complete molecular remission for more than 2 years. Blood *109*, 58-60.

Rowley, J. D. (1973). Letter: A new consistent chromosomal abnormality in chronic myelogenous leukaemia identified by quinacrine fluorescence and Giemsa staining. Nature *243*, 290-293.

Saito, Y., Uchida, N., Tanaka, S., Suzuki, N., Tomizawa-Murasawa, M., Sone, A., Najima, Y., Takagi, S., Aoki, Y., Wake, A.*, et al.* (2010). Induction of cell cycle entry eliminates human leukemia stem cells in a mouse model of AML. Nat Biotechnol *28*, 275-280.

Sanjuan-Pla, A., Macaulay, I. C., Jensen, C. T., Woll, P. S., Luis, T. C., Mead, A., Moore, S., Carella, C., Matsuoka, S., Bouriez Jones, T.*, et al.* (2013). Platelet-biased stem cells reside at the apex of the haematopoietic stem-cell hierarchy. Nature *502*, 232-236.

Sawyers, C. L. (1999). Chronic myeloid leukemia. New Engl J Med *340*, 1330-1340.

Schepers, K., Campbell, T. B., and Passegue, E. (2015). Normal and leukemic stem cell niches: insights and therapeutic opportunities. Cell Stem Cell *16*, 254-267.

Schmidt, T., Kharabi Masouleh, B., Loges, S., Cauwenberghs, S., Fraisl, P., Maes, C., Jonckx, B., De Keersmaecker, K., Kleppe, M., Tjwa, M.*, et al.* (2011). Loss or inhibition of stromal-derived PlGF prolongs survival of mice with imatinib-resistant Bcr-Abl1(+) leukemia. Cancer Cell *19*, 740-753.

Shah, N. P., Tran, C., Lee, F. Y., Chen, P., Norris, D., and Sawyers, C. L. (2004). Overriding imatinib resistance with a novel ABL kinase inhibitor. Science *305*, 399-401.

Silver, R. T., Woolf, S. H., Hehlmann, R., Appelbaum, F. R., Anderson, J., Bennett, C., Goldman, J. M., Guilhot, F., Kantarjian, H. M., Lichtin, A. E.*, et al.* (1999). An evidence-based analysis of the effect of busulfan, hydroxyurea, interferon, and allogeneic bone marrow transplantation in treating the chronic phase of chronic myeloid leukemia: developed for the American Society of Hematology. Blood *94*, 1517-1536.

Simonsson, B., Gedde-Dahl, T., Markevarn, B., Remes, K., Stentoft, J., Almqvist, A., Bjoreman, M., Flogegard, M., Koskenvesa, P., Lindblom, A.*, et al.* (2011). Combination of pegylated IFN-alpha2b with imatinib increases molecular response rates in patients with low- or intermediate-risk chronic myeloid leukemia. Blood *118*, 3228-3235.

Spangrude, G. J., Heimfeld, S., and Weissman, I. L. (1988). Purification and characterization of mouse hematopoietic stem cells. Science *241*, 58-62.

Stark, G. R., Kerr, I. M., Williams, B. R., Silverman, R. H., and Schreiber, R. D. (1998). How cells respond to interferons. Annu Rev Biochem *67*, 227-264.

Stuart, S. A., Minami, Y., and Wang, J. Y. (2009). The CML stem cell: evolution of the progenitor. Cell Cycle *8*, 1338-1343.

Swann, J. B., Hayakawa, Y., Zerafa, N., Sheehan, K. C., Scott, B., Schreiber, R. D., Hertzog, P., and Smyth, M. J. (2007). Type I IFN contributes to NK cell homeostasis, activation, and antitumor function. J Immunol *178*, 7540-7549.

Tabe, Y., and Konopleva, M. (2014). Advances in understanding the leukaemia microenvironment. Br J Haematol *164*, 767-778.

Takizawa, H., Boettcher, S., and Manz, M. G. (2012). Demand-adapted regulation of early hematopoiesis in infection and inflammation. Blood *119*, 2991-3002.

Takizawa, H., Regoes, R. R., Boddupalli, C. S., Bonhoeffer, S., and Manz, M. G. (2011). Dynamic variation in cycling of hematopoietic stem cells in steady state and inflammation. J Exp Med *208*, 273-284.

Talpaz, M., McCredie, K. B., Mavligit, G. M., and Gutterman, J. U. (1983). Leukocyte interferon-induced myeloid cytoreduction in chronic myelogenous leukemia. Blood *62*, 689-692.

Till, J. E., and Mc, C. E. (1961). A direct measurement of the radiation sensitivity of normal mouse bone marrow cells. Radiat Res *14*, 213-222.

Tokarski, J. S., Newitt, J. A., Chang, C. Y., Cheng, J. D., Wittekind, M., Kiefer, S. E., Kish, K., Lee, F. Y., Borzillerri, R., Lombardo, L. J.*, et al.* (2006). The structure of Dasatinib (BMS-354825) bound to activated ABL kinase domain elucidates its inhibitory activity against imatinib-resistant ABL mutants. Cancer Res *66*, 5790-5797.

Traer, E., Javidi-Sharifi, N., Agarwal, A., Dunlap, J., English, I., Martinez, J., Tyner, J. W., Wong, M., and Druker, B. J. (2014). Ponatinib overcomes FGF2-mediated resistance in CML patients without kinase domain mutations. Blood *123*, 1516-1524.

Trinchieri, G. (2010). Type I interferon: friend or foe? J Exp Med *207*, 2053-2063.

Trumpp, A., Essers, M., and Wilson, A. (2010). Awakening dormant haematopoietic stem cells. Nat Rev Immunol *10*, 201-209.

Trumpp, A., and Wiestler, O. D. (2008). Mechanisms of Disease: cancer stem cells--targeting the evil twin. Nat Clin Pract Oncol *5*, 337-347.

Uchida, N., Aguila, H. L., Fleming, W. H., Jerabek, L., and Weissman, I. L. (1994). Rapid and sustained hematopoietic recovery in lethally irradiated mice transplanted with purified Thy-1.1lo Lin-Sca-1+ hematopoietic stem cells. Blood *83*, 3758-3779.

Walter, D., Lier, A., Geiselhart, A., Thalheimer, F. B., Huntscha, S., Sobotta, M. C., Moehrle, B., Brocks, D., Bayindir, I., Kaschutnig, P.*, et al.* (2015). Exit from dormancy provokes DNA-damage-induced attrition in haematopoietic stem cells. Nature *520*, 549-552.

Wang, J. C., and Dick, J. E. (2005). Cancer stem cells: lessons from leukemia. Trends Cell Biol *15*, 494-501.

Wang, Y., Krivtsov, A. V., Sinha, A. U., North, T. E., Goessling, W., Feng, Z., Zon, L. I., and Armstrong, S. A. (2010). The Wnt/beta-catenin pathway is required for the development of leukemia stem cells in AML. Science *327*, 1650-1653.

Weisberg, E., Azab, A. K., Manley, P. W., Kung, A. L., Christie, A. L., Bronson, R., Ghobrial, I. M., and Griffin, J. D. (2012). Inhibition of CXCR4 in CML cells disrupts their interaction with the bone marrow microenvironment and sensitizes them to nilotinib. Leukemia *26*, 985-990.

Weisberg, E., Manley, P. W., Breitenstein, W., Bruggen, J., Cowan-Jacob, S. W., Ray, A., Huntly, B., Fabbro, D., Fendrich, G., Hall-Meyers, E.*, et al.* (2005). Characterization of AMN107, a selective inhibitor of native and mutant Bcr-Abl. Cancer Cell *7*, 129-141.

Weisberg, E., Manley, P. W., Cowan-Jacob, S. W., Hochhaus, A., and Griffin, J. D. (2007). Second generation inhibitors of BCR-ABL for the treatment of imatinib-resistant chronic myeloid leukaemia. Nature reviews Cancer *7*, 345-356.

Weissman, I. L. (2000). Translating stem and progenitor cell biology to the clinic: barriers and opportunities. Science *287*, 1442-1446.

Weissman, I. L., and Shizuru, J. A. (2008). The origins of the identification and isolation of hematopoietic stem cells, and their capability to induce donor-specific transplantation tolerance and treat autoimmune diseases. Blood *112*, 3543-3553.

Welch, J. S., Ley, T. J., Link, D. C., Miller, C. A., Larson, D. E., Koboldt, D. C., Wartman, L. D., Lamprecht, T. L., Liu, F., Xia, J.*, et al.* (2012). The origin and evolution of mutations in acute myeloid leukemia. Cell *150*, 264-278.

Welner, R. S., Amabile, G., Bararia, D., Czibere, A., Yang, H., Zhang, H., Pontes, L. L., Ye, M., Levantini, E., Di Ruscio, A.*, et al.* (2015). Treatment of chronic myelogenous leukemia by blocking cytokine alterations found in normal stem and progenitor cells. Cancer Cell *27*, 671-681.

Wilson, A., Laurenti, E., Oser, G., van der Wath, R. C., Blanco-Bose, W., Jaworski, M., Offner, S., Dunant, C. F., Eshkind, L., Bockamp, E.*, et al.* (2008). Hematopoietic stem cells reversibly switch from dormancy to self-renewal during homeostasis and repair. Cell *135*, 1118-1129.

Wilson, A., Laurenti, E., and Trumpp, A. (2009). Balancing dormant and self-renewing hematopoietic stem cells. Curr Opin Genet Dev *19*, 461-468.

Wilson, A., Oser, G. M., Jaworski, M., Blanco-Bose, W. E., Laurenti, E., Adolphe, C., Essers, M. A., Macdonald, H. R., and Trumpp, A. (2007). Dormant and self-renewing hematopoietic stem cells and their niches. Ann N Y Acad Sci *1106*, 64-75.

Wilson, A., and Trumpp, A. (2006). Bone-marrow haematopoietic-stem-cell niches. Nat Rev Immunol *6*, 93-106.

Woessner, D. W., Eiring, A. M., Bruno, B. J., Zabriskie, M. S., Reynolds, K. R., Miller, G. D., O'Hare, T., Deininger, M. W., and Lim, C. S. (2015). A coiled-coil mimetic intercepts BCR-ABL1 dimerization in native and kinase-mutant chronic myeloid leukemia. Leukemia *29*, 1668-1675.

Wright, D. E., Cheshier, S. H., Wagers, A. J., Randall, T. D., Christensen, J. L., and Weissman, I. L. (2001). Cyclophosphamide/granulocyte colony-stimulating factor causes selective mobilization of bone marrow hematopoietic stem cells into the blood after M phase of the cell cycle. Blood *97*, 2278-2285.

Wu, A. M., Till, J. E., Siminovitch, L., and McCulloch, E. A. (1967). A cytological study of the capacity for differentiation of normal hemopoietic colony-forming cells. J Cell Physiol *69*, 177-184.

Wu, J., Meng, F., Kong, L. Y., Peng, Z., Ying, Y., Bornmann, W. G., Darnay, B. G., Lamothe, B., Sun, H., Talpaz, M., and Donato, N. J. (2008). Association between imatinib-resistant BCR-ABL mutation-negative leukemia and persistent activation of LYN kinase. J Natl Cancer Inst *100*, 926-939.

Yamamoto, R., Morita, Y., Ooehara, J., Hamanaka, S., Onodera, M., Rudolph, K. L., Ema, H., and Nakauchi, H. (2013). Clonal analysis unveils self-renewing lineage-restricted progenitors generated directly from hematopoietic stem cells. Cell *154*, 1112-1126.

Yanez, A., Murciano, C., O'Connor, J. E., Gozalbo, D., and Gil, M. L. (2009). Candida albicans triggers proliferation and differentiation of hematopoietic stem and progenitor cells by a MyD88-dependent signaling. Microbes Infect *11*, 531-535.

Yokota, T., Oritani, K., Butz, S., Kokame, K., Kincade, P. W., Miyata, T., Vestweber, D., and Kanakura, Y. (2009). The endothelial antigen ESAM marks primitive hematopoietic progenitors throughout life in mice. Blood *113*, 2914-2923.

Yoshihara, H., Arai, F., Hosokawa, K., Hagiwara, T., Takubo, K., Nakamura, Y., Gomei, Y., Iwasaki, H., Matsuoka, S., Miyamoto, K.*, et al.* (2007). Thrombopoietin/MPL signaling regulates hematopoietic stem cell quiescence and interaction with the osteoblastic niche. Cell Stem Cell *1*, 685-697.

Zabriskie, M. S., Eide, C. A., Tantravahi, S. K., Vellore, N. A., Estrada, J., Nicolini, F. E., Khoury, H. J., Larson, R. A., Konopleva, M., Cortes, J. E.*, et al.* (2014). BCR-ABL1 compound mutations combining key kinase domain positions confer clinical resistance to ponatinib in Ph chromosome-positive leukemia. Cancer Cell *26*, 428-442.

Zhang, B., Ho, Y. W., Huang, Q., Maeda, T., Lin, A., Lee, S. U., Hair, A., Holyoake, T. L., Huettner, C., and Bhatia, R. (2012). Altered microenvironmental regulation of leukemic and normal stem cells in chronic myelogenous leukemia. Cancer Cell *21*, 577-592.

Zhang, B., Li, M., McDonald, T., Holyoake, T. L., Moon, R. T., Campana, D., Shultz, L., and Bhatia, R. (2013). Microenvironmental protection of CML stem and progenitor cells from tyrosine kinase inhibitors through N-cadherin and Wnt-beta-catenin signaling. Blood *121*, 1824-1838.

Zhang, P., Nelson, S., Bagby, G. J., Siggins, R., 2nd, Shellito, J. E., and Welsh, D. A. (2008). The lineage-c-Kit+Sca-1+ cell response to Escherichia coli bacteremia in Balb/c mice. Stem Cells *26*, 1778-1786.